JPL D-12626, Rev. C

Earth Observing System

Multi-angle Imaging Spectro-Radiometer

Science Data Validation Plan

James E. Conel[1]
William C. Ledeboer[1]
Thomas P. Ackerman[2, 3]
Roger Marchand[2,3]
Eugene Clothiaux[2]

[1]Jet Propulsion Laboratory, California Institute of Technology
[2]Pennsylvania State University
[3]Currently at Pacific Northwest National Laboratory

Jet Propulsion Laboratory
California Institute of Technology

December 10, 1999

JPL D-12626, Rev. C

Multi-angle Imaging SpectroRadiometer (MISR)

Science Data Validation Plan

Approvals:

David J. Diner

MISR Principal Investigator

Carol J. Bruegge

MISR Calibration/Validation Coordinator

The MISR web site should be consulted to determine the latest released version of this document (http://www-misr.jpl.nasa.gov)
Approval signatures are on file with the MISR Project

Jet Propulsion Laboratory
California Institute of Technology

TABLE OF CONTENTS

Part I: Common Elements--Management and AirMISR

Part II: Aerosol/Surface Algorithms and Products

Part III: TOA/Cloud Algorithms and Products

Appendix

GLOSSARY

ACE (Arctic Cloud Experiment)
ADAS (Atmospheric Data Acquisition System)
AERI (Atmospheric Emitted Radiance Interferometer)
AERONET (Aerosol Robotic Network)
AirMISR (Airborne Multi-angle Imaging SpectroRadiometer)
AQMD (Air Quality Management District)
ARL (Air Resources Laboratory)
ARM (Atmospheric Radiation Measurement)
ARM (Atmospheric Radiation Measurement)
ASCM (Angular Signature Cloud Mask)
ASD (Analytical Spectral Devices)
ASTER (Advanced Spaceborne Thermal Emission and Reflection Radiometer)
ATB (Algorithm Theoretical Basis)
ATSR (Along-Track Scanning Radiometer)
AVIRIS (Airborne Visible/Infrared Imaging Spectrometer)
AZM (Azimuthal Model)
BDAS (Band-Differenced Angular Signature)
BOREAS (Boreal Ecosystem-Atmosphere Study)
BRDF (Bidirectional reflectance distribution function)
BRF (Bidirectional Reflectance Factor)
BSRN (Baseline Surface Radiation Network)
CAPMON(Canadian Air Pollution Monitoring)
CCD (Charge-Coupled Device)
CLS (Cloud Lidar System)
CM (Calibration Mode)
CSAR (Coupled Surface-Atmosphere Reflectance)
CSSC (Cloud Screen Surface Classification)
DAAC (Distributed Active Archive Center)
DDV (Dense Dark Vegetation)
DFD (Data Flow Diagram)
DHR (Directional Hemispherical Reflectance)
DOE (Department of Energy)
DTED (Digital Terrain Elevation Dataset)
EOS (Earth Observing System)
EOSDIS (EOS Data and Information System)
ERBE (Earth Radiation Budget Experiment)
ESA (European Space Agency)
FOV (Field of View)
GEWEX (Global Energy and Water Cycle Experiment)
GM (Global Mode)
GPS (Global Positioning System)
GSFC (Goddard Space Flight Center)
HDR (Hemispherical-Directional Reflectance)

HDRF (Hemispherical-Directional Reflectance Factor)
ICD (Interface Control Document)
IFOV (Instantaneous Field of View)
IFRCC (In-flight Radiometric Calibration and Characterization)
IGAP (International Global Aerosol Program)
INS (Inertial Navigation System)
IOP (Intensive Operational Period)
ISIS (Integrated Surface Irradiance Study)
JPL (Jet Propulsion Laboratory)
L1B1 (Level 1B1)
L1B2 (Level 1B2)
LM (Local Mode)
MISR (Multi-angle Imaging SpectroRadiometer)
MODIS (Moderate Resolution Imaging Spectroradiometer)
NASA (National Aeronautics and Space Administration)
NGS (Navajo Generating Station)
NIR (Near Infrared)
NSA (North Slope of Alaska)
NSF (National Science Foundation)
ONR (Office of Naval Research)
PNNL(Pacific Northwest National Laboratory)
PAR (Photosynthetically Active Solar Radiation)
PI (Principal Investigator)
PSU(Pennsylvania State University)
RCCM (Radiometric Camera-by-camera Cloud Mask)
RH (Relative Humidity)
RLRA (Reflecting Level Reference Altitude)
SCAR-C (Smoke, Clouds and Aerosol Radiation - California)
SCF (Science Computing Facility)
SDCM (Stereoscopically-Derived Cloud Mask)
SDD (Software Design Document)
SDD (Software Design Document)
SGP (Southern Great Plains)
SHEBA (Surface Heat Budget of the Arctic Ocean)
SRD (Software Requirements Document)
SSFR (Solar Spectral Flux Radiometer)
SURFRAD (Surface Radiation Budget Network)
TASC (Terrestrial Atmosphere and Surface Climatology)
TOA (Top-of-atmosphere)
TOPEX/Poseidon (Ocean Topography Experiment)
TWP (Tropical Western Pacific)
UTM (Universal Transverse Mercator)
VNIR (Visible and Near Infrared)
WCRP (World Climate Research Programme)
WGS (World Geodetic System)
WRMC (World Radiation Monitoring Center)

Science Data Validation Plan

Part I: Common Elements--Management and AirMISR

James E. Conel
William C. Ledeboer
Jet Propulsion Laboratory

1. INTRODUCTION

1.1 PURPOSE

This Science Data Validation Plan describes the plans for validating a subset of the Multi-angle Imaging SpectroRadiometer (MISR) Level 2 algorithms and data products and supplying top-of-atmosphere (TOA) radiances to the In-flight Radiometric Calibration and Characterization (IFRCC) subsystem for vicarious calibration.

1.2 SCOPE

This plan deals only with MISR science data and algorithms. Reference *[M-7]* provides the theoretical basis of the ground-based retrieval algorithms. Plans for in-flight radiometric and geometric calibration of the instrument are described in *[M-12]* and *[M-13]* respectively. These plans also discuss validation of the L1B1 Radiometric Product and the L1B2 Geo-rectified Radiance Product. The MISR Experiment Overview *[M-1]* summarizes the measurement and science objectives, the missions and the science data products. Literature references used throughout this document are provided in Chapters 10 and 15. Within the text, these references are indicated by a number in italicized square brackets, *e.g., [1]*.

Elements described within this Science Data Validation Plan include:

(1) The MISR algorithms and parameters to be validated.

(2) The plans for validating MISR algorithms used to produce parameters contained within Level 2 algorithms, products and ancillary datasets.

(3) The plans for producing TOA radiances from field measurements for use in MISR calibration during the mission, the so-called *vicarious* procedure.

(4) Field experiments, including those completed to date and plans for future campaigns.

(5) Instruments required for field experiments, including ground and aircraft based sensors.

(6) Radiometer networks and special sites to be used in the validations.

(7) Data reduction procedures and software needed to generate validation data products containing MISR parameters from field measurements and compare them with standard MISR products.

(8) The roles and responsibilities of the participants in the validation process.

(9) The required deliverables from the validation team.

(10) The plans for archiving results of the validation activities.

1.3 DOCUMENT ORGANIZATION

Part I of this Science Data Validation Plan discusses elements that are common to all aspects of the MISR validation activity. These include an introduction to the MISR experiment, the management plan for validation activities, software and data management issues, and plans for the Airborne Multi-angle Imaging SpectroRadiometer (AirMISR).

Part II of this plan describes algorithms, instruments, field experiments to be used for validation of MISR Aerosol and Surface algorithms and products, both in the pre-launch and post-launch eras. The site selection, timing and aircraft scheduling, field operations, data acquisitions, data reductions, error analyses and archiving of results will be carried out mainly by personnel of the MISR validation team at JPL and are described herein. These activities are overseen by the Validation Scientist in cooperation with the Principal Investigator and the Calibration/Validation Coordinator.

Part III of this plan describes algorithms, field instruments, and field experiments to be used for Validation of MISR TOA/Cloud algorithms and products, both in pre-launch and post-launch time frames. The site selection, planning and execution of field experiments as well as data collection, data reduction, archiving for these activities are the responsibilities of the Validation Coordinator and the MISR Co-Investigator at the Pennsylvania State University. To avoid conflicts in aircraft scheduling, use of personnel (e.g., AirMISR flight crew) and equipment, the Validation Coordinator is responsible for coordination of aircraft and field experiment requirements with the MISR Validation Scientist.

Where feasible field experiments common to both Part II and Part III will be carried out simultaneously, but in general the activities of Part II are best pursued under clear skies, whereas those of Part III are generally pursued under cloudy conditions. Instrumentation utilized primarily in Part II investigations may be used for Part III studies, e.g., sphere scanning radiometers and diffuse/direct radiometers for measurement of selected radiation quantities (incident and reflected radiance, radiant exitance and irradiance), and fisheye cameras for assessment of cloud cover. Otherwise the experiments relating to Part II and Part III are seen to proceed largely independently.

1.4 MISR DOCUMENTS

References to MISR Project documents are indicated by a number in italicized square brackets prefixed by M, e.g., *[M-1]*.

[M-1] Experiment Overview, JPL D-13407.

[M-2] Level 2 Cloud Detection and Classification Algorithm Theoretical Basis, JPL D-11399, Rev. C.

[M-3] Level 2 Top-of-Atmosphere Albedo Algorithm Theoretical Basis, JPL D-13401, Rev. C.

[M-4] Level 2 Aerosol Retrieval Algorithm Theoretical Basis, JPL D-11400, Rev. C.

[M-5] Level 2 Surface Retrieval Algorithm Theoretical Basis, JPL D-11401, Rev. C.

[M-6] Level 2 Ancillary Products and Datasets Algorithm Theoretical Basis, JPL D-13402, Rev. A.

[M-7] Science Data Validation Algorithm Theoretical Basis, JPL D-13403.

[M-8] Science Data Validation Product Description, JPL D-14005.

[M-9] Science Data Validation Software Requirements, JPL D-14006.

[M-10] Algorithm Development Plan, JPL D-11220.

[M-11] Preflight Calibration Plan, JPL D-11392.

[M-12] In-flight Radiometric Calibration and Characterization Plan, JPL D-13315.

[M-13] In-flight Geometric Calibration Plan, JPL D-13228.

[M-14] Science Data Quality Indicators, JPL D-13496.

[M-15] Data Management Plan, JPL D-13584.

1.5 MEASUREMENT AND SCIENCE OBJECTIVES

The purpose of the MISR experiment is to acquire systematic multi-angle imagery for global monitoring of top-of-atmosphere and surface albedos and to measure the shortwave radiative properties of aerosols, clouds, and surface scenes in order to characterize their impact on the Earth's climate.

The instrument is scheduled for launch on the first Earth Observing System (EOS) spacecraft (EOS-AM1). See Experiment Overview *[M-1]* for more information and *[51]* for MISR retrieval methods.

1.6 MISR INSTRUMENT

The MISR instrument consists of nine pushbroom cameras. It is capable of global coverage every nine days, and flies in a 705-km descending polar orbit. The cameras are arranged with one

camera pointing toward the nadir (designated An), one bank of four cameras pointing in the forward direction (designated Af, Bf, Cf, and Df in order of increasing off-nadir angle), and one bank of four cameras pointing in the aftward direction. The same naming convention is used but designated Aa, Ba, Ca, and Da. Images are acquired with nominal view angles, relative to the surface reference ellipsoid, of 0°, 26.1°, 45.6°, 60.0°, and 70.5° for An, Af/Aa, Bf/Ba, Cf/Ca, and Df/Da, respectively. Each camera uses four Charge-Coupled Device (CCD) line arrays in a single focal plane. The line arrays consist of 1504 photoactive pixels and each line is filtered to provide one of four spectral bands. The spectral band shapes are centered at 446, 558, 672, and 866 nm.

MISR contains 36 parallel signal chains corresponding to the four spectral bands in each of the nine cameras. Each signal chain contains the output from the detectors in each CCD array. The zonal overlap swath width of the MISR imaging data (that is, the swath seen in common by all nine cameras along a line of constant latitude) is 360km, which provides global multi-angle coverage of the entire Earth in 9 days at the equator, and 2 days at the poles. The cross-track instantaneous field-of-view (IFOV) and sample spacing of each pixel is 275 m for all of the off-nadir cameras, and 250 m for the nadir camera. The constant across-track pixel dimension is achieved by varying focal length with view angle. Along-track IFOV's depend on view angle, ranging from 214 m in the nadir to 707 m at the most oblique angle. Sample spacing in the along-track direction is 275 m in all cameras. The instrument is capable of buffering the data to provide 4 sample x 4 line, or 1 sample x 4 line averages, in addition to the mode in which pixels are sent with no averaging. The averaging capability is individually selectable within each of the 36 channels.

There are several observational modes of the MISR instrument. Global Mode (GM) refers to continuous operation with no limitation on swath length. Global coverage in a particular spectral band of one camera is provided by operating the corresponding signal chain continuously in a selected resolution mode. Any choice of averaging modes among the nine cameras that is consistent with the instrument power and data rate allocation is suitable for Global Mode. Additionally, Local Mode (LM) provides high resolution images in all 4 bands of all 9 cameras for selected Earth targets. This is accomplished by inhibiting pixel averaging in all bands of each of the cameras in sequence, one at a time, beginning with the first camera to acquire the target and ending with the last camera to view the target. The instrument geometry limits the along-track length of Local Mode targets to about 300 km. Finally, in Calibration Mode (CM) the on-board calibration hardware is deployed and calibration data are acquired for the cameras. Calibration data will be obtained for each spatial sampling mode (see above) by cycling each channel through the various modes during the calibration period. Calibration Mode will be used on a monthly basis during routine mission operations, although early in the mission it will be used more frequently.

1.6.1 Science Objectives

Aerosols of natural and anthropogenic origin, including those from industrial and volcanic emissions, natural plant emanations, biomass burning and dust resulting from desertification, pro-

vide shortwave radiative forcing of the planetary radiation budget. The scientific objectives of MISR aerosol retrievals are: (1) to monitor globally the magnitude and natural temporal and spatial variability of sunlight absorption and scattering by aerosols in the Earth's atmosphere, particularly the troposphere, and to determine the shortwave radiative forcing of climate, (2) to improve our knowledge of the distribution of sources, transformations, and sinks of aerosols over the globe, as well as their global budgets (fluxes from surface emission and deposition, atmospheric generation rates, residence times), (3) to provide data for atmospheric correction of images acquired by MISR and other EOS platform instruments (MODIS and ASTER) to secure better estimates of surface reflectance properties.

Accurate hemispherical reflectance estimates are expected to be diagnostic of the influence of biophysical processes on surface-atmosphere interactions (both with respect to energy and mass transfer because of the strong correlation between hemispherical surface reflectance and photosynthetic and evapotranspiration rates. Angular signatures from surface cover types is also expected to lead to improved surface cover classifications and characterization as well as quantification of the time-evolution (change) of terrestrial ecosystems that result from natural processes such as canopy succession and species replacement, or anthropogenic activities like deforestation and processes leading to acid rain. Monitoring of ocean color provides a means of assessing marine biological productivity and changes with time. The scientific objectives of MISR surface retrievals are: (1) to study globally the magnitude and natural spatial and temporal variability of the sunlight absorption and scattering properties by the Earth's surface specifically through determination of the surface bihemispherical reflectance (the spectral albedo), (2) to provide improved land surface classifications and determinations of temporal change (dynamics) in conjunction with MODIS, (3) to make observations of ocean color in equatorial regions through improved measurements of water-leaving radiances from atmospheric correction of top-of-atmosphere radiances, supplementing observations of MODIS.

The importance of clouds to the Earth's climate is unquestioned, and as the Earth undergoes change, both natural and anthropogenic in origin, the physical properties of clouds are expected to change. Clouds play a major role in the Earth's energy balance. Unfortunately, even some of the most basic features of clouds (such as cloud top altitude) and important scientific quantities (such as the angular dependence of light scattered by clouds) are not easily determined on a global scale. Current models of the response of Earth's climate to increases in CO_2 and trace gases like methane are severely limited by ignorance of feedback processes associated with changes in cloud cover and cloud properties. Accurate cloud height determinations are lacking in existing cloud climatologies and are poorly represented in studies of severe storm phenomena. Lack of reliable estimates of cloud-top altitude hamper efforts to model three-dimensional radiative fluxes in climate feedback models. MISR's unique ability to view the same target from multiple directions will enable determination of cloud top altitude and velocity through stereo-imaging techniques, as well as, to better constrain the angular dependence of the solar reflectance for both clouds and the Earth sur-

face. The overall scientific objectives of MISR with regards to clouds are: (1) to detect clouds as a prerequisite to surface classification and to identify cloud-free lines of sight prior to the application of aerosol and surface retrieval algorithms, (2) to classify different types of cloud fields (e.g., by their apparent heterogeneity, spatial arrangement and altitude), and (3) to study, on a global basis, the effects of clouds on the spectral solar radiance and irradiance reflected to space.

1.7 SCIENCE DATA PRODUCTS

The MISR Science Computing Facility (SCF) and Distributed Active Archive Center (DAAC) represent the primary entities in which the functions of MISR science data processing will be implemented. The MISR SCF will support MISR science algorithm development, as well as quality assessment and validation of MISR data products. This will include generating those data and coefficients needed to run MISR science software at the DAAC. The MISR DAAC, which is shared with several other EOS instruments, is the facility at which software incorporating MISR science algorithms will operate in a high volume, real-time mode to produce standard science data products.

The generation of science data products can be divided into six subsystems within the Product Generation System. Each subsystem has at least one primary output product, but may have other secondary output products. It is convenient to conceptualize the processes within these subsystems as occurring in sequence, with the predecessor producing at least one complete product, a portion of which is the primary input for the successor. Each of these subsystems correspond to a processing level of a product generation flow, as shown in Figure 1. These levels conform generally to the EOS scheme from Level 1 to Level 4.

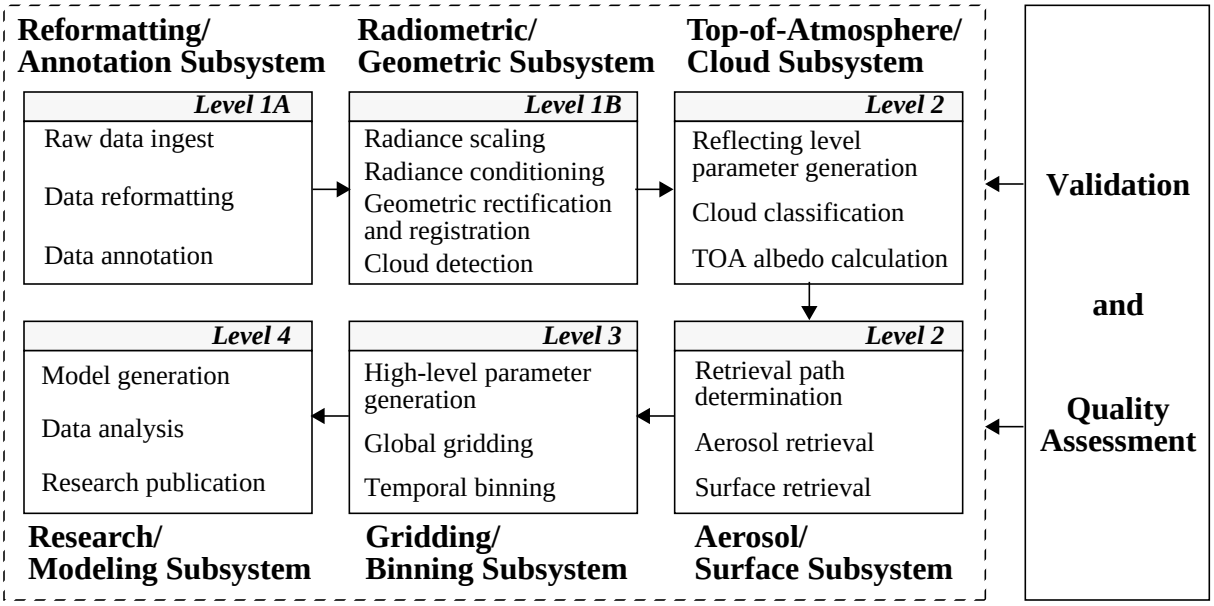

Figure 1: MISR Product Generation System

Standard products generated at the DAAC are critically dependent on calibration parameters and other lookup data, such as threshold datasets, atmospheric climatologies, aerosol and surface model datasets and the like, which must be produced at the SCF. Functions performed at the SCF are separated from DAAC activities because they require much closer scrutiny and involvement by the MISR Science Team than the MISR DAAC could provide. Updates to these data structures occur infrequently compared to the rate of standard product generation, and therefore fit into the more limited processing capabilities of the SCF. Other essential functions that have activities at the SCF include quality assessment, algorithm and data product validation, software development, and instrument operations.

1.8 REVISIONS

This plan will be updated periodically, or as warranted by new experiment developments. Future revisions will be issued as warranted in synchronization with the schedule for major software builds, and no less frequently than once per year, emphasizing the detail for work to be accomplished in the upcoming calendar year. All revisions to this document must be approved by the Principal Investigator. This release constitutes Revision C.

2. MANAGEMENT PLAN

2.1 INDIVIDUAL PARTICIPANTS AND ROLES

2.1.1 Principal Investigator

The MISR Principal Investigator (PI) has primary responsibility for the conduct of the MISR experiment and the direction of all MISR-related activities, including instrument development, operations, data management, data analysis, calibration, validation, and algorithm development. The PI possesses ultimate responsibility for selection of algorithms. Major elements of the PI's responsibilities are delegated as explained in the following subsections. The PI is David J. Diner of JPL.

2.1.2 Calibration/Validation Team Coordinator

The Calibration/Validation Coordinator, Carol J. Bruegge of JPL, oversees the joint onboard MISR calibration activities together with the science validation and vicarious instrument calibration effort. The role includes development and supervision and maintenance of a calibration facility, inherited from the MISR pre-flight calibration activity itself, that will be devoted exclusively to calibration and spectral characterization of field instruments and AirMISR. This role includes documentation of the calibration and validation efforts for both internal and external publication routes.

2.1.3 Validation Scientist

The MISR Validation Scientist, James E. Conel of JPL, assists the MISR Principal Investigator in overseeing the validation of MISR algorithms and data products. Algorithm development responsibilities include insuring that appropriate *in-situ*, aircraft-based, and space-based test data are acquired and used in testing MISR product generation algorithms and software before launch. The validation scientist is responsible for devising, writing, maintaining and implementing a plan for aerosol and surface products as well as schedule for MISR algorithm and data product validation, and is to be responsible for the validation budget. He will prepare experiment plans on an experiment by experiment basis, covering MISR plans delineating the experiment goals, the choice of field sites and the coordination of activities between aircraft overflight and ground teams. He will coordinate the choice of field validation activities with the Calibration-Validation Team Coordinator, members of the MISR Validation team, the MISR Science team, coordinate science and observational aircraft and field schedules with experiments carried on by NASA or other external organizations. The MISR Validation Scientist also coordinates the activities of a Field Engineer, a Data Management/Data Reduction Scientist, Field Algorithm Development Scientist, and a Software Subsystem Development Engineer. He will coordinate activities with the TOA/Cloud Validation coordinator (R. Marchand) and associated Co-Investigator formerly at Pennsylvania State University (PSU) and presently at Pacific Northwest Laboratories (PNL). The validation scientist also has responsibility for preparation of scientific papers describing validation developments in

the open literature and for episodic updates of the validation plan reflecting new lines of thought or important developments concerning MISR validation process.

2.1.4 Aerosol/Surface Validation Team

The Aerosol/Surface Validation team is based at JPL. The primary responsibilities of the Field Engineer, Mark C. Helmlinger, are acquisition, modification, calibration, maintenance and storage of all optical and meteorological instrumentation involved in the MISR field validation exercises. The Field Engineer is responsible for acquisition and storage of the raw observational data in the field and for its (near) real-time reduction as required to support field exercises. He has responsibility for development and maintenance of a JPL observation station designed to act as a local mode atmosphere/surface station for pre and post launch validation activities. The Validation Algorithm Scientist, Stuart Pilorz, will primarily be responsible for development and maintenance of all algorithms used for the reduction of optical data acquired from field and aircraft instruments. This includes the development of any new algorithms as required, adapted to the MISR theoretical formalism. The Validation Algorithm Scientist is also responsible for the writing and updating of the Science Data Validation ATB *[M-7]*. Working closely with the Validation Algorithm Scientist is the Validation Researcher, Wedad Abdou. She has a primary role in applying radiative transfer methodologies to the retrieval of surface radiometric parameters (e.g., BRF), participation on aerosol/surface closure studies, inclusion of aerosol models to calculate top-of-atmosphere radiances, and in the analysis of vicarious calibration results. The primary responsibilities of the Data Management Specialist (DMS) / Analyst, Barbara Gaitley, are to assemble field data from the acquiring entities external to JPL as well as from the JPL validation team, utilize the available laboratory and or field/acquired data to provide in-flight calibrations for MISR simulator instruments as well as other optical ground-based instrument data sets, maintain and upgrade existing software for reduction of field data and in addition work to provide routine (turnkey) editing capabilities and reductions for existing field instruments, (e.g. PARABOLA III of JPL, the MFRSR, the CIMEL and Reagan sunphotometers). She is responsible for the organization and maintenance of atmospheric, surface, and instrument calibration data acquired during field experiments into databases, its documentation for accessibility, so that quick access may be had by parties interested in complete traceability from field acquisition through calibration through deposition in the database. The Software Development Engineer, William Ledeboer, is responsible for establishing software requirements, designs, test plans, and test procedures. He is also responsible for implementation, integration, documentation and delivery of the validation software. With respect to algorithm development, his responsibilities are to insure that the software represents a thorough implementation of the algorithm requirements described in the relevant Algorithm Theoretical Basis (ATB) document(s). He works closely with the AirMISR data system team and is responsible for the generation of a routine processing approach for AirMISR calibrated and georectified data products.

2.1.5 TOA/Cloud Validation Team

Activities associated with validation of MISR TOA/Cloud products have been delegated to a team for which MISR team members and associates at Pennsylvania State University the have lead responsibilities. The lead individual formerly at PSU, and currently at PNL is MISR Co-Investigator Thomas P. Ackerman. He is assisted by researchers Roger Marchand and Eugene Clothiaux. Specifically these individuals will assume responsibility for the planning, coordination of activities with JPL (both field and AirMISR engineering teams) and NASA Dryden aircraft schedulers, the carrying out, the data reduction and publication of results for TOA/Cloud validation experiments. Members and associates of the MISR science team at JPL, University College London (Jan-Peter Muller), University of Illinois at Urbana (Larry Di Girolamo), and University of Arizona (Roger Davies) will also be involved in the TOA/Cloud Validation Team. The field experiments and data reductions for TOA/Cloud activities are predominantly independent of those carried out on behalf of Aerosol/Surface validation, although sharing of instruments and personnel may occur on an as needed basis.

2.2 SOFTWARE DEVELOPMENT

2.2.1 Objectives

The objectives of MISR validation software development activities are:

(1) Assist in the development, test and verification of MISR validation algorithms.

(2) Create a validation product generation system, running at the MISR Science Computing Facilities at JPL, Pennsylvania State University, University College London, University of Illinois, and University of Arizona, that will:

   (a) Ensure, through appropriate data management, that the raw field experiment data is maintained in its original form.

   (b) Implement the algorithms defined to generate the validation products.

   (c) Generate the data products needed to validate MISR algorithms and data products, and produce experiment reports and publications in the open literature.

(3) Implement the selection and ordering of appropriate granules of standard data products from the DAAC, corresponding to the times of coordinated field experiments/overflights.

(4) Facilitate the visualization and comparison of MISR and validation geophysical parameter retrievals.

2.3 DATA REDUCTION

2.3.1 Data Product Generation

The objective of reducing MISR validation data is to produce validation data products as defined in *[M-8]*. These products contain raw instrument data (Level 0), observables derived from raw data (Level 1) and geophysical parameters resulting from science retrievals (Level 2). Table 1 is a high-level summary of the Validation Products to be generated from the Validation Team activities.

Table 1: MISR Science Data Validation Products

Name	Processing Level
Field Raw Data Products	0
Field and Airborne Instrument Calibration Products	1
Field Instrument Products	1, 2
AirMISR Radiometric Product	1B1
AirMISR Georectified Radiance Product	1B2
Vicarious Calibration DN Product	0
Vicarious Calibration TOA Radiance Product	1
Validation TOA/Cloud Products	2
Validation Aerosol/Surface Products	2

Figure 2 is the context diagram for the MISR validation data product generation process. This figure identifies all of the external interfaces for this process, including all required inputs and the destinations of the various products.

MISR validation data products will be used for retrieval comparison and analysis. In addition, the TOA radiance and DN products will be delivered to the MISR In-Flight Radiometric Calibration and Characterization (IFRCC) subsystem for use in vicarious calibration of the flight instrument.

Most of the cloud validation data analysis will be performed at Pennsylvania State University, especially analysis of those data associated with ground-based measurements. In large measure, the data provided by ARM and other groups is quality controlled. Nonetheless, the validation analysis will include examining the data quality and calibration of these sensors.

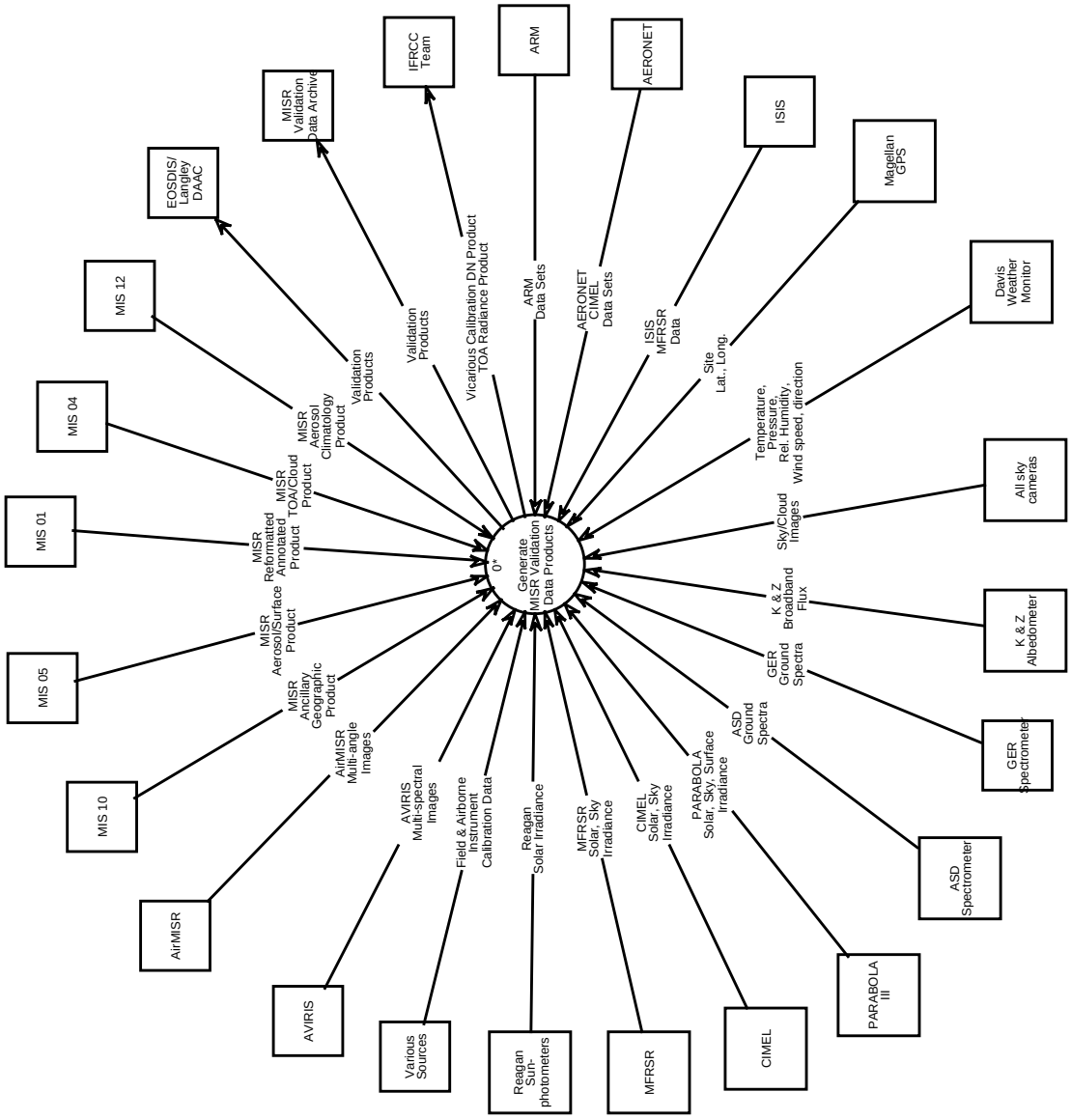

Figure 2: MISR Validation Product Generation Context Diagram

2.3.2 Archiving of Results

Measurement data from all field experiments as well as the parameter retrievals, comparisons and experiments reports will be archived both at the MISR SCF and at the appropriate DAAC (see Figure 2). The principal motivation is to allow recovery of the experimental conditions and permit complete traceability as well as characterization of the measurements.

Detailed descriptions of how the data will be archived will be included in the Data Management Plan *[M-15]*. Validation data will be archived at the scientific computing facility at which the product is generated as well as at the Langley DAAC.

2.3.3 Role of EOSDIS

MISR Science Data Validation will interact with EOSDIS through the DAACs. MISR Level 2 data products will be retrieved from the appropriate DAAC for comparison with ground and aircraft-based retrievals. The Level 1 data for all ground-based field exercises will also be archived at JPL and will be available to investigators concerned with MISR validation activities.

3. AIRMISR

3.1 INSTRUMENT DESCRIPTION

In 1996 the EOS Project Science Office at the NASA Goddard Space Flight Center (GSFC) approved the construction of an airborne MISR simulator, designated AirMISR. The primary mission of AirMISR is to (1) collect MISR-like data sets to support the validation of MISR geophysical retrieval algorithms and data products; (2) underfly the EOS-AM1 MISR sensor to provide an additional radiometric calibration path and to assist with in-flight instrument performance characterization; and (3) enable scientific research utilizing high quality, well-calibrated multi-angle imaging data. A secondary mission is to serve as a technology testbed for advanced, lightweighted MISR cameras for future remote sensing platforms.

AirMISR is a pushbroom imager utilizing a single spare MISR camera built into a pivoting gimbal mount. See *[15]* for a complete instrument description. A single data run is divided into nine segments, each at a specific MISR look angle. The gimbal pivots aftward between segments to repeat the pushbroom data acquisition of the same area on the ground from the next angle. This process is repeated until all nine look-angles of the target area are collected. The swath width is governed by the single camera field-of-view, and varies from 11 km in the nadir to 32 km at the most oblique view angle. The along-track image length at each angle is dictated by the timing required to obtain overlap imagery at all angles, and varies from about 9 km in the nadir to 26 km at the most oblique angle. Thus, the nadir image dictates the area of overlap that is imaged from all nine look angles. This approach ensures identical calibration at all angles, a useful feature in utilizing the instrument as part of the spaceborne MISR calibration. The AirMISR instrument flies aboard the ER-2 platform at an altitude of 65,000 to 70,000 feet above sea level. Thus adjustments in the calculated FOV must be made for targets at elevations above (or below) sea level.

JPL adopted the following approach in developing the instrument:

(1) MISR brassboard, protoflight spares, and existing ground support equipment were adapted for the camera optics, electronics, and data system. This ensures that AirMISR is closely matched in spectral and radiometric performance to the spaceborne MISR. The use of existing components, assemblies, and facilities minimized the development costs.

(2) The gimbal provides images at all nine MISR angles during a 13-minute flight line. The computer-controlled gimbal supports a number of different operating modes, including the standard nine-angle sequence as well as alternative angle sequences for specific studies and algorithm validations.

(3) MISR-equivalent pixels can be constructed by binning raw pixels in the ground data processing, taking into account the full resolution and frequency updates of existing Inertial Navigation System (INS) and Global Positioning System (GPS) pointing corrections as well as other look-angle scaling factors. From ER-2 alti-

tude, the AirMISR camera has an instantaneous footprint of 7 m cross-track x 6 m along-track in the nadir view and 21 m x 55 m at the most oblique angle. Lines of image data are acquired every 40.8 msec, resulting in an along-track sample spacing, regardless of view angle, of 8 m for an aircraft ground speed of 200 m/sec. Thus, it is possible to generate samples which match MISR pixel dimensions at any view angle, and to compensate for the variable footprint dimensions with angle in the ground data processing. It is also possible to make use of the higher resolution imagery if desired.

(4) Sets of MISR calibration photodiode assemblies were incorporated into the design to test their ability to supplement laboratory calibrations. A detector-based calibration approach is one of the innovations included in the spaceborne MISR on-board calibrator, and is essential to meeting the demanding radiometric accuracy requirements of the experiment. High accuracy radiometry of AirMISR is necessary in order for it to provide a useful calibration pathway for the spaceborne instrument, and detector-based methods are also integral to AirMISR laboratory calibrations.

(5) Room for an additional camera to be incorporated at a later date (e.g., to incorporate new spectral channels, or to enable the benchmarking of new technology camera components) was reserved within the instrument.

AirMISR has been partially operational since 1997, and became fully operational for unrestricted science data collection in approximately November, 1998. The instrument has flown as part of numerous engineering and several science flights. Diner *et al. [15]* describe some of the early results. Because the instrument specifications are those of the MISR cameras themselves, the radiometric performance is equivalent to that of MISR, with signal-to-noise ratios in the range from 700 at target reflectances of 100% to 100 at 2% ground reflectance, for individual pixels. Pointing to a specific ground target and stability of the overlapping fields-of-view for various view angles mainly depends upon stability of the ER-2 flight path, *e.g.*, straight and level, with pre-programmed start time. (Camera model and camera orientation relative to airframe are also involved). However the large AirMISR field of view and relatively good surface resolution (about 7 m at nadir) help to ensure that overlapping views of the surface target are secured and that distinctive surface features will be secured for target location. In addition, high accuracy and temporal resolution GPS and INS data obtained by the ER-2 help to determine image orientation for motion and attitude correction. Ground tie-pointing is used for additional geometric calibration.

3.2 INSTRUMENT STATUS

Following several deployments, a number of engineering issues remained with the instrument. A technical review was held at JPL on July 15, 1998 to solicit external advice on how to address the engineering issues. A brief description of the most significant issues, and plans for dealing with them is given here:

(1) The most significant issue was that the rotating gimbal was not reliably moving to all 9 acquisition angles. This has been determined to be due to excessive cable drag and an unbalanced condition of the rotating drum. Rework and flight testing has eliminated the problem.

(2) Flight software timing problems resulted in an allocation of computer resources between acquisition of image data and navigational data that results in a typical rate of 10% dropped image lines. A detailed analysis of the software timing was undertaken and a software rework carried out, culminating in a checkout flight in winter 1999. The fixes have largely eliminated dropped or corrupted lines upon data acquisition and greatly reduced need for such fixes in the ground data processing software.

(3) Some remaining engineering issues of a more minor nature, and implementation of the on-board diode calibrators, is scheduled for some time in 2000.

Each of the engineering checkout flights has been coupled with specific science objectives as described below so that the instrument continues to perform as a science instrument as part of the validation activities wherever possible

3.3 DATA REDUCTION

An automated data processing system is being developed to produce corrected, radiometrically calibrated, geo-rectified images from raw data acquired by AirMISR. Processing includes correction of images for corrupt or missing data, radiance conversion and scaling using laboratory measured calibration coefficients, resampling of ER-2 navigation data, and georectification of AirMISR images. AirMISR data reduction will proceed according to the following steps.

3.3.1 Unpacking

AirMISR flight data consists of image, navigation, engineering and log files. These files are unpacked from the tarred compressed file delivered by the flight operations team and installed in a standard directory structure.

3.3.2 Log File Analysis

The in-flight log file produced by the instrument is analyzed to determine how many runs (target overpasses) were attempted, the desired camera angles for each run and whether or not the camera angles were achieved based on the optical switch readings.

3.3.3 Navigation Data Processing

ER-2 navigation data is used to create a Hierarchical Data Format (HDF) file containing re-sampled navigation data for use in image georectification.

3.3.4 Image Correction and Radiometric Calibration (Level 1B1)

AirMISR images are corrected to replace dropped lines and corrupt data with linearly interpolated values. Radiometric calibration coefficients determined from laboratory measurements are applied and the resulting radiances are scaled in the same manner as MISR to produce an HDF product. The radiances are traceable to système international (SI) units.

3.3.5 Image Georectification (Level 1B2)

The georectification uses the navigation data to correct for aircraft attitude changes and co-registers the spectral and multi-angle images. The images are projected to terrain, defined by the Digital Terrain Elevation Dataset (DTED) Level 1, as well as to the ellipsoid defined by World Geodetic System 1984 (WGS84). Projected images are resampled to 27.5 m resolution on a Universal Transverse Mercator (UTM) grid.

3.3.6 DAAC Ingest Metadata Generation

Data required to submit AirMISR data products to the Langley DAAC are obtained from the flight log file, README files and user input.

3.3.7 Geophysical Parameter Retrieval (Level 2)

Modified MISR algorithm development codes will be used to retrieve geophysical parameters.

3.3.8 Plans

An Interface Control Document (ICD) for delivery of AirMISR data to the Langley DAAC is still under review at JPL and LaRC. The first phase of development focused on implementing the functionality needed to create Level 1B1 and 1B2 data products. Subsequently, we concentrated on automating and streamlining the production process such that raw data could be used to create DAAC-ready products with a minimum of operator/analyst intervention. MISR prototype algorithm development codes are being modified for use with AirMISR Level 1B2 products to retrieve aerosol, surface, and cloud parameters. Additional plans in the near future include:

(1) Updating of the Data Quality Indicator fields in the Level 1B2 product to reflect radiometric and geometric data quality.

(2) Inclusion of additional metadata into the AirMISR standard products.

(3) Release of AirMISR ICD.

(4) Re-processing of AirMISR flight data and delivery of data products to Langley DAAC

3.4 EXPERIMENT CAMPAIGNS

3.4.1 Nature Of AirMISR Field Campaigns

Each field campaign is designed to obtain ground measurements of atmosphere and surface simultaneously with AirMISR overflight of the target. Each target chosen addresses one or more validation issues of aerosol, surface reflectance, or cloud algorithm validation. The experiments are carried out under clear sky conditions, unless cloud validation activities are involved. In order to compensate for possible aircraft pointing and other stability or navigational issues, it has been decided to duplicate each overpass at a given azimuth (down and back). Typically three azimuth directions are chosen: (1) duplicate expected ground path of MISR ground track, about 190°, and reverse, about 10°, (2) solar principal plane and reverse, (3) line bisecting (1) and (2), and the reverse, for a total of six individual lines. Including the solar principal plane observations introduces the possibility of measuring aerosol scattering phase angles approaching 180° and also the surface reflectance near the so-called hot-spot, coinciding with the direction of retro-reflection from the ground.

3.4.2 Schedules

Tables 2, 3, and 4 summarize the AirMISR field campaign program from late 1998 through 2002. Included in the charts are experiment locations, types, aircraft coverage sought and status. The future schedule will probably be modified as to location, timing, and content to fit with status of AirMISR, the ER-2 aircraft schedule, unforeseen problems with MISR, its calibration or data interpretation, and occurrence of other EOS validation efforts or related field campaigns.

In the latter part of CY 1998 and throughout CY 1999 two engineering flights for AirMISR were planned to check operability of the instrument/aircraft system after the latest instrument rework. Table 2 lists five targets for these missions that provided high priority data for algorithm validation studies. The plan was to have each such overflight accompanied by the full complement of ground observations at the chosen site thus leading to complete validation experiments in each case regardless of whether the goals were predominantly engineering or predominantly science.

Tables 3 -5 present experiments planned for the FY 2000 -2002 flight seasons. They represent (1) previously scheduled experiments that were postponed or cancelled because of unavailability of AirMISR, (2) new experiments added to satisfy needs of MISR team members. These experiments will be carried out as funding, flight hours, weather conditions, and aircraft availability permit.

Table 2: Science Experiments Involving AirMISR completed during late 1998 and 1999

SITE -DATE	EXPERIMENT TYPE	AEROSOL TYPE	BOUNDARY CONDITION	AIRCRAFT INSTRUMENT	STATUS
Rogers Lake, CA November, 1998	Engineering check-out of drum rework, vicarious calibration of AirMisr	Ambient	homogeneous dry playa	AirMISR, RC-10	Completed December 11, 1998. Full complement of aerosol and surface measurements
San Joaquin Valley (Buena Vista Reservoir) February-March, 1999	Engineering check-out of new flight software, vegetation BRF, path radiance analysis over Reservoir	Ambient	Winter wheat and alfalfa canopies, water	AirMISR, RC-10	Aborted due to weather, AirMISR engineering problems
Lake Tahoe, California- May 7, 1999	Aerosol over deep lake water	Smoke or ambient	Deep (fresh) water	AirMISR, MAS, RC-10	Incomplete, got some lines, missed target, high clouds
Monterey Bay (Marina)- June 13-July 2, 1999	Stratus cloud albedo and cloud BRF. Aerosol recovery over deep water	Marine aerosol for clear sky option	Dark water, coastal sage scrub	AirMISR, RC-10, MAS	Clear sky flights over both deep and near shore water and land targets
Konza Prairie, Kansas, July 11-18, 1999	Grassland BRF	Ambient	First and second year grass canopy after burning, plus other indigenous cover types	AirMISR, RC-10, MAS, SSFR	Completed with associated ground BRF and aerosol measurements
Lake Tahoe, CAlifornia - October 12-21, 1999	Biomass smoke/ ambient aerosol over deep and shallow lake waters	Smoke from prescribed burns and/or ambient	Shallow and deep water, low winds, small waves	AirMISR, RC-10	Completed with ground obs on shore and on lake.

Table 3: Proposed AirMISR Schedule for FY 2000

SITE -DATE	EXPERIMENT TYPE	AEROSOL TYPE	BOUNDARY CONDITION	AIRCRAFT INSTRUMENT	STATUS
Lunar Lake, Nevada - Launch + 2 months	Vicarious calibration of MISR	Ambient	Playa lake surface	AirMISR, RC-10	Planned
Lake Mendota, WI, Feb 15-Mar 9, 2000	Snow and Ice BRF (SOLDE)	Ambient	Snow/Ice	AirMISR, MAS, RC-10,AVIRIS	Planned
ARM-CART - March 5-30, 2000	Cloud and Radiation Expt.	Clouds or Ambient	Grass/fallow fields/ farmlands/snow	AirMISR,MAS,RC-10	Planned
SAFARI-2000, South Africa, Namibia, Botswana, August, 2000	Aerosol sources transport, transformation, sinks, Savannah BRF; Calibration of AirMISR and MISR	Biomass burning, industrial	Savannah, pan surfaces	AirMISR, MAS, RC-10	Planned

Table 4: Proposed AirMISR Schedule For FY 2001

SITE-DATES	EXPERIMENT TYPE	AEROSOL TYPE	BOUNDARY CONDITION	AIRCRAFT INSTRUMENTS	STATUS
Hawaii - January 2001	Clouds/MOBY	Marine, ambient	Deep ocean water	AirMISR, RC-10, MAS	Proposed
Lunar Lake, Nevada, April, 2001	MISR Vicarious Cal.	Ambient	Homogeneous dry playa	AirMISR, MAS, RC-10	Proposed
Dry Tortugas, Florida - May-June, 2001	Saharan dust over ocean	Dust	Marine waters	AirMISR, RC-10	Proposed
San Joaquin Valley, CA; August, 2001	BRF of grasses and broadleaf crops	Ambient	Vegetation canopies	AirMISR, RC-10	Proposed
Lunar Lake, Nevada, Sept., 2001	MISR Vicarious Cal.	Ambient	Homogeneous dry playa	AirMISR, MAS, RC-10	Proposed

Table 5: Tentative AirMISR Schedule for FY2002

SITE-DATES	EXPERIMENT TYPE	AEROSOL TYPE	BOUNDARY CONDITION	AIRCRAFT INSTRUMENTS	STATUS
TBD - February 2002	Scattered cumulus and cirrus	Ambient	TBD	AirMISR, RC-10	Proposed
Lunar Lake, Nevada, April 2002	MISR Vicarious Cal.	Ambient	Homogeneous dry playa	AirMISR, MAS, RC-10	Proposed
Wind River Canopy Crane, Washington - June, 2002	BRF of Old Growth Forest	Ambient	DDV	AirMISR, MAS, RC-10	Proposed
Boardman, Oregon, Potlatch Tree Farm - July, 2002	BRF of broadleaf trees (poplar)	Ambient	Broadleaf	AirMISR, MAS, RC-10	Proposed
Lunar Lake, Nevada, April 2002	MISR Vicarious Cal.	Ambient	Homogeneous dry playa	AirMISR, MAS, RC-10	Proposed

Science Data Validation Plan

Part II: Aerosol/Surface Algorithms and Products

James E. Conel
William C. Ledeboer
Jet Propulsion Laboratory

4. VALIDATION OVERVIEW

4.1 OBJECTIVES

MISR aerosol/surface science data validation is a subsystem of the MISR project. This subsystem is being developed and operated to accomplish the following objectives:

Prelaunch -

(1) Validate selected MISR Level 2 science algorithms.

(2) Demonstrate the ability to make field measurements of radiometric quantities.

(3) Demonstrate the ability to generate aerosol microphysical properties from field optical measurements, and compare such retrievals where possible with direct measurements of similar properties.

(4) Demonstrate the ability to retrieve from ground measurements the bidirectional reflectance function and the hemispherical directional reflectance function in selected target areas

(5) Establish equivalences of retrievals of geophysical parameters between MISR solar radiometer systems and between AERONET network instruments and retrievals such as CIMEL.

(6) .Calculate top-of-atmosphere (TOA) radiances as required for vicarious calibration of the MISR simulator AirMISR and MISR on orbit.

(7) Make field measurements of selected parameters contained in MISR ancillary data sets, for example, aerosol models including: (1) column-effective single scattering albedos and single scattering phase functions, these leading to (2), column equivalent size distributions and complex refractive indices. This will be known as the *augmented* approach, as it combines several observational ground data sets to recover specific aerosol models *[M-7]*, and goes beyond mere recovery of the aerosol spectral optical depth or characterization of size distribution by a single (Angstrom) parameter.

Postlaunch -

(1) Validate selected MISR Level 2 science data products.

(2) Continue to validate MISR Level 2 algorithms as needed.

(3) Produce aerosol size and compositional models from the field data for comparison with assumed MISR ancillary data sets

(4) Deliver TOA radiances to the In-flight Radiometric Calibration and Characterization (IFRCC) subsystem as required for in-flight vicarious calibration.

(5) Intercomparisons of MISR retrievals with established AERONET and ISIS networks of solar radiation instruments.

The MISR science data validation objectives will be accomplished by conducting field experiments coordinated with overflights of airborne instruments and after launch, MISR. Data from the field and aircraft flight experiments will be analyzed both before leaving the field and subsequently at the MISR SCF, to retrieve geophysical parameters via the independent algorithmic pathways available. The pathways represent: (1) retrievals via the conventional as well as modified ground based methods and (2) retrievals via the novel MISR approach involving nine multi-angle observations of a target area carried out in one geometrical plane but at two azimuth angles (in fore and aft view directions) relative to the Sun. In addition all exercises with AirMISR, both pre and postlaunch, will secure observations of the target in four additional azimuths, the principal plane of the Sun, and in a plane bisecting the principal plane of the Sun and the principal plane including the local ground track. These latter tracks will help characterize in a more complete way both the aerosol scattering regime and the surface BRF.

Table 6 summarizes the different experiment types in terms of purpose (across) and type (down) of data collected and compared. As an example of how to read the chart, there are two types of vicarious calibration experiments: one involving MISR and ground-based instruments operated by the MISR team, and one involving MISR and a MISR airborne simulator. These are usually carried out simultaneously in practice. Figure 3 illustrates the primary operations of the Science Data Validation Subsystem from the field experiment activity through production of experiment reports. Different types of experiments will include different subsets of the elements shown, but will follow a similar operational flow.

Table 6: MISR Validation Experiment Measurement Comparisons

EXP. / **MEAS.**	Calibration & Inter-calibration		Airborne Inst. Cal. & TOA Radiance Intercomparison		Algorithm Validation		Product Validation			Vicarious Calibration	
MISR[1]							X	X	X	X	X
Air MISR[2]				X	X	X			X		X
AVIRIS[3]			X								
non-MISR Ground[4]		X				X		X			
MISR Ground[5]	X	X	X	X	X		X			X	

MISR Validation Measurement Types:

1 - Parameters from Level 2 science data products and ancillary data sets.
2 - Parameters retrieved from AirMISR measurements.
3 - Parameters retrieved from AVIRIS measurements including near-TOA upwelling radiances
4 - Parameters retrieved from ground based networks or sites (AERONET, ISIS, ARM) as well as from other instrument teams.
5 - Parameters retrieved from MISR ground based instrument measurements by validation team

MISR Validation Experiment Types:

Calibration and Inter-calibration
Airborne Instrument Calibration
TOA Radiance Intercomparison
Algorithm Validation
Product Validation
Vicarious Calibration

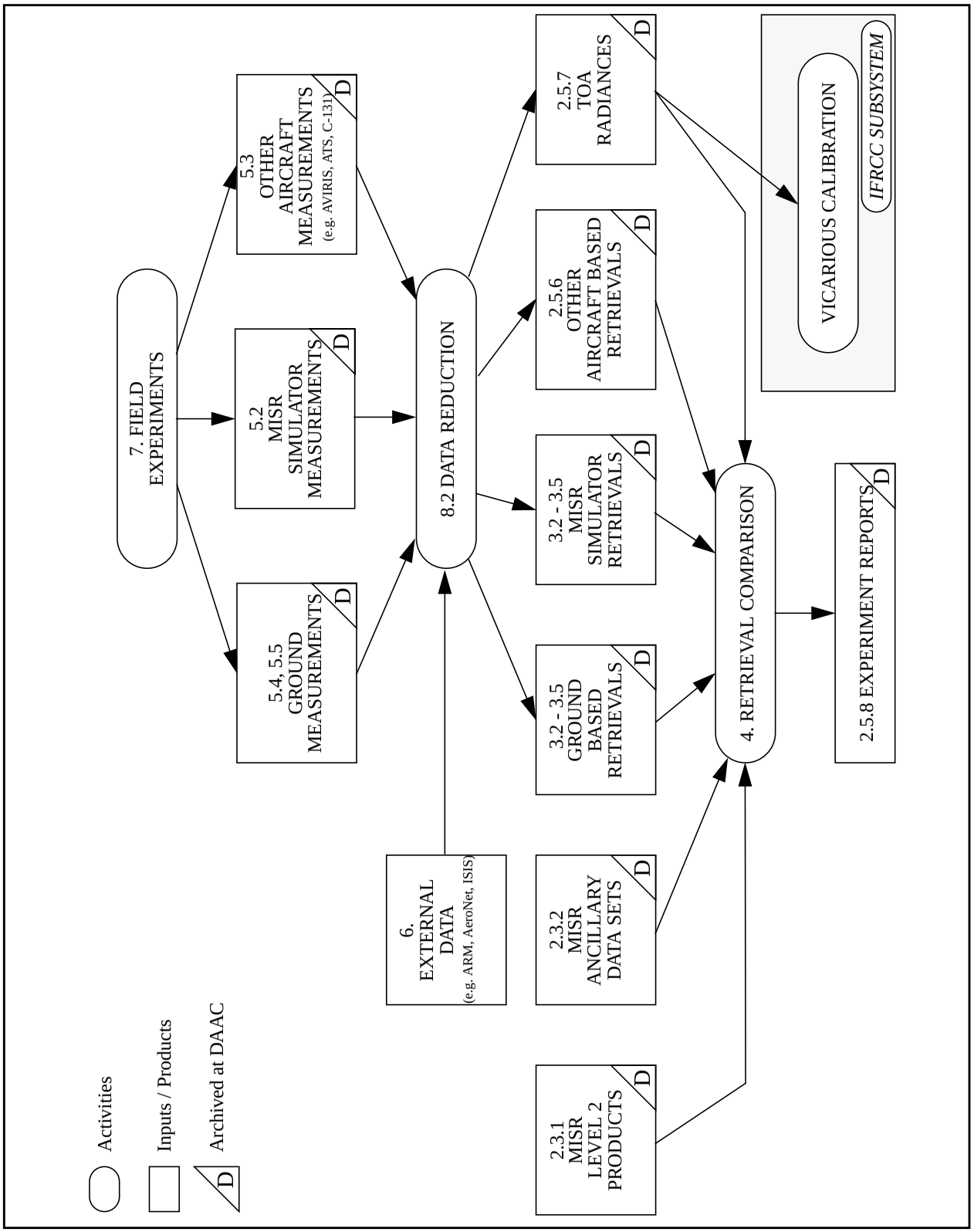

Figure 3: MISR Science Data Validation Subsystem Operation

4.2 APPROACH

4.2.1 Components of the program

General - Algorithm validation components have been alluded to previously, and constitutes a comparison between (a) geophysical products retrieved by applying MISR retrieval algorithms to surface or tropospheric-leaving radiances measured either by MISR simulator instruments or top-of-atmosphere (TOA) radiances measured by MISR with (b) geophysical products retrieved from downwelling sky and direct solar radiation measured at the surface then applying conventional plus augmented retrieval algorithms to such measurements. Both the systematic and random errors in each pathway (*e.g.*, down - looking and up- looking) are evaluated to detect biases in each. In addition to downwelling and surface-reflected radiation components, it will be possible to utilize AirMISR to measure selected upwelling angular radiance components thus securing additional important large scattering phase angle constraints on aerosol scattered radiance

Radiance closure - As an essential part of the validation process, comparisons are also made between: (1) both downwelling and upwelling radiances *calculated* by an atmospheric model using the ground-retrieved geophysical products and (2) downwelling radiances *measured* at the ground and upwelling radiances *measured* by a calibrated MISR simulator at altitude. This provides a radiatively consistent atmospheric and surface model against which MISR multiangle radiances, and associated products, are to be compared. The use of both up and downwelling radiance comparisons in the ground-based part guards against possible sources of bias introduced by factors such as layering of aerosols in the atmosphere. Without use of the upwelling determinations by the simulator (AirMISR), layering ambiguities, where present in highly turbid conditions, may remain. Air MISR observations used to secure large phase angle radiances also provide crucial data for separation of spherical and nonspherical particle scattering models.

The MISR validation program is one of continuing algorithm validation throughout both prelaunch and post-launch time frames. The prelaunch phase certifies the principal mathematical transformations between radiance measurements and geophysical parameters retrieved by MISR. The post-launch phase certifies that the retrieved products agree or disagree with ground-based retrievals, establishes quality control limits for the retrieved parameters by both ground and MISR pathways based on formal analyses of the errors, as well as determination of biases present and offers a basis for improving the algorithms incrementally if this step is needed.

After MISR is in orbit and operational, the Level 2 science data products (available from the DAAC) will be compared with results obtained from concurrent field experiments and aircraft underflights and from comparisons with results accumulated in observational networks.Two types of validation field campaigns aimed specifically at MISR products are planned: (1) stand-alone ground based retrievals of aerosol, surface, or cloud properties, coinciding with MISR orbital overpasses, and (2) ground-based measurement campaigns coinciding with MISR orbital overpasses

and with simultaneous underflights by the AirMISR, (3) A third type of ground measurement campaign may be possible, and is included here for completeness, although not specifically carried out by the MISR Validation Team, *e.g.*, that coinciding with MISR overpasses, simultaneous underflights by the AirMISR and airborne direct aerosol sampling experiments made using independent aircraft. Results of experiments (1), (2), and (3) will also be used to calculate TOA radiances for possible use in MISR (vicarious) calibration. The observational networks and special sites to be used for long-term comparisons thus far consist of the AERONET solar and sky radiometer network and ISIS radiometer (spectral irradiance) networks. Radiometric and other observations from the ARM CART site in Oklahoma and the MFRSR stations at such locations as PSU, will also play an important role. The IMPROVE network designed to monitor horizontal *visibility* in scenic areas of the United States, and including determinations of microphysical aerosol properties, may provide local windows into direct measurements of aerosol properties. This highly desirable type of information will need to be transformed to optical depth before it is of direct use.

4.2.1.1 Included and Excluded Elements in the MISR validation plan

The MISR science data validation program **includes** the following elements:

(1) Gathering together of existing conventional ground-based retrieval (inverse) methods for aerosol abundances and microphysical properties.

(2) Conversion of these conventional retrieval methods to MISR formalism, where necessary (e.g., non-Lambertian reflectance generalized to Bidirectional Reflectance Distribution Function or BRDF).

(3) Development of new software to analyze data for MISR needs specifically: (1), retrieval of BRDF from sphere-scanning radiometer (PARABOLA III) measurements that include contributions of diffuse incident radiation, (2) analysis and software development for combination of CIMEL, MFRSR, PARABOLA III, REAGAN observations to provide separations of aerosol scattering parameters, e.g., single scattering albedo, single scattering phase function, size distribution and composition (complex refractive index)

(4) Procurement and adaptation/modification of essential field instruments for direct solar, diffuse sky and ground-reflected radiation measurements to implement retrievals.

(5) Organization of field campaigns at selected land surface and ocean targets encompassing essential parts of the MISR aerosol climatology and surface reflectance types.

(6) Organization of coordinated measurement campaigns on the ground with MISR simulator overflights.

(7) Routine laboratory and field calibration of the field instruments.

(8) Special field experiments aimed at acquisition of local network measurements for determination of averaging and (optimal) interpolation procedures

(9) In-flight characterization (calibration/noise measurement) of the MISR aircraft simulators using ground targets and the reflectance-based vicarious method, both to study and augment calibration of the simulators for possible use in radiance-based calibration of MISR itself.

(10) Development and use of differential GPS techniques for accurate (1 m) location of surface targets.

(11) Development of procedures and algorithms for automated rectification and registration of MISR-simulator multi-angle scenes that are suitable for application of the MISR data reduction algorithms. These are to use Global Positioning (GPS) and Inertial Navigation System (INS) data on aircraft geographic location and spatial orientation gathered during a mission.

(12) Implementation of parameter retrievals based on MISR algorithms using the calibrated rectified and registered aircraft simulator data.

(13) Intercomparison campaigns with other EOS-related validation field programs including vicarious calibration (TOA radiance) intercomparisons and network or local observations (AERONET, ISIS, SGP ARM).

(14) Carrying out of field experiments

(15) Specific evaluation of the sensitivity of MISR aircraft simulator and field instrument capability to validate MISR algorithms consistent with the demonstrated sensitivity of each MISR surface and aerosol retrieval strategy

(16) Implementation of retrievals based on MISR algorithms using the calibrated aircraft simulator data

(17) Comparisons of ground-based and simulator -based results and analysis of errors and biases

(18) Intercomparison campaigns with other EOS-related validation field programs (SCAR-C) and network or local observations (AERONET, ISIS, ARM site, Oklahoma).

(19) Postlaunch product validations using aircraft simulator underflights, field campaigns, retrievals from other EOS sensors at particular sites.

(20) Postlaunch sub-grid point determinations of aerosols, ozone, water vapor abundances, RH determinations for comparison with MISR assumed values. Such campaigns may be carried out at stations such as AERONET where other standard measurements are carried out (*e.g.*, Dobson or Brewer Spectrometer observations of ozone column abundances).

At present the aerosol and surface reflectance program **excludes** validation of:

(1) Ocean surface BRDF descriptions, Cox-Munk wave facet model, foam and white-cap models

(2) Cloud masks as well as TOA cloud albedo, RLRA and azimuthal model studies. These properly belong under the Cloud Validation Activity, Part II of the present plan

(3) Assumptions of the MISR aerosol climatology and the climatology itself excepting comparisons resulting directly from full field measurement campaigns.

(4) SMART Dataset entries excepting comparisons resulting directly from field measurement campaigns where full radiatively consistent models are derived from the MISR ground validation activity

(5) Other ancillary data sets used in the MISR retrievals excepting comparisons resulting directly from field measurement campaigns.

(6) Calibration or validation exercises that may be required for other EOS or specific satellite sensors (*e.g.*, MODIS, ASTER, POLDER, ATSR-2, or MSX).

(7) Validation of data assimilation areal-average predictions of the water vapor distribution by weather models used for RH determinations. We simply plan to make local measurements and compare with MISR input values.

(8) At launch, retrievals of LAI and fAPAR for vegetation canopies

(9) At launch, retrievals over bright homogeneous targets such as snow and ice. However continuing efforts to secure algorithm validation sets in conjunction AirMISR will be carried out in the postlaunch time frame.

See Part III: TOA/Cloud Algorithms and Products for a discussion of some of these points.

4.2.2 Approaches to aerosol product validation

The aerosol and related geophysical parameters are summarized in Chapter 5, Table 9.

Two main approaches to algorithm and product validation are possible: (1) field experiments of short duration at specific sites that seek to isolate aerosols of given characteristics cast against chosen surface reflectance backgrounds, and (2) long term comparisons of ensemble averages of aerosol optical depth and properties gathered at permanent maintained installations instrumented as to make measurements automatically over time. These latter intercomparisons will carry the statistical strength of large numbers of observations from both ground-based and MISR-derived pathways. A third approach that will evolve is thorough knowledge of sources of error in the ground-based measurements and methods of data reduction.

Pre-launch algorithm validation objectives will be accomplished by conducting field experiments involving ground-based measurement campaigns coordinated precisely with overflights of aircraft-borne MISR simulator instruments *e.g.*, AirMISR. Such experiments will be carried in a limited time frame seeking clear weather and uniform, stable atmospheric conditions and homogeneous or inhomogeneous surface targets to maximize probability that physical conditions under which the algorithms being tested are proper. The aerosol evaluations will be done at the local scale as evaluated from time series data on aerosol optical depth at ground stations and spatial variability as evaluated from scatter in AirMISR retrievals.

In postlaunch time, radiance data from the MISR instrument itself and the derived geophysical parameters obtained via the MISR pathway, are of principal interest. The aerosol validation data sets now expand to include: (1) those acquired from AirMISR underflights and field campaigns at a small number of specific sites and times. These include local measures of a radiatively consistent aerosol model plus ground BRF data, (2) time series of observations from the extensive AERONET and ISIS ground network stations. The long term properties returned from (1) include aerosol optical depths and aerosol microphysical properties (local aerosol climatologies), and from (2) the surface spectral diffuse and direct irradiance. Validation of the MISR aerosol products and ancillary data will thus compare statistical distributions from ground-based retrieval and retrievals for a site acquired from multiple MISR overpasses. The issue of horizontal scale for application of data from any CIMEL or ISIS station needs to be evaluated on a case-by-case basis. The present world-wide distribution of AERONET stations, both permanent installations and seasonal, is shown in Appendix A, Figure 1. The present distribution of SURFRAD stations with MFRSR instruments is also shown in Appendix A, Figure 2, along with the continuous ARM-CART site and intermittent MISR-JPL station.

In pre-launch and in post-launch time comparisons between time series values at selected network stations and retrievals based on AirMISR measurements will also be carried out to test the feasibility of the intercomparison approach. One such site will constitute a MISR Local Mode site established at Jet Propulsion Laboratory. The JPL AERONET station data for this specific location will be downloaded locally and passed through the MISR retrieval pathway as opposed to the Goddard AERONET pathway.

An important issue already alluded to for aerosol validation in both pre and post launch time frames is that of scale. MISR seeks to report aerosol products at the scale of 17.6 km, whereas field experiment data and automatic station data pertain instantaneously to a scale of a few km. There are three possible ways in which the scaling-up issue may be approached: (1) use local networks of ground stations, interpolating and or averaging the results, (2) use AirMISR to supply larger scale footprint data (~ 10 km) validating locally the MISR-like retrievals from AirMISR using ground data, then averaging to the 10 km scale, (3) use time series retrievals from single ground stations, averaging over time as a measure of the spatial variation (Taylor-like hypothesis). Methods (2) and (3) will be carried out at selected sites. Method (1) will be employed wherever local networks can be established. These network applications will be limited because of fiscal constraints and availability of instruments.

4.2.3 Validation of MISR-calculated surface irradiance

Downwelling flux at surface (irradiance) and upwelling flux (radiant exitance). These are calculated for a site from the MISR-retrieved aerosol properties using a radiative transfer model during the MISR reductions. These are termed here intermediate radiation quantities since they are calculated in process of obtaining surface HDRF and BRF and BHR. These quantities are sum-

marized in Chapter 4, Table 8. Validation of the intermediate quantities is simply direct comparison of the MISR-calculated quantity at a maximum resolution of 275 m, and its direct measurement at a local site. The local sites will consist of local-mode MISR retrievals at pixel size (order of 250 m) These measurements may be carried out in cooperation with other groups using a local networks of stations involving MFRSR instruments to provide a local spatial average of incident irradiance. The MFRSR instruments will also operate as part of the NOAA ISIS network. The ISIS stations are widely separated geographically. Long time series measurements of incident spectral irradiance and radiant exitance are available from one collocated pair of MFRSR (diffuse-direct) radiometers at one tower location at the SGP ARM site and at stations forming SURFRAD that focus on surface radiation balance. The irradiance measurements described will also be used for long-term statistical comparisons of surface and MISR retrievals. A Local Mode MISR site at Jet Propulsion Laboratory will provide a time series of downwelling diffuse and direct irradiance measurements as well as optical depth with the MFRSR. Optical depths are retrieved from global and diffuse irradiance measurements as described in *[26]* and *[27]*. The present distribution of SURFRAD stations with MFRSR instruments is also shown in Appendix A, Figure 2, along with the continuous measurement ARM-CART site and intermittent MISR-JPL station.

4.2.4 Validation of Bidirectional Reflectance Factor (BRF) and related quantities

The BRF and related quantities are summarized in Chapter 5, Table 9. PARABOLA III measurements are taken as the basis for ground-based BRF retrieval, the calculation of HDRF and BHR and the validation of all three quantities. The simplest strategy is direct comparison between the BRF/HDRF derived from the multi-angle measurements of AirMISR for a site with surface and sky radiance measurements of the same site supplied by PARABOLA III. The BRF is obtained from AirMISR and MISR measurements by the use of parameterized BRF models (in particular the Martonchik-Raman-Pinty-Verstraete (MRPV) three parameter model). The MRPV model evaluations will be compared to BRF determinations directly from PARABOLA III measurements. The BRF is obtained from PARABOLA III data by solution of the fundamental integral equation describing reflection of diffuse and direct incident light at the surface. The BRF data obtained from the ground will also be fitted to the MRPV model for comparison of the parametric fits and evaluation of uncertainties. In particular experience has proved that the integral equation approach is most successfully applied to data from smooth targets (such as dry playas, possibly grassy cover), whereas a model fitting procedure can best be applied to inhomogeneous terrain such as scrublands.

An important issue for the BRF comparison is expansion of local ground measurements to the 1.1 km scale reported by MISR. PARABOLA can deliver observations detailed surface observations at angular FOV of 5° over surface areas up to a few hundred meters in diameter. Local direct comparisons are therefore possible at the Local Mode scale of MISR pixels. Some simple scaling methods involving use of normal incidence HDRF measurements made with a portable (ASD) spectrometer are being investigated to help extrapolate PARABOLA measurements to larg-

er scale. This should be successful if the normal incidence HDRF is largely independent of surface albedo. Extrapolations to 1.1 km will also be carried out using AirMISR, evaluating the local comparisons at AirMISR resolution with PARABOLA.

Seasonal measurements of BRF at selected vegetation sites will be attempted to help support investigations of retrievals of seasonally dependent biophysical variables (LAI, FPAR, NDVI, water content, ground reflectance).

Long time series of surface properties that range over seasons between MISR and ground measurement with PARABOLA III type instruments will be limited. The present BRF validation strategy focuses on intermittent measurements at specific sites, possibly implemented with towers or cherry-pickers, to get above tall canopy structures of large (tall) stature. BOREAS (see *[72]*) is one such experiment site that has been used over deciduous and needle forests. That site can be occupied intermittently over the years as resources permit. A crane facility is now operational over old growth needle forest in Wind River Forest, Washington, which can be used for both above- and within canopy studies down to ground level. Additional tower facilities may be built for ecosystem and other EOS validation activities as part of an EOS-wide test site validation program *[81]* but these sites have yet to be defined or constructed. These facilities will be utilized as they become available and/or aircraft and field exercises permit.

4.3 INPUTS

4.3.1 MISR Level 2 Products

For actual validation experiments, Level 2 Aerosol/Surface *[M-4], [M-5]* and TOA/Cloud *[M-2], [M-3]* products will be imported for comparison with ground and MISR simulator based retrievals. These products both at local mode and full MISR scale, will be selected based on their space and time correlation with field experiments and observations made by network instruments. Data will be selected and ordered using the ECS Client software, which provides the user interface to EOSDIS.

In addition to the Global Mode data from standard products generated at the DAAC, Local Mode products produced at the MISR SCF will also be compared to the validation products.

4.3.2 Ancillary Data Sets

ACP, TASC and SMART *[M-6]* data sets, available at the SCF, will be utilized in comparisons of ground and MISR or MISR simulator based retrievals.

4.3.3 External Data

While most of the MISR field experiment types shown in Table 6 are capable of providing

local validations of MISR geophysical parameters, we will take advantage of other, non-MISR, sources of field data in both the prelaunch and postlaunch validation phases. These sources include the ARM, AERONET and ISIS instrument networks. Additional stations from other long-established networks and data sources compiled from them (*e.g.*, the Global Energy Balance Archive, GEBA, *[60], [59]* and IMPROVE network *[17], [47], [48]* will also be employed. These all apply principally to the post-launch era.

4.4 ACTIVITIES

4.4.1 Field Experiments

Field validation campaigns for MISR involve coordinated ground-based measurements of atmospheric, aerosol optical and surface reflectance properties at selected field targets, combined with overflights of AirMISR. The field measurement campaigns and timing correspond to geographic locations where aerosols and surface reflectance conditions most relevant to MISR climatologies are likely to be found. The ground-based optical measurements are used to characterize radiatively and derive the aerosol model before, during and after the time of overflight. Ground measurements of the full downwelling sky and upwelling surface directional radiances are made for calculation of target bidirectional reflectance factors. These are carried out with the specially constructed sphere-scanning radiometer (PARABOLA III). Ground-based measurements of downwelling spectral irradiance are performed using a single MFRSR instrument. These measurements are used for comparison of the spectral irradiances calculated from a radiative transfer code as part of the ground-based portion of radiative closure experiments and also as part of the MISR surface/aerosol retrieval.

The aircraft simulator (AirMISR) performs multi-angle multi-azimuth passes over the target area, the first pass coinciding in time and direction with the local expected MISR ground track and sun angle, and subsequent passes, six in all, in six azimuths that characterize the emergent radiance in the nine MISR view directions and four wavelengths. The additional passes are in the solar principal plane and approximately normal to that plane. The additional passes help characterize both aerosol scattering properties over an increased range of scattering angles, and the ground reflectance over additional azimuth directions relative to Sun incidence direction. A complete field exercise with the simulator includes a vicarious ground-based calibration of the simulator in-flight (as opposed to the laboratory calibration), although for reasons of logistics and timing, may be carried out on separate days.

Simultaneous direct aerosol sampling from ground and by aircraft perhaps along vertical profiles are desirable if available in order to extract connections between remotely determined quantities and directly measured ones. But for reasons of fiscal and manpower constraints are not the primary focus of the aerosol validation program. Collocation of ground stations making direct aerosol scattering, size, and chemistry measurements will be sought when possible. such a net-

work, the IMPROVE network, has been mentioned. Direct aerosol sampling by aircraft throughout the atmospheric column are thought to be the best way to characterize the aerosols present. Local measures with lidars may be carried out, especially at JPL and at ARM, sites where these instruments operate on a regular basis.

While most measurements needed for constraint of experimental conditions locally are made routinely as part of field campaigns, additional important observations will be imported as available, for example:

(1) Ground-based scattering measurements by nephelometry or chemistry and size from Air Quality Management labs or individual investigators

(2) Aircraft data on direct aerosol measurements

(3) Lidar measurements on backscatter coefficients and vertical structure of aerosol loading

(4) Nephelometer measurements of aerosols at the surface

(5) Ocean mooring data on wind speed, direction and wave characteristics

(6) Downwelling / upwelling water spectral radiance measurements

(7) Weather records and air mass trajectories,

(8) Radiosonde profiles of moisture and temperature

(9) Calibration, dark current, vignetting correction files from ASAS or AirMISR laboratory calibrations.

4.4.2 Algorithm and Software Development

Except where noted, well-tested conventional ground-based algorithms will be used to retrieve MISR geophysical parameters from surface measurements made in the field. These algorithms are fully described in *[M-7]*, including modifications that form the augmented aerosol/surface retrieval procedures. Parameter retrieval from MISR simulator measurements and MISR itself will be performed using the Level 2 Aerosol/Surface algorithms.

Software and procedures will be developed that implement the conventional and MISR algorithms and that create the products needed to compare and evaluate various retrieved MISR parameters. An incremental approach is being used to developing the validation software. This approach allows new and existing field campaign data to be reduced even while the system is being developed.

The purpose of the validation software is to provide a complete, integrated tool for processing field experiment measurements, measurements from network sites, and MISR simulator measurements, and generating the corresponding validation parameter subsets. This processing will in-

corporate external data and assumptions as specified in the SRD *[M-9]* reflecting the relevant ATBs. The software will facilitate comparison and evaluation of the generated parameter subsets.

Many of the algorithms used in MISR validation are tested and verified through the implementation of prototype codes. Most of the retrievals done from ground-based instruments are currently performed with these codes as follows:

Table 7: Ground-based Instrument Retrieval Codes

Instrument	Retrievals
Reagan	Aerosol optical depth
MFRSR	Diffuse-to-direct irradiance ratio
CIMEL	Almucantar and principal plane radiances
PARABOLA III	Surface reflectance BRDF
ASD	Surface reflectance spatially averaged over flight sensor

The MISR validation team will make use of a multi-instrument approach in order to provide for the retrieval of aerosol and land surface products, and top-of-atmosphere radiances, as derived from in-situ instruments. Figure 4 depicts these instruments (shown with rectangular boxes with rounded edges), output products (square boxes), and processing flow (codes are depicted with ovals). Going from the lower left corner of the figure, we can describe each of these elements in turn:

Figure 4: Multi-Instrument Approach

(1) A sun-tracking radiometer ("sunphotometer") provides for the optical depth components, including the aerosol optical depth, as a function of time-of-day. The Reagan instrument is our baseline sunphotometer. If there is an aircraft of satellite overpass, we extract the components measured at that time of day.

(2) We make use of a the ASD field-portable moderate resolution spectroradiometer to provide a measure of the surface BRF for a nadir-view angle. Data are spatially averaged over a ground footprint equivalent to the spatial scale of interest - i.e. the sensor to be validated or calibrated.

(3) The PARABOLA III relative surface BRF data are applied to the ASD retrievals. These extend our surface reflectance inputs to the MISR or AirMISR view angles.

(4) The CIMEL and MFRSR sky-viewing radiometers are used to define the aerosol properties se.g., the effective column single scatter albedo and scattering phase function. The radial size distribution functions and complex refractive index are adjusted and input into a MIE and radiative transfer codes. An aerosol model is established when agreement between the measurements and code output radiance and irradiance is found.

(5) Once this type of radiative closure is obtained, *e.g.*, between the code outputs and measurements, an aerosol model, surface reflectance function, and top-of-atmosphere radiances are delivered as data products which result from the experiment.

Development phases for the validation product generation system include requirements analysis, system design, prototyping/implementation, testing, documentation and maintenance. Functional requirements are derived from the algorithms defined in the Science Data Validation ATB *[M-7]*. Data products are created in Hierarchical Data Format (HDF) and will be archived at the Distributed Active Archive Center (DAAC) at Langley Research Center (LaRC). The system also produces full, browse and thumbnail size Graphical Interchange Format (GIF) images.

Materials that will be delivered from the Software Development Engineer to the validation team include the following:

(1) Machine-readable source code listing, with embedded comments, for all programs, scripts, and program building.

(2) Automated procedures to compile, link and execute the programs.

(3) Module architecture description, expressed in the form of data flow diagrams (DFD's) and structure charts.

(4) A description of the mapping of code units into the major transformational steps specified in the ATB. For large or complex units, a second-level DFD showing processing steps is desirable.

(5) A description of the development environment, e.g., machine type, operating system and version, and programming languages.

(6) Software User Guide indicating how to set up and operate the software.

(7) Test data and procedures.

4.4.3 Data Reduction

Data reduction begins when raw instrument data arrives at the MISR SCF. These data are stored in a dedicated area known as the MISR Validation Data Archive. Raw data typically requires interactive filtering and/or formatting prior to use by retrieval codes. Filtering includes exclusion of data during periods where clouds or other obstructions blocked an instrument aperture and separation of calibration and data points. Reformatting of data is currently required due to differences between the PC-based programs which do the data acquisition from the instruments and the UNIX codes used for data reduction.

Validation parameters are currently retrieved using separate codes for each field instrument. An integrated retrieval method is under development using an iterative technique which will perform ground-based Level 1 and Level 2 retrievals simultaneously.

4.4.4 Retrieval Comparison

These retrievals must be compared and evaluated against several criteria (e.g. results of error analysis) to determine if the validation was successful or to identify the cause of the discrepancy.

4.5 OUTPUTS

As indicated in Figure 2, several outputs from the validation process will be archived at the DAAC including ground and aircraft measurements, ground based retrievals, MISR simulator retrievals, TOA radiances, other aircraft based retrievals and experiment reports. These outputs will be aggregated into various products described in *[M-8]*.

4.5.1 Ground and Aircraft Measurements

Raw data from ground and aircraft instrument measurements constitutes an intermediate output of each field experiment. These data fall in three major categories.

(1) **Ground measurements -** Solar, sky and ground spectral radiances (Reagans, MFRSR, CIMEL, PARABOLA III, GER, ASD), meteorological data, nephelometry, direct aerosol sampling

(2) **MISR simulator measurements -** Multi-angle spectral images (AirMISR).

(3) **Other aircraft measurements -** Spectral atmospheric extinction (ATS), meteorology, aerosol/cloud properties, radiometry (C-131A), aerial photographs (RC-10), nadir-viewing spectral images (AVIRIS).

4.5.2 Ground-based Retrievals

Measurements by the ground based instruments using will be reduced using conventional algorithms to determine the following parameters:

(1) **Reagan sunphotometers:** aerosol spectral optical depth, ozone optical depth, column abundance of water

(2) **MFRSR:** imaginary part of the aerosol refractive index and an average Lambertian surface reflectance. Also used to provide separate local spectral irradiance and radiant exitance observations for estimates of local spectral BHR.

(3) **CIMEL:** aerosol spectral optical depth, aerosol scattering and absorption properties

(4) **PARABOLA III:** hemispherical directional reflectance factor (HDRF)bidirectional reflectance factor (BRF), hemispherical directional reflectance (HDR) and bihemispherical reflectance (BHR)

(5) **GER:** spectral bidirectional reflectance and atmospheric transmittance

(6) **ASD:** average reflectances of large natural target areas

(7) **Albedometer**: the albedometer provides total surface irradiance and radiant exitance for separate evaluation or for calculation of local BHR (albedo). AirMISR retrievals

MISR algorithms will be used to retrieve the following parameters from flight instrument and simulator (**AirMISR**) data products: aerosol optical depth, hemispherical-directional reflectance factor (HDRF), bihemispherical reflectance (BHR), bidirectional reflectance factor (BRF), directional hemispherical reflectance(DHR), PAR - integrated BHR and DHR and reflecting level reference altitude (RLRA).

4.5.3 Other Aircraft Based Retrievals

Measurements by other airborne instruments will be used to determine the following parameters:

(1) **AVIRIS:** multispectral images and near TOA calibrated radiance measurements.

4.5.4 TOA Radiances

Vicarious calibration of both AirMISR as well as the MISR instrument itself require respectively near TOA (top of atmosphere) or TOA radiances. These can be calculated using an RTC employing the following methods and independent field measurements:

Method I: Regular reflectance based

(1) Surface reflectance measurements via PARABOLA III and ASD

(2) Measurements using CIMEL, REAGAN, and MFRSR to secure aerosol abundance together with absorption/scattering (single scattering, phase function) model

(3) Use RTC to calculate TOA radiances with (1) and (2)

Alternatively the radiative transfer code is solved for TOA radiance from:

Method II: Radiance propagation method

(4) Measurements using CIMEL, REAGAN, and MFRSR to secure aerosol abundance together with absorption/scattering (single scattering, phase function) model

(5) Direct measurement of surface-leaving radiance at all exit and azimuth angles using PARABOLA III

AirMISR aboard the ER-2 flies at an altitude of 20 km, close to but not at TOA. The standard RTC employed for all ground-based retrieval work, has been modified to calculate within atmosphere AirMISR upwelling radiance.

Validation field campaigns will make the necessary field measurements to provide as inputs to the RTC which will be used to calculate within atmosphere as well as directional TOA radiances. These radiances are supplied to the IFRCC subsystem for use in vicarious calibration.

The second method named here the radiance propagation method will employ ground leaving radiances measured by PARABOLA. These surface leaving radiances are propagated through the atmosphere using the RTC and the derived atmospheric model. This step bypasses the need to calculate surface BRF, hence replaces a derived (BRF) with a measured (surface leaving radiance) quantity in the model. This method places the burden of accurate radiometric calibration on the PARABOLA instrument.

Method III: Radiance-based

(6) An alternative to use of a radiative transfer code and field measurements of the atmosphere and surface, is the so-called radiance-based method which involves direct measurement of the upwelling TOA (or near TOA) radiance by a well-calibrated spectral radiometer operating from an aircraft platform close to the top of the atmosphere. Two such instruments will be employed for radiance-based calibration of MISR, namely AirMISR and AVIRIS. This places the burden of accurate radiance measurement on AirMISR. This issue continues to be the subject of investigation. At issue is the radiometric stability of AirMISR in flight compared to laboratory calibrations, plus state of knowledge of aircraft and instrument orientation, airspeed, flight altitude, in short not only radiometric calibration, but also the head scanning rate and geometry. When verified, these radiances are also supplied to the IFRCC subsystem for use in vicarious calibration.

4.5.5 Experiment Reports

Each experiment will be documented in an experiment (or campaign) report which will be archived at the DAAC along with other validation outputs. The report will include:

(1) Experiment objectives

(2) Site selection criteria and descriptions

(3) Ground based instrumentation used

(4) Aircraft instrumentation employed, Description of measurements, including MISR data if applicable, calibration data.

(5) Results, including description of parameter retrievals

(6) Conclusions, including results of retrieval comparisons

4.5.6 Peer Reviewed Publications

Results and conclusions from these experiments will be published in the open literature.

4.6 SCHEDULE

The schedule for MISR aerosol/surface validation activities is shown in Table 8 in terms of several categories of milestones and the time periods in which they will be achieved.

Table 8: Aerosol/Surface Validation Algorithm, Software Milestones and Instrument Issues

Prelaunch (1/94 to 12/99)	On-orbit Check-out &Postlaunch (12/99 to 6/05)
Algorithms 1) Langley method for aerosol optical depth retrieval from Reagan sunphotometers and MFRSR 2) Size inversion on extinction. Obtain code from King 3) Field and laboratory calibrations of sunphotometers, PARABOLA III 4) Ozone, water vapor retrievals, validation with independent data sets such as CAPMON (ozone) and/or MARK IV (water vapor) 5) Intercalibration of instruments at periodic field intercomparisons 6) Develop methods for retrieving phase function and complex index of refraction from CIMEL, MFRSR, and other measurements 7) Implement methods for retrieving albedo and complex index of refraction from MFRSR measurements, e.g., diffuse-direct method *[41]* 8) Develop methods for calibrating PARABOLA III and editing data 9) Implement diffuse light corrections to BRF 10) TOA radiances via radiance propagation method 11) Combined extinction and aureole inversions 12) Combined CIMEL, Reagan, MFRSR analysis to get aerosol parameters, complete closure process 13) Implement local download of CIMEL data for JPL algorithm processing 14) Implement radiance/irradiance comparisons with MFRSR and ISIS results 15) Implement CIMEL intercomparisons at AERONET stations and/or reduce CIMEL data by JPL and Goddard pathways	

Table 8: Aerosol/Surface Validation Algorithm, Software Milestones and Instrument Issues

Prelaunch (1/94 to 12/99)	On-orbit Check-out &Postlaunch (12/99 to 6/05)
Software 1) Code for retrieval of optical depth from Reagan sunphotometer measurements 2) Code for retrieval of optical depth from MFRSR measurements using Langley algorithm 3) GER code for retrieval of moderate resolution spectral optical depth 4) ASD code for retrieval of field spectra, interpolated standard method 5) Size inversion, spectral (King) 6) Diffuse light correction for PARABOLA (Martonchik method) 7) Development of PARABOLA III calibration, editing and data reduction code. 8) Adapt MRPV model to PARABOLA III data for inhomogeneous terrain 9) Adaptation of RTC for TOA radiance calculations via three methods of Section **4.5.4**. 10) Adaptation of CIMEL data reduction code (from T. Nakajima) for MISR use. 11) Design and development of prototype integrated data reduction/analysis system 12) Combined extinction, aureole and TOA radiance/irradiance inversions 13) Combined CIMEL, Reagan, MFRSR analysis for best fit aerosol parameters 14) Closure analyses of BRF together with aerosols for simulations and for selected field data sets. 15) Turnkey systems in place for aerosols, surface, TOA/cloud, TOA radiances	

Table 8: Aerosol/Surface Validation Algorithm, Software Milestones and Instrument Issues

Prelaunch (1/94 to 12/99)	On-orbit Check-out &Postlaunch (12/99 to 6/05)
Instruments	
1) Auto-tracking Reagan sunphotometers (2) 2) Manual Reagan sunphotometers (2) 3) MFRSR (1) 4) CIMEL (1) 5) Dual ground based camera system (Nikons with data backs and fisheye lenses) 6) Acquisition of PARABOLA III, calibration and adaptation for MISR use. 7) Design and construction of stabilized marine mounting platform for instruments 8) Construct high mount to increase PARABOLA III surface footprint	1) Maintain calibrations/intercomparisons of all instruments 2) Augment instrument arrays to define small scale networks, e.g., REAGAN and MFRSR
Field Experiments	
1) EOS Intercalibration at Lunar Lake 2) AirMISR vicarious calibration at Roger's Lake 3) Various algorithm validation exercises on aerosol, surface geophysical products 4) Survey and location of additional field targets, continuous effort through period 5) Establish local mode sites for post launch validation exercises covering BRF localities with connections to LAI FAPAR, model studies, AERONET stations for optical depth, SURFRAD (ISIS) stations for spectral irradiance	1) MISR vicarious calibration at Lunar Lake 2) Aerosol optical depth intercomparisons with AERONET stations 3) Surface irradiance intercomparisons with SURFRAD MFRSR stations 4) BRF intercomparisons at calibration and vegetation canopy sites 5) Pacific Northwest (smoke, conifer forest BRF, broadleaf BRF) 6) Monterey (marine aerosol) 7) Lake Tahoe (ambient aerosol over shallow and deep lake waters) 8) L.A. Basin (aerosol/BRF climatology/chemistry/size) 9) San Nicholas (BRF, marine aerosol climatology) 10) Intercalibration at AERONET, ISIS sites 11) Lunar Lake (calibration/BRF) 12) Cooperative experiments with EOS groups 13) Maintain MISR field instrument and AirMISR calibrations 14) Troubleshoot any MISR calibration or retrieval disagreements

Table 8: Aerosol/Surface Validation Algorithm, Software Milestones and Instrument Issues

Prelaunch (1/94 to 12/99)	On-orbit Check-out &Postlaunch (12/99 to 6/05)
Procedures 1) Concepts for parameter retrieval comparison and analysis 2) Identify sources of ground based radiometric network data 3) Concepts for error analysis 4) Develop methods for comparing MISR, aircraft and ground based parameter retrievals 5) Develop methods for accessing ground based radiometric network data 6) Develop methods for accessing simulated MISR data and ancillary data sets 7) Complete testing of retrieval comparison procedures using field data and simulated MISR instrument data 8) Identify local mode aerosol (AERONET), radiation (ISIS) and BRF (TBD) sites for long term analysis	
Documentation 1) Science Data Validation Plan 2) Science Data Validation Plan, Rev. A 3) Science Data Validation Plan, Rev. B 4) Science Data Validation Plan, Rev. A 5) Software Requirements Document 6) Software Design Document 7) Science Data Validation ATB 8) Open literature publications on calibration and algorithm validation exercises 9) Intercomparison studies at high altitude sites 10) Ozone column abundance retrieval validation by comparisons with surface Brewer spectrometry at CAPMON stations 11) Software User's Guide 12) Water vapor retrieval validation with interferometry	1) Science Data Validation Plan, Rev. C and beyond as warranted 2) Open literature on combined CIMEL, Reagan, MFRSR plus sensitivity study on albedo and refractive index retrievals 3) PARABOLA III Instrument description and calibration 4) VIcarious calibration of AirMISR 5) Vicarious calibration and updates of MISR 6) Intercomparisons of MISR aerosol and BRF retrievals 7) Statistical tests using AERONET and other field results of MISR natural mixtures as deduced from Climelikely and SMART analyses for land and oceans

5. VALIDATION RETRIEVALS

5.1 VALIDATION ALGORITHM THEORETICAL BASIS DOCUMENT

The purpose of the Science Data Validation ATBD *[M-7]*, a document separate from the present Plan, is to provide a specification of the science/physics and mathematical formulas involved in converting instrument measurements into data sets that provide specific parameters, or that can be used for further processing such as the RTC. The document is restricted to consideration of *aerosol and surface* parameters, except for cloud height, speed, and cloud motion direction that can be dealt with by simple photographic/stereoscopic methods. Other closely-related MISR ATBD's are listed in Section 1.4.

The Science Data Validation ATBD provides:

(1) A description of the validation concept

(2) A formal documentation of the data, algorithms, and software used in the validation process

(3) A document by which the algorithms can be reviewed, e.g., by the EOS Science Peer Review Board

The Science Data Validation ATB also contains:

(1) A brief characterization of the validation strategy, including references to other works.

(2) A description of the validation products relevant to (i) the surface/aerosol models, (ii) the vicarious calibration of AirMISR and MISR, and (II) MISR data product validation.

(3) A description of the input data, namely those data required from MISR, AirMISR, field instruments, together with ancillary data sets.

(4) A discussion of the instrument characteristics and Level 1 processing of the input data, where appropriate.

(5) The theoretical basis for algorithms used in deriving validation products, including assumptions, limitations, caveats.

(6) A description of the software implementation for validation algorithms, including limitations,

(7) A description of steps that will be taken to assess errors in recovered surface/ aerosol models, and how such errors are accounted for in product validation data products for AirMISR and MISR.

Table 9: Radiometric Quantities Calculated At Surface During MISR Retrievals And Measured In Field

Parameter Recovered as Part of MISR Retrieval	Field Instruments	Field Method of Recovery
MISR-CALCULATED SPECTRAL IRRADIANCE AND RADIANT EXITANCE		
Direct Solar Irradiance	Reagan, CIMEL, MFRSR, PARABOLA III	For sunphotometers and PARABOLA III, time-dependent direct measurement. For MFRSR, derived from total irradiance using measured diffuse sky component
Total Spectral Irradiance	MFRSR	Time-dependent direct measurement with unshadowed instrument
Diffuse Solar Irradiance	MFRSR, PARABOLA III	Time-dependent direct measurement. With MFRSR, separated from total irradiance using measurements with sun shadowed. With PARABOLA III, estimated by integration over upward hemisphere excluding pixels with direct sun
Radiant exitance	PARABOLA III, Kipp and Zonen albedometer	Time-dependent direct measurements. Determination from PARABOLA III requires integration of measured surface-reflected radiances over downward hemisphere. Upper and lower hemisphere wavelength integrated value with albedometer
SPECTRAL MULTIANGLE RADIANCES		
Downwelling Multiangle Radiances (surface incident radiance)	PARABOLA III, CIMEL	PARABOLA III and CIMEL measurements, calculation of downwelling radiance at surface including multiple reflections with atmosphere from MISR-retrieved aerosol and surface models

Table 9: Radiometric Quantities Calculated At Surface During MISR Retrievals And Measured In Field

Parameter Recovered as Part of MISR Retrieval	Field Instruments	Field Method of Recovery
Upwelling Multiangle Radiances (surface leaving radiance)	PARABOLA III	PARABOLA measurements, calculation from MISR-estimated downwelling radiance at surface together with calculated BRF using MISR-retrieved aerosol and surface models

Table 10: MISR Science Data Validation Parameters

Parameter	Field Instruments	Field Method of Recovery at Specific Sites
AEROSOL		
Total column optical depth τ_t	Reagan, MFRSR,CIMEL, GER	Langley method for both instantaneous and time-average values. Also derived from separate determination of direct irradiance component obtained using the diffuse/direct (MFRSR) radiometer and the Langley method
Rayleigh scattering optical depth τ_R	Determined from atmospheric pressure at site	Formula relating pressure to τ_R
Chappuis ozone absorption, τ_{Oz_3}	Reagan, MFRSR, CIMEL	Linear fits to residual $(\tau_{tot} - \tau_R)$ spectral optical depth in simultaneous retrieval with aerosol optical depth under assumption of second derivative of optical depth variation with wavelength is minimum
Tropospheric aerosol optical depth τ_a	Reagan, MFRSR, CIMEL	Derived from total column aerosol optical depth measurement by subtracting Rayleigh and other gaseous contributions, and estimating stratospheric component.
Water vapor column abundance	Reagan, CIMEL, MFRSR, PARABOLA III	Modified Langley method using relationships between atmospheric transmittance in water band and water column abundance derived from MODTRAN atmospheric transmittance code after adjustment for gaseous and aerosol transmittances.
Stratospheric aerosol optical depth, τ_s	Approximately from high mountain sites, and retrievals with Reagan, CIMEL, and MFRSR	Langley method

Table 10: MISR Science Data Validation Parameters

Parameter	Field Instruments	Field Method of Recovery at Specific Sites
Column equivalent aerosol size distribution, *dN/dr* from spectral extinction measurements alone	Reagan, CIMEL,MFRSR, PARABOLA III	. Also according to constrained inversion of governing integral equation relating size and Mie extinction functions to observed aerosol spectral optical depth.
Column equivalent aerosol single scattering phase function	CIMEL,PARABOLA III, Reagan, MFRSR	Derived from simultaneous inversion of sky radiance measurements in the solar almucantar together with spectral optical depth determinations using direct solar irradiance. Iterative procedure with RTC to account for multiple scattering. Procedure changes total scattering phase function to achieve rms best fit to measured almucantar and other sky radiances. Aerosol single scattering phase function is derived from total by formula weighting aerosol and Rayleigh scattering components, using estimate of single scattering albedo for aerosols
Column equivalent aerosol size distribution from combined spectral extinction and aureole measurements	CIMEL, Reagan, MFRSR, PARABOLA III	Using estimate of total single scattering phase function derived from almuncantar radiances, carry out simultaneous inversion of
Column equivalent aerosol particle complex refractive index	MFRSR, CIMEL, Reagan	Estimate real index and *dN/dr* from solar extinction and aureole scattering, employ multemporal diffuse /direct obs + radiative transfer model to estimate ground albedo and imaginary index. Adjust imaginary index so derived by minimizing differences between measured surface spectral irradiance and spectral irradiance calculated with RTC

Table 10: MISR Science Data Validation Parameters

Parameter	Field Instruments	Field Method of Recovery at Specific Sites
Column equivalent aerosol single scattering albedo, ϖ_0	Reagan, CIMEL, MFRSR, PARABOLA III	Calculated from Mie theory and radiative transfer code, given best estimates of aerosol size distribution and particle refractive index from above retrievals
SURFACE		
Bidirectional reflectance factor (BRF)	PARABOLA III	Solve integral equation representing surface reflectance boundary condition by iteration for the Bidirectional Reflectance Distribution Function (BRDF). Inputs from PARABOLA include direct and diffuse incident radiances and surface-reflected radiance measured over sky and ground hemispheres
Bidirectional reflectance factor (BRF)	PARABOLA II	Solves for maximum likelihood model (five parameters) consistent with all temporal PARABOLA III scans of upwelling and downwelling radiance
Hemispherical directional reflectance factor, HDRF	PARABOLA III	Surface-reflected radiance measured by PARABOLA III, divided by incident irradiance obtained by integration of measurements over upward (sky) hemisphere
Bihemispherical Reflectance, BHR	PARABOLA III, MFRSR operated looking sequentially up, and down with shadow arm in rest position	Numerical integration of HDRF from PARABOLA III measurements. Also as ratio of surface irradiance to radiant exitance measured with MFRSR
Directional Hemispherical Reflectance, DHR	PARABOLA III	Numerical integration of the BRF over the hemisphere

Table 10: MISR Science Data Validation Parameters

Parameter	Field Instruments	Field Method of Recovery at Specific Sites
PAR, BHR and DHR	PAR band, PARABOLA III	(1) Determine PAR BRF from PARABOLA III measurements, (2) determine PAR HDRF as ratio of surface reflected PAR radiance to incident PAR irradiance, (3) determine PAR DHR by numerical integration of the PAR BRF over the hemisphere. Same procedures, but use spectral PARABOLA measurements and numerical spectral integration
CLOUD		
Cloud bottom/top height	All sky cameras geographically oriented, set on measured baseline.	Stereoscopic analysis of simultaneous image pairs.
Cloud speed	All sky cameras geometrically oriented, set on measured baseline	Measure displacements in time lapse photo images of recognizable cloud points
Cloud motion direction	All sky cameras geometrically oriented, set on measured baseline	Measure cloud motion relative to camera coordinates in successive time lapse images

Table 9 summarizes all of what will be termed here intermediate radiation quantities that are calculated as part of MISR standard processing for the retrieval of surface reflectance parameters. The intermediate quantities result from use in an RTC of the preferred MISR-retrieved aerosol model or models. Table 10 summarizes the MISR Science Data Validation Parameters described in the following sections. Note that some activities related to cloud height and cloud motion determination have been retained, these to help assess windspeeds aloft in assessment of bulk airmass motions.

For descriptions of methods of aerosol, surface, and calculation of surface radiation retrievals employed with MISR observations refer to *[M-2], [M-3]*, *[M-4]*and *[M-5]*.

5.2 RADIATIVE TRANSFER CODE

The one-dimensional radiative transfer code MRTC used in MISR validation work is based on the discrete ordinate matrix operator method of *[25]*. The associated atmosphere/surface model is described by the number of atmospheric layers, the optical properties (aerosol and Rayleigh-scattering optical depths, phase functions, and single scattering albedos) of each layer, the surface directional reflectance characteristics (analytical/empirical models or measurements), and the altitude of the aircraft/spacecraft observations. In its current configuration the code computes the direct and diffuse components of the radiance fields and associated fluxes (irradiance and radiant exitance) at both the surface and the aircraft/spacecraft altitude and the sky and surface leaving radiance in arbitrary directions. These results allow a direct comparison to measurements from the various ground-based instruments, from the MISR aircraft simulator AirMISR, from AVIRIS, from MISR itself. The code can also be used to process ancillary retrieval algorithms employing ground-leaving and sky radiances to derive full bidirectional reflectance factors for the surface from PARABOLA measurements. The code has been benchmarked and verified against a second code based on the adding-doubling method of *[24]*. The results obtained by the two codes agree to within 0.1%.

5.3 RETRIEVALS OF RADIOMETRIC QUANTITIES

5.3.1 Direct solar irradiance at the surface

5.3.1.1 Field determination

The time-dependent direct solar irradiance is determined in the field from Reagan and CIMEL sunphotometer measurements, from global irradiance measurements with the MFRSR by subtraction of the measured diffuse incident component, and from selected observations with the sphere-scanning radiometer PARABOLA III, *e.g.*, in the latter case, those sky hemisphere pixels that include the Sun in its entirety. The irradiance is reported at a variety of wavelengths characteristic of the instruments employed (See Chapter 7). The direct measurement ordinarily assumes that the diffuse component contributed by the solar aureole is negligible. This may not always be

the case, *e.g.*, for heavy aerosol burdens such as smoke. The direct measurement obtained from the diffuse-direct instrument (MFRSR) is a derived quantity and is sensitive to the magnitude of the diffuse correction, which must therefore be determined accurately. The direct component measured with the MFRSR is also dependent upon a laboratory measured cosine-correction function supplied by the manufacturer. This function, which varies with both zenith angle and azimuth, can be a source of error in retrieval of the direct component if the function is not accurately measured and the instrument accurately leveled and oriented with respect to north in the field (few tenths of a degree). The cosine correction function is periodically remeasured by the manufacturer and has for MISR purposes been determined at eight regularly spaced azimuths rather than the usual four.

5.3.1.2 MISR value

The direct irradiance is calculated from the retrieved total optical depth.

5.3.2 Diffuse solar irradiance at the surface

5.3.2.1 Field determination

The diffuse irradiance field at the surface including multiple reflections between sky and ground is determined directly from field measurements using the diffuse-direct (MFRSR) radiometers. The diffuse irradiance is reported at six wavelengths characteristic of such instruments. Radiometric calibration of the MFRSR is preferably carried out in the field using the Langley method for determination of zero airmass instrument response (V_0); a more accurate calibration of the diffuse component (accurate to 1% absolute for a new calibration) is performed by the manufacturer. This NIST traceable recalibration NIST is carried out in the laboratory by the manufacturer using an integrating sphere. An average value for the solar exoatmospheric irradiance over the instrument bandpasses is required to recover instrument calibration constants for each channel in terms of solar irradiance units. The instrument filter functions but not the spectral response functions are supplied by the manufacturer and are used for this purpose.

The diffuse spectral irradiance at the surface is also determined using PARABOLA III by integration over the sky hemisphere of the measured incident spectral radiance by interpolation to Gauss points in the sky hemisphere.

5.3.2.2 MISR value

The diffuse irradiance is calculated from the retrieved aerosol model coupled with the retrieved surface BHR.

5.3.3 Total irradiance at the surface

5.3.3.1 Field determination

The total (global) irradiance at the surface is measured directly by an MFRSR instrument, and approximately from PARABOLA III sky observations by integration over the sky hemisphere of the measured incident sky radiance. The measurement includes contributions from multiple reflections between sky and ground. The measured radiances also include both solar aureole and direct solar components.

5.3.3.2 MISR value

For MISR, the total position-dependent irradiance $E_{x,y}(\mu_0)$ at the surface for given solar zenith angle is calculated using: (1) the locally retrieved aerosol model and optical depth obtained from the MISR aerosol retrieval, (2) the calculated local bihemispherical reflectance for non-isotropic incident radiation (BHR), the black surface irradiance (E_b), and (3) the bottom-of-atmosphere (BOA) bihemispherical albedo for isotropic incident radiation (s). The irradiance is given by a highly-accurate approximation as the ratio of black surface irradiance to one minus the product of the local bihemispherical reflectance and the BOA bihemispherical albedo.

5.3.4 Radiant exitance from the surface.

5.3.4.1 Field determination

The radiant exitance is determined by integration of projected surface-reflected radiances measured with PARABOLA III over the downward-looking hemisphere. The radiant exitance may also be inferred from direct measurements by inverting the MFRSR radiometer head to view the downward hemisphere.

5.3.4.2 MISR determination

For MISR the radiant exitance is determined from an integration of the calculated projected surface reflected radiance over the upward hemisphere.

5.3.5 Surface-incident radiance

5.3.5.1 Field determination

Measured at a point using PARABOLA III. Includes multiply scattered radiation between sky and ground.

5.3.5.2 MISR determination

MISR does not report values for the multiangle surface-incident radiance, but this can be calculated for the aerosol and surface BRF models adopted based on MISR retrievals. These radiances are calculated as part of the surface retrieval package.

5.3.6 Surface-leaving radiance

5.3.6.1 Field determination

The surface-leaving radiance is measured in the field using PARABOLA III. The extent of the surface area covered by such observations depends upon the instrument IFOV, height of the instrument above the surface and local nature of the surface topography and atmospheric scattering conditions. In practice, topographic conditions and atmospheric attenuation will limit the radial distance of the area of coverage, but this area will not in general be precisely defined.

5.3.6.2 MISR determination

For MISR the surface leaving radiance is determined for the retrieved aerosol model from the product of the local BRF times the incident radiance integrated over the upward hemisphere)

5.4 RETRIEVALS OF AEROSOL PARAMETERS

5.4.1 Column optical depth

5.4.1.1 Description

The total column optical depth is a dimensionless parameter indexing light attenuation throughout the entire vertical atmospheric column and, in the optical region covered by MISR measurements, is the sum of components due to molecular (Rayleigh) scattering, aerosol scattering, and minor gaseous absorptions due to ozone, nitrogen dioxide and water vapor. To isolate the aerosol optical depth, estimates of the Rayleigh scattering, gaseous and water vapor absorptions must be supplied. The MISR aerosol optical depth is reported at 555 nm, whereas typically the field-derived values are reported at 6 to 10 narrow bandpasses between 390 and 1030 nm.

5.4.1.2 Total optical depth retrieval using ground-based measurements

The total atmospheric optical depth τ is determined from the ground using solar radiometer observations and the Langley method. This method has been used for many years to determine atmospheric turbidity and is based on the premise that direct atmospheric transmission obeys Beer's Law. Thus for observations of the direct solar irradiance under uniform stable skies, a plot of logarithmic instrument response versus airmass yields the average total optical depth for each channel as the slope the distribution of sample points so obtained. The average optical depth together with uncertainties of slope and intercept is determined using conventional least square techniques on

sample collections weighted to provide equal airmass increments. Calibration of solar radiometers and other field instruments is discussed in Section 7.

For observations with instruments that determine both global (total) incident irradiance together with independent measurement of the diffuse component, the direct irradiance component is obtained from the total by subtraction after adjustment for the incidence angle and a correction for angular response of the receiver *[26], [27]*.

The average determination of slope for Langley plots (logarithm of response vs. airmass) may be made without regard to absolute calibration of the instrument to obtain a day long estimate of τ if the skies are stable. Generally there are time-dependent changes in abundance of scatterers and absorbers present, and knowledge of V_0 is required to estimate an instantaneous optical depth. If V_0 is known and stable over the day, then a two-point Langley fit may be used to calculate an instantaneous optical depth corresponding to the solar measurement at given airmass. This retrieval gives the time history of optical depth to coincide with aircraft overflights or MISR overpass. Since the instantaneous optical depth retrievals are sensitive to uncertainty in V_0, more so in morning and evening, the uncertainties will be reduced by averaging over time intervals around the time of aircraft or MISR overpass.

The separation of aerosol optical depth τ_a from τ requires determination of the molecular (Rayleigh) scattering optical depth τ_R, the ozone absorption optical depth τ_{Oz}, and the nitrogen dioxide optical depth τ_{NO_2}. Here we assume that NO_2 absorption to be negligible. Also of use is the water vapor column abundance, derived from the water vapor optical depth τ_W. Recovery of each of these components of the total optical depth is described below.

The aerosol optical depth retrieval according to the Langley method does not depend upon the assumption of a particle shape model for the aerosol components. The column equivalent total optical depth is simply derived from the measured light attenuation relative to the determined instrument response at zero airmass, assuming that the diffuse irradiance from the solar aureole is negligible compared to the direct solar irradiance.

5.4.1.2.1 Standard column ozone abundance

5.4.1.2.1.1 Description

The standard ozone column abundance represents combined tropospheric and stratospheric components, measured in Dobson units (milliatm-cm).

5.4.1.2.1.2 Field determination

The most important absorbing gaseous component in the MISR spectral region is ozone. The instantaneous ozone column abundance is estimated using the Chappuis band absorption repre-

sented in the residual spectral optical depth (total optical depth - Rayleigh optical depth). The procedure adopted, due to Flittner *et al. [20],* involves fitting of the aerosol wavelength optical depth variation simultaneously with the absorption band profile of ozone contained in MODTRAN III subject to the constraint that the second derivative of the aerosol spectral profile remain small. See *[M-7]* for details. No special assumption about variation of the aerosol optical depth with wavelength or with time is required. The procedure of *[20]* will be validated against independent determinations of ozone column abundance carried out either by: single line interferometric measurements, or (2) comparisons with retrievals from standard UV absorption spectrometers such as Dobson or Brewer.

5.4.1.2.2 Rayleigh scattering optical thickness

5.4.1.2.2.1 Description

The optical thickness of the Earth's atmosphere due to molecular scattering is proportional to atmospheric pressure with a spectral variation in the optical region of approximately λ^{-4}. Used to define residual spectral optical depth due to aerosol scattering, and ozone, and nitrogen dioxide absorption.

5.4.1.2.2.2 Field determination

Determined from atmospheric pressure measurement and assuming the spectral variation (approximately λ^{-4}) given in *[25]*.

5.4.1.2.3 Water vapor column abundance

5.4.1.2.3.1 Description

Number of cm of water vapor present per unit area in the atmospheric column condensed to liquid water.

5.4.1.2.3.2 Field determination

Determined from optical depth measurements at 940 nm by sunphotometry. The optical depth due to water vapor absorption is related to the column abundance of water vapor (gm/cm^2). The optical depth due to water vapor is derived from the water band transmittance after isolation of water absorption from aerosol and molecular scattering contributions. The MODTRAN III atmospheric transmittance code is used to provide the relationship between broad band attenuation as measured by the sunphotometers and detailed line by line absorption representing the actual atmospheric absorption. See *[M-7]* for details.

5.4.1.2.4 NO_2 absorption

5.4.1.2.4.1 Description

A measured stratospheric NO_2 abundance is usually expressed as a slant column amount in molecules per square cm. The actual vertical column abundance is calculated from the slant column abundance by dividing by the airmass. NO_2 absorptions may be present in the optical depth spectra taken during high altitude calibration of sunphotometers and may need to be accounted for in retrieval of column ozone abundance at such sites. The wavelength of maximum NO_2 absorption is at 400 nm falling rapidly to both shorter and longer wavelengths. If needed, the absorption spectrum adopted is contained in MODTRAN III.

5.4.1.2.4.2 Field determination

No independent determinations of NO_2 will be carried out. A climatological average value of 4.3×10^{15} molecules/cm^2 is assumed for NO_2 column abundance *[29]*.

5.4.1.3 Aerosol optical depth retrieval with AirMISR

AirMISR will employ retrieval strategies identical to those of MISR itself. The following discusses the MISR strategy from the viewpoint of AirMISR.

Following MISR, the AirMISR aerosol retrieval process is implemented using three ancillary MISR-constructed data sets. The first, the Aerosol Climatology Product (ACP) contains microphysical and scattering characteristics of a set of globally representative aerosol types upon which the retrievals are based, the specification of mixtures of pure aerosol types that comprise candidate models to be used in the retrievals, and a geographical and seasonal measure of the climatological likelihood of each mixture. The second, the Terrestrial Atmosphere and Surface Climatology (TASC) Dataset, gives baseline meteorological fields and ozone abundances to be used in the absence of real time data for these variables. The third, the Simulated MISR Ancillary Radiative Transfer (SMART) Dataset, contains radiation fields obtained by a forward calculation that are used to generate the *near*-TOA equivalent reflectances (radiances). The AirMISR observations are compared to these calculated fields case by case to implement the aerosol retrieval according to χ^2 criteria. The SMART Dataset is generated using stratified atmospheric models and aerosol models found in the ACP. The calculations are carried out for various relative humidities (RH) of the aerosol layer and for a range of assumed aerosol optical depths. The calculations are carried out for two surface reflectance boundary conditions representing: (1) oceans or large dark water bodies and (2) a spectrally black surface, which is used in the retrievals over land. Further details on the ancillary data sets are contained in *[M-6]*. The adopted MISR retrieval approach depends upon whether: (1) the viewed region contains dark water or land, (2) the surface contains dense dark vegetation, or (3) the land surface is heterogeneous or homogeneous in reflectance.

The MISR aerosol retrieval is obtained over 17.6 km regions that are topographically simple, free of obscuration, cloud or cloud shadow contamination, illumination shadowing, and over water, glitter contamination. The aerosol retrieval procedure is described in detail in *[M-4]*.

AirMISR will be available for algorithm and post-launch product validation work. Implementation of the procedure with AirMISR is similar to that for MISR itself, except that a smaller area is analyzed and the observations and calculations are carried out within rather than at the top of the atmosphere.

5.4.2 Compositional model identifier of best-fit aerosol model

5.4.2.1 Description

For MISR retrievals this parameter specifies the mixture of pure aerosol components in the ACP including effects of relative humidity, that provided the best fit obtained comparing AirMISR-measured radiances with radiances contained in the SMART Dataset. Both spherical and non-spherical aerosol scattering models are included. The MISR inventory of aerosol properties is based upon size distribution descriptors imported from aerosol climatologies as reported in the scientific literature. The descriptions include both dry and wet particle values the latter at specified RH. Once a compositional model is determined from the AirMISR retrieval, the size distribution parameter is obtained from the ACP database.

To provide connections with conditions implied by application of the AirMISR aerosol retrieval procedure, the following ancillary field measurements will be carried out as part of field algorithm and product validation exercises: (1) Continuous RH at ground level, (2) column water vapor abundance from solar radiometry as function of time, (3) vertical distribution of absolute humidity (gm water/cm^3) from temperature and RH aloft, obtained by balloon observations, (4) column ozone abundances from Chappuis band-based retrievals.

5.4.2.2 Comparison of ground-based and MISR-retrieved aerosol optical models.

The aerosol optical and microphysical properties sought independently from ground based optical measurements presently include: (1) estimates of the column equivalent particle size distribution, (2) column equivalent single scattering phase function, and (3) column equivalent complex refractive index; these currently assume spherical homogeneous particles. These quantities are used to calculate single scattering albedo, extinction and scattering cross sections, all under assumption of the Mie scattering theory.

A comparison of the field-determined and MISR-retrieved aerosol models will be carried out: (1) by a direct comparison of the aerosol properties generated from these independent pathways, and (2) by comparison of the downwelling sky radiance and surface irradiance implied by the MISR aerosol retrieval generated with an RTC with actual values of these quantities measured

by the field instruments. Any disagreement generated by these comparisons outside the uncertainties associated with each pathway will be classified as a systematic error and used as a basis for analysis of the retrieval algorithms and ancillary assumptions for both pathways. Statistical hypothesis testing will be utilized to assess significance of differences found.

The instrumentation used for retrieval of particle size distribution by inversion of the spectral optical extinction and sky radiance measurements, include Reagan and CIMEL sunphotometers, the MFRSR diffuse-direct radiometer, and the sphere-scanning radiometer PARABOLA III. The CIMEL sky photometer in particular is used to characterize the single scattering phase function and the particle size distribution from light scattering measurements in the solar aureole and from polarization measurements at one wavelength (870 nm).

5.4.2.2.1 Relative Humidity

5.4.2.2.1.1 Description

For MISR the relative humidity (RH) is a value corresponding to the boundary layer**.**

5.4.2.2.1.2 Field determination

A capacitance method at ground level using a standard (Davis) meteorological package determines time history. Aloft, RH is measured as a function of pressure altitude by an atmospheric sounder package using capacitance method (hygristors).

5.4.2.2.2 Particle size distribution

5.4.2.2.2.1 Description

These parameters describe aerosol particle size distributions according to specified models such as log-normal and power law distributions. These functions give number of particles per unit volume per unit radius interval or log(radius interval). The volume distribution, particle volume per unit volume per unit radius interval, is usually more indicative of multimodal aerosol populations, and is thus reported here.

5.4.2.2.2.2 Field determination

Effective column values for the size distributions are estimated from inversion of spectral extinction, solar almucantar, and principal plane measurements. The retrievals will eventually include complete sky hemisphere radiances measured with PARABOLA.

The algorithm of King, *et al*. *[40]* will be employed with essentially instantaneous optical depth observations obtained with the Reagan and MFRSR instruments, and thus a time-history of the size population will be obtained. This algorithm is a constrained linear inversion on the spectral

optical depth alone. These provide an effective size retrievals applicable to the line of sight air path to the Sun., although the MFRSR direct beam irradiance is a quantity derived from the total global irradiance by subtraction of the diffuse sky irradiance measurement.

The CIMEL observations on the other hand involve both the solar direct beam but also sweep out the complete almucantar and principal plane, and therefore involve a considerable potential scattering volume of the troposphere in addition to the line of sight path to the Sun. The CIMEL retrievals depend upon a homogeneous clear sky assumption, and the observations are screened to attempt to secure such a condition. Reduction of the CIMEL sky radiance observations for size distribution proceeds according to the methodology of Nakajima *et al. [58]*.

The CIMEL procedure is divided into two steps. (1) Estimation of the scattering phase function of aerosols is carried out by removing a theoretical estimate of the Rayleigh scattered and multiply scattered radiance from the aureole data. To constrain these calculations the total and aerosol optical depths are taken as known from the direct beam sunphotometer reductions. An estimate of the surface reflectance is employed either from the diffuse/direct reductions or preferably from direct measurements with PARABOLA III and possibly ASD data. (2) Once an estimate of the total scattering phase function is secured and corrected for multiple scattering an estimate of the volume spectrum (or equivalently the radial size distribution function) is obtained by inverting simultaneously the total optical thicnkess and scattering phase function estimates. The procedure begins with a first estimate of the phase function as represented by the observed almucantar sky radiance distribution. Improved estimates of the phase function are obtained by successive corrections for the multiply scattered component until agreement between calculated and measured almucantar radiances are reduced to the noise level in the data. The limits on radius interval for the retrievals have been determined to lie between 0.06-10 μm.

Except under homogeneous stable atmospheric conditions these determinations (King- and Nakajima *et al*.-based) are both column equivalent values that may differ from the column equivalent values reported by MISR both because of viewing geometry and the volume of troposphere sampled. The MISR values represent averages in space (over MISR view angles of 70.5°) through the aerosol scattering layer, and over time (about seven minutes/scene).

5.4.2.2.2.3 Surface-based measurements with integrating nephelometry

Integrating nephelometer measurements provide multispectral extinction coefficients from surface-based stations. These measurements give estimates of the power law exponent (in wavelength) in Angstrom's law which are simply related to the so-called Junge parameter of a power law size distribution formula. If the exponent in Angstrom's law is α, then the Junge exponent in the radius size distribution law is $\nu = \alpha+2$. Nephelometer measurements will be employed where available as further constraints on column aerosol properties.

5.4.2.2.2.4 Aircraft determinations of size distribution

Aircraft measurements of direct aerosol properties are fundamental in specifying connections between remote and directly measured size distributions. The C-131A or other aircraft direct measurement will be utilized whenever available. We will take advantage of direct measurements between ground and aircraft determinations by participating in available field exercise where these measurements are available.

5.4.2.2.3 Complex index of refraction

5.4.2.2.3.1 Definition

The complex refractive index of refraction is a fundamental quantity for describing electromagnetic wave propagation in continuous media, and for scattering by aerosol particles immersed in air. In addition to dimensions (radius for spherical particles) and wavelength of light, the complex index of refraction determines the particle extinction, scattering and absorption properties of particles, in the case of spherical particles according to the Mie theory. The imaginary index determines the degree of absorption of light by aerosol particles and hence is a major determinant of climatic impact of the presence of aerosols. The complex refractive index is an index of aerosol composition, and may be computed from the mass fraction of end-member components in an internal mixture with formulas given, for example, by Pilnis *[65]*.

5.4.2.2.3.2 Field determination

This is a column-effective value estimated at the MISR and closely adjacent wavelengths. The imaginary part of the complex index is estimated from modeling of diffuse/direct irradiance observations together with the average surface (Lambertian) reflectance. These estimates are used in the inversion algorithm for determination of the single scattering phase function and for determination of the size distribution (see for example, Nakajima, *et al. [58]*. Both spectral extinction, and solar almucantar measurements are employed. A measured value of the surface spectral reflectance (possibly non-Lambertian) is also supplied if there is substantial disagreement with the value determined from diffuse/direct analysis. Once a phase function and size distribution model have been evolved that satisfy (in a least square sense) the solar almucantar radiances, the downwelling irradiance is calculated from the code and compared to a measured value of the surface irradiance (supplied by MFRSR). The calculated irradiance at the surface proves to be largely insensitive to the real part of the refractive index (and also to the surface reflectance for low turbidity conditions), but quite sensitive to the imaginary component. Consequently, the imaginary part is adjusted (if needed) until agreement is achieved between the measured and calculated irradiances. With this refined estimate of the complex index, a new iteration is begun to improve the single scattering phase function model and the size distribution. Finally, a comparison is made between model-calculated radiances using this refined aerosol model and other sky radiance measurements provided by PARABOLA not to this point used in the analysis. Another check is supplied by using

the retrieved size distribution and the aerosol compositional estimate to calculate the total aerosol optical depth. Both the sky radiance comparison and the optical depth comparison just described, will be used as figures of merit for the aerosol model retrieval.

To summarize, the field observations used involve the following instruments: (1) Reagan sunphotometers to obtain spectral extinction, (2) CIMEL sunphotometers to obtain spectral extinction and sky radiance measurements in solar almucantar, (3) MFRSR radiometer to obtain separately the diffuse and direct incident irradiances, PARABOLA III to measure sky radiance in directions other than solar almucantar and principal plane, and to supply an estimate of the surface non-Lambertian reflectance.

5.4.2.2.4 Scattering and extinction coefficients

5.4.2.2.4.1 Description

The scattering and extinction coefficients represent effective (size distribution weighted) column average values for both MISR and field methods.

5.4.2.2.4.2 Field determination

The appropriate coefficients are calculated from the field-retrieved particle size distribution and the retrieved complex index of refraction using Mie theory.

5.4.2.2.4.3 MISR values

The appropriate cross-sections are established within the ACP as a function of RH using the assumption of Mie scattering theory for spheres and randomly oriented spheroids for non-spherical aerosols.

5.4.2.2.5 Aerosol single scattering albedo

5.4.2.2.5.1 Description

The effective single scattering albedo is the ratio of the total energy scattered in all directions in a single scattering event to the total incident wave energy. For spectral values the wavelength interval is taken to be that of the MISR channels, although the field measured quantities are at the bandpasses of the sunphotometers and other instruments employed. The MISR values will be determined by interpolation between the field-determined quantities.

5.4.2.2.5.2 Field determination

The single scattering albedo for the average wavelengths of sunphotometer band passes is calculated from the retrieved particle size distribution using inversions on the spectral extinction and aureole scattered solar radiance and the best retrieved complex refractive index model.

5.4.2.2.5.3 MISR value

The column single scattering albedo is provided in the ACP for each compositional model.

5.4.2.2.6 Aerosol single scattering phase function

5.4.2.2.6.1 Description

The single particle single scattering phase function describes the redistribution of energy in space resulting from the scattering of a plane electromagnetic wave by an aerosol particle. In the present context, the particles are assumed to be spherical, homogeneous, and optically isotropic.

5.4.2.2.6.2 Field determination

The column-effective aerosol single scattering phase function is derived from solar almucantar and spectral extinction measurements together with a radiative transfer code to extract singly and multiply scattered aerosol and molecular components. The radiative transfer calculations may employ as first approximations the refractive index and surface (Lambertian) reflectance estimates provided by analysis of diffuse/direct ratio observations from the MFRSR according to the scheme elaborated by *[41]* and *[42]*. The diffuse/direct values of the reflectance should represent a large area average for the Lambertian reflectance, but actual field-measured values of the surface (possibly non-Lambertian) spectral reflectance will be supplied by PARABOLA III or ASD observations are preferable, if these can be taken as representative of a large area. The principal instrument used for determination of the scattering phase function is the CIMEL sky/sun photometer which provides the diffuse sky radiance in the solar almucantar as well as the spectral extinction determination. These measurements are used in the inversion algorithm of Nakajima *et al. [58]*, which estimates the phase function from the almucantar radiance measurements, using the radiance actually observed as a function of scattering angle as a first approximation. The radiative transfer code is used to estimate the multiply scattered component, and by iteration, successive approximations are developed. At each stage the code calculates the total solar almucantar radiance and compares the calculated and measured values. Iterations continue until a prescribed rss limit, determined by sky variability and instrument noise, is achieved. The aerosol single scattering phase function is separated from the total scattering phase function (which includes Rayleigh and aerosol components together) using formulas given by Nakajima *et al.[58]*.

The aerosol model, which includes composition estimate, size distribution estimate, and the phase function estimate is finally checked by comparison with other field measurements in a kind of closure experiment. In particular comparisons are made with the downwelling spectral irradiance as measured with the MFRSR, and the sky radiance pattern in directions other than the solar almucantar obtained with PARABOLA III. Also, from the aerosol model, the effective column value of the aerosol optical depth will be calculated and compared with the observed values. The calculation requires an estimate of the effective column size distribution, the effective aerosol ex-

tinction coefficient obtained from calculations using Mie theory, and integration over the column, in which the particle number distribution is assumed uniform with height over the scattering layer.

5.4.2.2.7 Nonspherical particles

5.4.2.2.7.1 Description and distinctive features of scattering

Nonspherical particles contain surface irregularities (departures from sphericity) on the order of the wavelength in size. Such particles are still usually thought of as homogeneous and optically isotropic, although no formal calculations of the scattering behavior, like those possible with Mie theory for spheres or for spheroidal shapes, are actually carried out here.

The principal effect on the phase function of nonspherical particle scattering is to increase values of the sideward scattering phase function around a scattering angle of 120°and to decrease the overall asymmetry of the phase function. Forward scattering is less affected and remains comparable for spherical and nonspherical cases as described in *[45]* and *[67]*. Increased absorption (from calculations) reduces the differences in scattering properties between spherical and irregularly shaped particles, The degree of linear polarization is reduced over that from Mie particles as described in *[56]*. The effects of particle shape are greatest for dry desert aerosols or dust or unhydrated types of urban origin and less for other types having a significant liquid water components. The effect of nonsphericity decreases with increasing wavelength. Nonsphericity can lead to uncertainty in refractive index using the method of *[87]* if the analysis is based on kernels derived from Mie theory. Using the radiative transfer and library method of Tanaka, *et al.[83]*, Nakajima *et al. [57]* found that nonsphericity of dust from so-called yellow sand events leads to much larger than expected values for both the retrieved real and imaginary parts of the refractive index. (It may be, however, that the higher than expected parts of the refractive index for such turbidity events are due to presence of iron oxides [goethite or hematite] of high complex refractive index (see for example *[14]*) coating or permeating individual particles and thus giving rise to the characteristic yellow color.)

Detection of nonspherical particles is under investigation as part of the study of nonuniqueness of component properties. For example, it has been shown possible in several simulations to match arbitrary radiances with a spherical model, providing a willingness to accept size distributions and variation of refractive index with wavelength which are nonphysical. That is spherical particles seem able to serve as basis functions for representation of observed phase functions, although the multiplier coefficients might be nonphysical. It is hoped that when investigating radiance distributions produced by non-spherical particles, that principles of parsimony may emerge to judge whether spherical particles form the best fit or not. Currently under development is an algorithm in which the phase function and single scattering albedo are estimated by iteration without recourse to an inversion kernel assembled from spherical particle phase functions and extinction coefficients. Such an approach would allow greater flexibility in determining presence of nonspherical particles.

The plan is to use code based upon a T-matrix approach to generation of phase functions in the non-spherical case. To assess sensitivity of retrievals to nonspherical particles, such particles (ellipsoidal) will be used to generate simulation data sets, from which aerosol properties will be inferred using both spherical and non-spherical assumptions.

5.4.2.2.7.2 Field determination

For possible presence of scattering by nonspherical particles, we follow the strategy outlined in *[34]*. This focuses on the characteristic behavior of the single scattering phase function of non-spherical scattering particles around 120° scattering angle in a comparison relative to the phase function for spherical particles around the same angle. Estimates of the single scattering phase function are retrieved from clear sky observations of the solar almucantar radiance using algorithms of *[56]*, and *[58]*. Currently all estimates of multiple scattering are carried out under the assumption that the scattering particles are spherical.

Two estimates of the phase function at this stage are now available for comparison: (1) that derived from the observations after correction for multiple scattering (termed P_a in *[34]*) and reproducing the actual measured almucantar radiance to within the noise of the data, and (2) that derived from the particle size distribution extracted from the combined phase function and optical extinction retrieval assuming spherical homogeneous particles and refractive index (termed P_s in *[34]*).

Presently the MISR validation effort does not extend beyond these analyses of particle shape. Several options remain open to provide some check on the actual MISR retrievals. for which a non-spherical scattering model is indicated: (1) We will routinely take the MISR-retrieved aerosol model (spherical or nonspherical), calculate the downwelling sky radiance pattern as well as the irradiance at the surface using a radiative transfer code, and compare with actual observations taken by the field instruments. (2) On selected occasions, we may acquire samples of the aerosol by direct sampling from ground or aircraft, for comparison with ground retrieved model. (This is a procedure carried out in *[34]* on individual particles. This option seems more likely to produce unaltered aerosol samples, especially on occasions where dust is a predominant component.

5.4.2.2.7.3 Distinction of spherical/nonspherical models using AirMISR

Observations with CIMEL limit the maximum scattering phase angle that may be recovered from ground to about 120 .On the other hand it is known that significant differences exist between the phase functions of spherical and those of non-spherical distributions at scattering phase angles of about 140 .For field experiments in which both surface and AirMISR observations are available, AirMISR observations in the solar principal plane will be used to extract scattered intensity at larger phase angles, which theoretically can extend to near 180 although increasingly not without complication from surface reflected light. The additional AirMISR observations, especially over dark

targets, will be used to estimate the relevance of nonspherical distributions in the scattering.

5.4.2.2.7.4 Aerosol microphysical properties directly from aircraft observations.

It is uncertain what role direct determinations of aerosol properties by aircraft observations will play in the MISR ground validation effort because of the expense. It may occur that direct sampling by aircraft will be possible for some field campaigns, *e.g.*, SAFARI -20000 as well as post launch product validation exercises. The present emphasis for MISR ground validation must be on generation of radiatively closed aerosol models rather than pursuit of differences or similarities between radiative and direct sampling properties.

5.4.2.3 Uniqueness of aerosol and surface models derived

Uniqueness of the ground-derived model atmosphere is not necessarily an issue for verifying MISR data products. What we are required to do is show that the resulting BOA and TOA radiances obtained using the ground-retrieved model are consistent with ground-measured BOA radiances and with upwelling TOA radiances measured by MISR or AirMISR. We know that the optical depth retrievals do not suffer from uniqueness problems. The BRF determination is also considered unique, unless topographic relief is involved that prevents observation of an entire area from interior points. For purposes of TOA radiance calculation, the test areas are always chosen large, flat and uniform, so that this problem is not present.

Aerosol property retrievals may suffer from nonuniqueness problems because the RTC is only constrained by BOA and TOA radiance measurements, and not by particle or radiance measurements within the atmosphere The existence of accurate ground data will however verify consistency of the validation retrieval, namely, (i) the radiance calculated at BOA with the MISR or AirMISR-derived aerosol model may be compared with ground measurements, and (ii) if the calculated and measured BOA radiances are consistent, confidence in the correctness of the MISR or AirMISR product may be judged by statistical tests comparing magnitude and scatter between this product and an equally consistent one derived by the ground-based pathway. There is no definitive literature known to us on the question of uniqueness of aerosol inversions based upon radiative transfer methods. Uniqueness, whether in terms of vertical structure or component properties is a topic of current research.

5.4.3 Hemispherical-directional reflectance factor (HDRF)

5.4.3.1 Description

The hemispherical directional reflectance factor for nonisotropic incident radiation is equal to the ratio of the reflected radiance from the surface into a single direction to the radiance reflected into the same direction from an ideal Lambertian target into the same beam geometry and illuminated under identical atmospheric conditions.

5.4.3.2 Field determination

To recover HDRF at the surface, use is made of PARABOLA III measurements, namely the surface-reflected radiance and the surface irradiance which is obtained from an integration of the projected incident sky and solar radiance over the upward hemisphere The HDRF is calculated from its defining equation as the ratio of the reflected radiance in a chosen direction to the incident irradiance.

5.4.4 Bihemispherical reflectance (BHR)

5.4.4.1 Description

The bihemispherical reflectance (BHR) for non-isotropic incident radiation represents the ratio of the radiant exitance to the irradiance. It can also be defined in terms of the HDRF as the integral of the HDRF over the upward hemisphere divided by π.

5.4.4.2 Field determination

The field-based retrieval of the BHR follows from its definition as the ratio of the total exitance to the total irradiance. At present, the radiant exitance at a site is measured using PARABOLA III. The irradiance is determined by PARABOLA III measurements and also by measurements with the shadowband radiometer (MFRSR) after extrapolation to PARABOLA III wavelengths and bandpasses.

5.4.5 Bidirectional reflectance factor (BRF)

5.4.5.1 Description

The bidirectional reflectance factor (BRF) is a limiting form of the HDRF defined for the special condition of surface illumination by a parallel beam of radiation and zero incident diffuse illumination (see *[M-5]*). It is the ratio of the radiance reflected in a specific direction to the total incident radiance.The condition of illumination described corresponds physically to an atmosphere of zero optical depth. This is a hypothetical circumstance for actual Earth surface observations, even at the highest elevations.

5.4.5.2 Field determination

The method for obtaining the BRF on the ground relies on PARABOLA III measurements of the surface-reflected radiance, PARABOLA III or sunphotometer measurements of the direct solar irradiance at the surface and PARABOLA III measurements of the incident diffuse radiance from the sky hemisphere for all angles of the solar incidence direction between zero and 90°. These data are utilized to implement a numerical solution of a two-dimensional Fredholm integral equation (second kind) giving the relationship between them, which merely represents the conservation

of reflected energy at the surface. It is to be noted that requirements on the incident radiance measurements for the complete range of solar zenith angles preclude complete natural determination of the BRF from field measurements for any latitude on the Earth north or south of about 23° from the Equator and then only during certain portions of the year when the Sun reaches the zenith. In practice, this restriction will be circumvented using: (1) interpolation methods to fill out the missing sky irradiance data or (2) approximate empirical or theoretical physically based models of the surface reflectance properties to fill out the reflectance function.

5.4.6 Directional hemispherical reflectance (DHR)

5.4.6.1 Description

The directional hemispherical reflectance (DHR) bears the same relationship to the BHR as does the BRF to the HDRF. That is, the surface is illuminated by a parallel beam of radiation from the sun, with no diffuse illumination. The DHR represents the ratio of the total exitance to the total incident irradiance for the assumed conditions of zero diffuse illumination. This condition of illumination is in general a hypothetical circumstance for Earth surface observations, even at the highest elevations.

5.4.6.2 Field determination

Once the BRF is derived from surface measurements (see Section 5.4.5.2) the DHR follows by numerical calculation of the integral over the hemisphere of this quantity, divided by the solar exoatmospheric irradiance at the appropriate incidence angle.

5.4.7 PAR - integrated BHR and DHR

5.4.7.1 Description

The photosynthetically active radiation (PAR) is defined as the solar radiation incident at the surface by direct and diffuse illumination integrated over the spectral range 400 - 700 nm.

5.4.7.2 Field determination

PARABOLA III has a PAR broad band filter (about 400-700 nm) included in the scanning head that will provide direct measurements of PAR-integrated incident and reflected radiance, hence by integration of the irradiance and radiant exitance. Hence BHR can be calculated (Section 5.4.4.2). In addition, the individual spectral channels available with PARABOLA III, which approximate closely those present on MISR, can be used to provide narrow band BHR values. An independent estimate of PAR-integrated BHR, using the MISR method of calculation from monochromatic values and the assumption of linear spectral variation between channels, will thus be obtainable.

5.5 ASSUMPTIONS AND LIMITATIONS

The following assumptions are made with respect to the ground based aerosol, surface, and cloud product retrievals using the validation algorithms.

Aerosol Products

(1) At present aerosol particles are taken to be spherical, homogeneous, whether hydrated or solid (*e.g.*, dust, sea salt). Future extension to non-spherical particle scattering is under way. Uniqueness of aerosol recoveries in presence of BOA and TOAR observations is also subject of active study.

(2) The (complex) particle refractive index is assigned initially, allowed to evolve to value consistent with sky and sun observations, diffuse/direct observations, and possibly direct measurements, not otherwise restricted.

(3) The atmosphere is taken to be plane-parallel, laterally homogeneous, but with (possible) vertical layering in radiative transfer modeling as specified by ancillary measurements such as radiosonde or lidar backscatter soundings and inferences on composition that may be forthcoming.

(4) Column-effective optical depths, aerosol phase functions and aerosol size distributions and compositions are implied for all retrievals, *i.e.*, no regard to actual layering that may be present in the atmosphere is possible from the retrievals themselves, although the derived model will be consistent radiatively with all radiance observations available.

(5) For most solar radiometer analyses of the direct solar irradiance, except heavy haze conditions such as smoke, the diffuse solar aureole component will be considered negligible in magnitude compared to the direct solar irradiance component. The exception to this are diffuse/direct irradiance measurements carried out with the MFRSR, where the individual components are determined separately.

(6) For interpretation of sky radiance measurements leading to aerosol properties, the surface will be assumed to be flat, homogeneous, and (presently) Lambertian. Relaxation of the Lambertian assumption and incorporation of full BRF is in place for MRTC.

(7) For calculation of effects due to ozone and water vapor absorption present in the spectral solar radiometer data, the line measurements contained in MODTRAN III for these constituents will be assumed. Ozone column abundances will be obtained from simultaneous retrievals along with aerosol optical depth, not otherwise imported from external data sources.

(8) If needed, extraction of optical depths due to NO_2, will employ absorption data contained in MODTRAN III and climatological values for column abundances taken from literature or other sources used as required. Presently NO_2 is ignored in retrievals.

(9) Adjacency effects in interpretation of solar radiometry are ignored, as are diffuse radiances present in the solar aureole.

(10) The Cox-Munk *[12]* wave facet model is currently adopted together with the foam reflectance model based on Monahan and O'Muircheartaigh *[54]* and Koepke *[44]* for aerosol retrievals over water, given the surface wind speed measured at the standard height of 10 m.

Surface Products

(1) The plane-parallel approximation for radiative transfer in the atmosphere and at the surface are adopted.

(2) Adjacency effects are ignored at the scales at which the surface reflectance parameters are reported.

(3) Validations are restricted to comparisons of BRF reflectance model parameters obtained from AirMISR or MISR retrievals and ground-based measurements with PARABOLA III. Validation of empirical extensions seeking connections between derived BRF and biophysical quantities (*e.g.*, LAI, FPAR, green biomass) are not included

(4) Experience shows that derivation of BRF from PARABOLA III data sets over inhomogeneous terrain are not practical as a general rule. (This excludes the problem introduced by partial solar incidence angle coverage as is usually the case in Northern Hemisphere observations north of 23° north latitude.) Hence solution using the integral equation procedure will be restricted to certain homogeneous targets. For inhomogeneous targets, the maximum likelihood best fit model will be adopted.

6. RETRIEVAL COMPARISONS

6.1 MEASURES OF SUCCESS

Data verification experiments are carried out to check accuracy of parameters derived from MISR algorithms, discover biases between ground-based and MISR retrieval pathways, if any, and to monitor accuracy and quality of the data products produced by MISR over time. Also an error assessment of TOA radiances as part of vicarious calibration, depends on uncertainties in ground measurements of atmospheric and surface parameters, which arise from natural variability or inherent instrument error. The ground-based data sets are generated in the present experiments by independent mostly conventional approaches using instruments and methods that have a long history of development and use. Furthermore, care has been taken to understand the error budgets of each method employed. Some preliminary statements concerning error analyses are included here for a few cases, but it is emphasized that more work needs to be done to understand uncertainties (precision and accuracy) for many parameters sought by ground-based methods These are the subject of ongoing investigations and instrument intercomparisons.

Successful validation of a MISR algorithm (and products derived therefrom) here implies that the following criteria be met:

(1) Agreement of values (aerosol optical depths, microphysical properties, HDRF, BRF, HDR, BHR, cloud heights, etc.) derived or assumed by MISR and derived by ground-based pathways to within expected errors for each pathway.

(2) For aerosol and surface properties, radiance closure to within expected errors of the MISR and ground-based pathways. Closure tests are describe next.

6.2 RADIANCE AND IRRADIANCE CLOSURE TESTS

Additional radiatively based tests of the ground based retrievals of aerosol properties and surface reflectances will be to check for closure between calculated and measured upwelling and downwelling atmospheric radiances by various pathways. Closure, as the term is used here, implies agreement within expected uncertainties between measured irradiance and downwelling radiance at the surface with calculated irradiance or downwelling radiance supplied using a radiative transfer code. In practice, favorable agreement will be decided by a weighted chi-square test, where the weighting is inversely proportional to uncertainties present in each pathway. The result of non-closure implies the inadequacy of either model atmospheric parameters, surface parameters, or possibly both. Four separate pathways are possible involving ground measurements and measurements from either MISR or AirMISR.

(1) Comparison of multi-angle upwelling radiances measured by MISR and AirMISR with radiances calculated by an RTC using atmospheric parameters and surface reflectances derived from the ground-based measurements.

(2) Comparison of measured downwelling surface radiances and irradiances and upwelling surface radiances and radiant exitances with such quantities calculated by a radiative transfer code using atmospheric parameters and surface reflectances derived from MISR algorithms and the MISR measurements.

(3) Comparison of downwelling and upwelling radiances measured by ground based instruments with downwelling and upwelling radiances calculated by a radiative transfer code using parameters derived from analysis of the ground based and surface measurements themselves.

(4) Comparison of measured downwelling radiances and the irradiance at the surface with downwelling radiances and irradiance at the surface when the surface reflectance is measured and the aerosol model (composition and size distribution) is specified by direct measurements, say with aircraft This is characterized as a *complete* closure experiment

For these tests, the radiances within the solar almucantar and in the principal plane used in the aerosol property retrievals with the CIMEL procedure are specifically excluded in the comparisons. Sky radiances measured in other directions by PARABOLA III as well as irradiance at the surface supplied by MFRSR, are utilized.

Radiance closure testing in the manner described will result in a well specified model for the aerosols present. If downward-only closure is possible because of the unavailability of upwelling radiance measures from AirMISR or from AVIRIS, then some error in the model may be introduced because of discrete layering of the aerosol distribution vertically. Inclusion of an adjustment for upwelling TOA (or near TOA) radiances in the aerosol model, removes this ambiguity *[M-7]*. Thus with respect to validation of MISR aerosol models, specification of the upwelling radiative components is complete. There may remain differences between this radiatively consistent retrieval and results of direct measurement of the aerosol components actually present.

6.3 ERROR ANALYSIS

The objective of error analysis is to determine the expected errors in parameter retrievals according to the ground-based pathway and according to the AirMISR (or ASAS) pathways. (MISR has its own error budget). Errors can be both systematic and random in nature. Systematic errors are independent of time. An example of systematic error in solar radiometry and in the aircraft simulator instruments is adoption of incorrect values for the instrument calibration constants or incorrect determinations of cosine response formulas in the case of shadowband radiometry at the surface. Random errors are time-varying; a persistent source of random error is instrument noise, and in solar radiometry, atmospheric variability and fluctuations in turbidity. The first purpose here is to identify, from a ground-based perspective, sources of error in measured parameters and methods of estimation of these errors rather than to present completed analyses. Wherever possible analytical formulas for error propagation will be sought, but where this is not possible because of analytic complexity, or because the retrieval is algorithmic, error propagation will be car-

ried out by end-to-end simulations. Error propagation studies will be described fully in *[M-7]*. The ground-based parameters for which error budgets can be generated are listed in Tables 11-13 together with presently known sources of error.

Table 11: MISR Aerosol Parameters and Error Sources

Parameter	Measuring Instruments	Method of recovery	Error sources	References
Total column optical depth, τ_t	Reagan, MFRSR, CIMEL	Langley, diffuse/ direct ratio	**Instrumental:** (1) Unmapped detector nonlinearity (2) Long- term changes in sensitivity (3) Dark current uncertainty (4) Temperature sensitivity and drift (5) Recording errors (personnel factors) (6) Spectral response functions **Calibration:** (1) Uncertainty in V_0 (2) Uncertainties of standard irradiance sources used to derive V_0 equivalence in SI units (3) Uncertainties in extraterrestrial solar irradiance **Imposed by atmosphere:** (1) Diffuse sky radiance in Reagan FOV (2) Diffuse sky correction with MFRSR (3) Temporal changes in atmospheric transmission during measurement sequence (4) Uncertainties from presence of gaseous absorptions, principally water vapor (5) Inhomogeneous vertical distributions	*[77], [70], [5], [62]*

Table 11: MISR Aerosol Parameters and Error Sources

Parameter	Measuring Instruments	Method of recovery	Error sources	References
Rayleigh scattering optical depth τ_R	Determined from atmospheric pressure at site	Proportional to surface pressure	(1) Different formulas lead to small differences in τ_R (2) Inaccurate or time-varying pressure at site elevation	*[25]*
Chappuis ozone optical depth, τ_{O3}	Reagan, MFRSR, CIMEL, ATS	Linear and non-linear retrievals from residual ($\tau_{tot} - \tau_R$)optical depth, comparisons with Brewer spectrophotometer values for column O3	(1) Uncertainty in V_0 (2) Real spectral variations in aerosol optical depth violating minimum second derivative constraint of retrieval algorithm (3) Errors in ozone absorption coefficients adopted, pressure and temperature dependence.	*[39]*, *[3]*
Tropospheric, aerosol optical depth τ_a	Reagan, MFRSR, CIMEL	Derived from total optical depth measurement by subtracting Rayleigh and other gaseous contributions, estimating stratospheric component	Accuracy of determination depends on accuracy of τ_t determination and accuracies of extracting ozone and possibly other gaseous and stratospheric components, and water vapor.	*[77]*, *[70]*, *[5]*

Table 11: MISR Aerosol Parameters and Error Sources

Parameter	Measuring Instruments	Method of recovery	Error sources	References
Water vapor column abundance	Reagan, CIMEL, MFRSR, PARABOLA III	Modified Langley	(1) Inaccurate aerosol correction (2) Poor knowledge of radiometer calibration, spectral response (3) Uncertainties in water vapor calibration law derived from water vapor transmission atmospheric transmission model used, (e.g., MODTRAN) (4) Presence of condensed water (droplets) or water ice crystals in path, rendering MODTRAN III-derived law for water vapor less accurate	*[69], [7]*
Stratospheric aerosol optical depth, τ_s	ATS, estimate from Reagan retrievals assuming negligible tropospheric value	Langley	See discussion for τ_t above	*[70]*
Equivalent aerosol size distribution, *dN/dr* from spectral extinction measurements	Reagan, CIMEL,MFRSR, PARABOLA III	Constrained inversion of governing integral equation relating size and Mie extinction functions to observed optical depth.	(1) Measurement errors in τ_a, quadrature errors and uncertainty in form of kernel function for scatterers present. (2) Smoothing operator effect for small particles (3) Presence of non-spherical or inhomogeneous particles (4) wrong choice of complex index (5) inhomogeneous particles (6) External multicomponent mixtures	*[40], [38], [62]*

Table 11: MISR Aerosol Parameters and Error Sources

Parameter	Measuring Instruments	Method of recovery	Error sources	References
Equivalent scattering phase function $P(\Theta)$	CIMEL, PARABOLA III, AirMISR	Constrained inversion of governing integral equation relating size distribution and Mie light scattering functions to observed scattered radiation in solar aureole. AirMISR extends range of Θ	(1) Finite (vignetted or poorly defined) field-of-view of observing sunphotometer (2) Scattered light from out of field (3) Uncertain correctness for multiple scattered radiance in solar aureole (4) presence of non spherical or inhomogeneous particles (5) Limited range of observation near Sun with poor angular resolution	*[61], [74], [56]*
Equivalent aerosol particle complex refractive index	MFRSR, CIMEL, Reagan	Estimate real index and dN/dr from solar extinction and aureole scattering, employ temporal diffuse /direct observations + RT model to estimate ground albedo and imaginary index	(1) Radiometer calibration uncertainty and limitations on S/N for diffuse light measurement. (2) Limitations of model and/or sensitivity of method (3) Presence of non-spherical or inhomogeneous particles	(to be supplied)
Equivalent single scattering albedo, ϖ_0	Reagan, CIMEL, MFRSR, PARABOLA III	Calculated from Mie theory and radiative transfer code, given size distribution and particle refractive index	(1) Uncertainties in size distribution and aerosol complex refractive index (2) Presence of nonspherical or inhomogeneous particles	(to be supplied)

Table 12: MISR Surface Parameters and Error Sources

Parameter	Measuring instrument	Method of recovery	Error sources	References
Bidirectional reflectance factor (BRF)	PARABOLA III	Solve Fredholm integral equation of second kind representing surface reflectance boundary condition by iteration	(1) Radiometric uncertainty in measured sky and ground-leaving radiances (2) Missing observations for latitudes where Sun does not reach zenith	(in preparation)
Hemispherical directional reflectance factor, (HDRF)	PARABOLA III	Surface-reflected radiance divided by incident irradiance	Radiometric uncertainty in measured sky and ground-leaving radiances	(in preparation)
Bihemispherical Reflectance (BHR)	PARABOLA III MFRSR operated looking up and down	Numerical integration of HDRF derived from PARABOLA III measurements, ratio of surface irradiance to radiant exitance measured with MFRSR	Uncertainties inherited from measurement of HDRF from PARABOLA III observations, uncertainties in calibration of MFRSR	(in preparation)
PAR BHR,DHR	PARABOLA III	see above descriptions for spectral values of BHR and	Radiometric uncertainty in PARABOLA III measurements of ground and sky radiances in PAR band	(in preparation)
Direct Irradiance at surface	Reagan, CIMEL, MFRSR, PARABOLA III	Direct measurement at surface. Instrument calibration constants converted to equivalent solar exoatmospheric irradiance equivalent and by laboratory calibration	Uncertainty in instrument calibration constant and in exoatmospheric solar irradiance. Pointing direction with PARABOLA III not directly on Sun	(in preparation)

Table 12: MISR Surface Parameters and Error Sources

Parameter	Measuring instrument	Method of recovery	Error sources	References
Diffuse irradiance at surface	MFRSR, PARABOLA III	Direct measurement by MFRSR at surface, angular integration of sky radiance by PARABOLA III, conversion of instrument calibration constants to exoatmospheric solar irradiance	Uncertainty in instrument calibration constant and in exoatmospheric solar irradiance. Uncertainty in: (1) solar aureole contribution with PARABOLA III because of 5° FOV and scattered light , (2) in calibration constant, (3) influence of mixed sky-surface pixels near horizon	(in preparation)
Radiant exitance at surface	PARABOLA III, MFRSR	Integration of direct radiance measurements over downward hemisphere, conversion of instrument calibration constants to exoatmospheric solar irradiance. Direct measurement by MFRSR with shadow arm out of FOV	Uncertainty in: (1) in calibration constant, (2) influence of mixed sky-surface pixels near horizon. Uncertainty in instrument calibration constant and in exoatmospheric solar irradiance.	(to be supplied)

Table 13: Field Calibration of Airborne Instruments; Determination of TOA Radiances from Ground Measurements

Parameter	Measuring Instrument	Method of Recovery	Error sources	References
Pure reflectance-based at (or near) TOA radiances	Reagan, CIMEL, PARABOLA III, MFRSR	(1) Measure ground target BRF with PARABOLA, HDRF with ASD spectrometer (2) Determine atmospheric parameters from field optical measurements (3) calculate radiances near or at TOA with RT code according to	(1) Uncertainties in ground BRF, e.g., areal scatter of magnitudes and directional properties (2) Uncertainties in atmospheric parameters, optical depth, diffuse transmission function (3) Uncertainty in path radiance from (2). (4) Uncertainties in RT code calculations	see *[5]*, apply error propagation to Eq (7)
Ground radiance method	PARABOLA III, CIMEL Reagan MFRSR	(1) Determine directional surface leaving radiance with PARABOLA (2) use RT code with measured surface-leaving radiances as substitute for derived BRF at lower boundary (3) estimate atmospheric properties for calculation of path radiance and diffuse transmission (3) propagate surface radiances to TOA via RTC.	(1) Measurement error in surface leaving radiances (2) Uncertainties in path radiance from measured atmospheric properties and optical depth (3) Uncertainty in diffuse transmission function generated from field data and RT code simulations	see *[5]*, apply error propagation to Eq (7) written in terms of surface leaving radiance

6.4 ERROR ESTIMATES FOR AEROSOL AND SURFACE PARAMETERS

Tables 10and 11 have assembled the MISR aerosol and surface parameters and some sources of measurement error expected in retrieval of these parameters. Here preliminary estimates of the accuracies of measurement for the optical depth and surface BRF are provided.

6.4.1 Total optical depth

6.4.1.1 Characteristics

Coverage: Local

Spatial/Temporal Sampling: ~MISR pixel resolution, but expandable in scale by measurements over networks of sites plus interpolation and averaging. Measurements at selected sites during intensive field campaigns

Estimates of accuracy of ground-based retrieval of total optical depth using solar radiometers for validation of both MISR products and retrieval algorithms in pre and post-launch time frames are described here. Errors for other column equivalent quantities needed to derive aerosol optical depth from local ground observations, including, ozone optical depth, and atmospheric pressure will be given in *[7]*, together with uncertainty analyses for particle size distribution, aerosol complex refractive index, phase function and single scattering albedo.

6.4.1.2 Theoretical Accuracy of total optical depth retrieval

Resolution of digital recording of ground-based radiometer response (Reagan automated instruments) is 1 part in 2^{16} (~1/66000), with actual instrument noise from photodiode and opt-amp sources about one-eighth of this Ehsani *[16]*. From error propagation, with this level of uncertainty in radiometer output, the standard error of determination of V_0 is $O(10^{-5}\text{-}10^{-6})$ and the standard error of optical depth determination is of $O(10^{-6})$.

In practice the limit on instrument calibration is best established by multiple local determination of V_0 on clear stable days and/or at high altitude observing sites. Bruegge, *et al. [6]* indicate relative determinations of V_O to a few percent, and total optical depth retrievals to 0.02. Recently, Erxleben and Reagan *[19]* have applied wavelet filtering techniques to improve V_0 determinations for Reagan solar radiometers. These indicate reductions in uncertainty of V_0 to $O(1\%)$ or less, leading to optical depth determinations of this order of uncertainty.

6.4.1.3 Detection of total optical depth fluctuations

Studies of response of identical Reagan solar radiometers operating side by side show that optical depth fluctuations present in both records are recoverable to ~ 0.0001.

6.4.1.4 Caveats on optical depth retrieval errors

Reductions of ground-based observations usually neglect diffuse component present in solar aureole in angular field of view of radiometers. In some circumstances (for example thick smoke, clouds) diffuse light may contribute heavily to or dominate observed BOA irradiance. Magnitude and influence of the diffuse component is discussed by Shaw *[73]* who gives a maximum relative error in optical depth determination of 0.025 for moderate turbidity and airmasses less than about 6. See Reference *[M-7]* for additional discussion. Optimal conditions for comparison with MISR EOS data include clear (cloud free) skies that are so describable for the period of a MISR observation (*e.g.*, about 7 minutes per site). Strictly ground-based observation is the line-of-sight path to Sun at any given time.

Inferences to larger areas are obtained by averages of network observations (where available) covering dimensions on the order 17.6 km, averages obtained from time series at single stations, where the sampling time interval ΔT of fluctuations present is that required for a test air parcel to cover a distance $X = \underline{U}\,\Delta T$ where $\underline{U}$ is a measure of the average horizontal wind speed in the aerosol-bearing layer, and X is 17.6 km. This latter will be recognized as an application of a form of Taylor hypothesis (see Stull *[80]*). This application needs to be checked against ~ 20 km network averages for typical areas and observing conditions.

6.4.2 Surface Bidirectional Reflectance Factor (BRF)

6.4.2.1 Characteristics

Coverage: Local

Spatial/Temporal Sampling: Sampling at MISR pixel resolution (~250 m in Local Mode) of selected field campaign site.

Estimated accuracy of ground-based retrieval of the BRF from directional sky and ground radiance measurements is given here. Observations are assumed available with PARABOLA as a standard instrument for basis of validation of MISR algorithms and products, e.g., surface bidirectional reflectance factor (BRF) and other closely-related parameters that can be derived from it (*e.g.*, hemispherical directional reflectance factor, HDRF, bihemispherical reflectance, BHR, etc.). *[5]*. The three principal error sources for retrieval of BRF from ground-based observations are: (1) accuracy of sky and ground radiance retrieval with PARABOLA, (2) instrument noise, (3) errors in total optical depth retrieval constraining the direct solar spectral irradiance incident at the surface, (4) algorithm errors. The BRF retrieval method is that of Martonchik *[49]*. Improvements in the accuracy of retrieval of the BRF in this fashion did not depend upon choice of 0.5% as opposed to one percent for the convergence criterion.

6.4.2.2 Theoretical accuracy

(1) A error source in determination of BRF is described as algorithm error. Simulations were performed using the three-parameter BRF model of Rahman-Pinty-Verstraete *[68]* according to the iterative retrieval scheme described above. To estimate algorithmic error, the data and optical depth for these simulations are considered perfectly measured. (a) Algorithm errors: Generally the errors in retrieved BRF are very large when either the sun incidence or view angles are greater than 80°. For angles at 75° the error is 3% and falls to less than 1% for sun angles less than 75° (b) Round-off numerical errors: no impact. (c) Total optical depth errors: Optical depth errors of 10% lead to increases in retrieval error by factor of five. Methods to limit errors in absolute optical depth retrieved values are described under MISR ground-based algorithms Practical uncertainties. Further study of sky turbidity, view angle dependencies for PARABOLA-based BRF retrievals are under way.

(2) Radiometric calibration errors. The dynamic range of PARABOLA measurements is 10^{20}. The lower part of the range is calibrated by measurements with an integrating sphere. The standard errors of least squares fits of such observations are wavelength dependent. For example at 550 nm these errors imply an uncertainty of *O*(1%) in the radiance recovery. Neglect of diffuse light altogether in the error tally leads to an error in BRF determination proportional to error in measured direct solar irradiance Where the diffuse light component itself is O(10%), of the illumination, a systematic overestimate of the BRF by about 10% occurs. Calibration of PARABOLA III in the direct solar irradiance range is being carried out.

6.4.2.3 Caveats on BRF retrieval errors

(1) Spatially inhomogeneous surface reflectance. Natural targets are inhomogeneous, and the resulting variations in reflectance properties at the scale of PARABOLA observations must be averaged spatially, either by occupying multiple sites, or by binning pixels from any one site. This problem is under study. (2) Scaling to larger areas. The typical PARABOLA footprint for an instrument height of two meters and 80 degree view angle from the horizontal, is ~20 meters in diameter. The scaling to 1.1 km must involve AirMISR, whose nadir pixel size is 7 m and footprint size~9 km. (3) The simulation of algorithm error sources described below assumes a homogeneous target. ((4) Possible uncertainties in the solar irradiance are not considered. (5) As with Reagan solar radiometers PARABOLA instrumental noise is considered negligible compared to other sources. (6) errors in total optical depth retrieval we believe can be constrained to *O*(1%) by application of noise filter techniques to our solar radiometer observations.

6.5 UNCERTAINTIES IN TOA RADIANCES

Table 14 assembles the principal sources of error encountered in calculation of TOA radiances from ground-based measurements according to two approaches: (1) conventional reflectance-based method using ground targets, and (2) a radiance method in which the BRF boundary condition is replaced by measured values of the reflected radiances at the boundary, obtained from PARABOLA, thus bypassing the need to calculate a BRF for the surface. Utility of the second method is that the TOA radiance estimate can be obtained from ground-leaving measurements confined to the time interval of overflight. Note here that the term “radiance method” refers to propagation of surface-leaving radiance through the measured atmosphere rather than measurement of upwelling radiance by an airborne radiometer; this latter method has been termed “radiance-based”. (3) A third formulation is possible in which the TOA radiance is written as a function of the surface HDRF. The HDRF is measured as a function of solar zenith angle for view direction normal to the surface using the ASD field spectrometer, but remains unmeasured for the remaining view directions required of the TOA radiance model. A full description of the HDRF must therefore be derived from the BRF using PARABOLA measurements. Hence except for normal incidence measurement, there is no advantage in working in terms of the HDRF as opposed to the BRF. The following Table 14, enumerates the principal factors and their sources either as measured quantities or as calculated from an atmospheric model. The notation is taken from *[M-5]*.

Table 14: Principal sources of error in TOA radiance derived from surface measurements

Method	**Path radiance (L^{atm})**	**Total and aerosol optical depths (τ. τ_{aer})**	**Atm. Trans. (T)**	**Incident radiance at surface (L^{inc})**	**Surface BRF ($R_{x,y}$)**	**Surface HDRF ($r_{x,y}$)**	**Surface reflected radiance (L^{refl})**
Method (1), Reflectance-based with BRF	Atm. model	Solar radiometry, aerosol model retrieval	Atm. model	PARABOLA measurement	PARABOLA measurement of $L_{inc,}$ L_{refl}, plus model calculation	Not required	PARABOLA measurement, part of BRF retrieval
Method (2), Radiance	Atm. model	Solar radiometry, aerosol model retrieval	Atm. model	Not required	Not required	Not required	PARABOLA measurement
Method (3), Reflectance-based with HDRF	Atm. model	Solar radiometry, aerosol model retrieval	Atm. model	PARABOLA measurement	PARABOLA measurement of L_{inc}, L_{refl}, plus model calculation	ASD measurement at normal incidence, otherwise PARABOLA + integration	PARABOLA measurement, part of BRF retrieval

The path radiance and atmospheric transmission function (T) calculated from the atmospheric model are themselves subject to uncertainty and have individual error budgets involving the factors involved, namely aerosol optical depth, aerosol size distribution, and aerosol compositional model.

The TOA radiance error budget is the subject of active investigation.

6.6 SCALING ISSUES

Differences in scale of observation between the ground-based and MISR observations are thought to represent a large possibly dominant source of uncertainty. The ground-based values are representative of smaller volumes of the atmosphere (aerosols) or surface (surface reflectance parameters) as compared to MISR. Table 15 lists the horizontal sampling of MISR aerosol and surface and surface irradiance parameters together with the estimated horizontal sampling of the ground-based procedures for these parameters.

The uncertainties over the MISR-reported areas will be estimated by measures of the scatter in reported values pixel-by-pixel over the averaged areas. The uncertainties in ground values will be assesses as: (1) averages in values over networks of surface stations (when and where available), together with standard deviations, (2) averages in optical depth over time series centered at and around the time of overflight, with scatter of values as estimators of the uncertainty.

Use of AirMISR in helping to resolve scaling issues will be required. Even here however, the MISR aerosol retrievals reported at 17.6 km will not be fully addressable and it will be necessary to use subsets of pixels over MISR local mode sites for this purpose. The chain of comparisons will then be from ground -> AirMISR -> MISR.

Table 15: Horizontal sampling of Level 2 aerosol and surface parameters

Parameter name	MISR horizontal sampling	MISR minimum horizontal sampling	Approximate ground-based sampling	Comments on ground-based sampling
Aerosol optical depth	17.6 km	275 x 704 m	~ 5 km (single station)	Depends on sky homogeneity and thickness of aerosol scattering layer. Optical thicknesses are line-of-sight to Sun, whereas almucantar scans depend upon solar zenith angle θ_0, and, in single scattering approximation, samples on the surface of a cone bounding a volume through the aerosol scattering layer(s) of half angle θ_0 about the zenith direction.
HDRF, BRF, BHR, DHR	1.1 km	275 x 704 m	r_s ~ 3.7 m for H= 1.0 m. H~25 m for r_s = 140 m or one-half pixel size (see comments)	Direct retrievals from PARABOLA III. To avoid horizon effects from topography and mixed pixels of sky and ground, vertical scan must be limited up to angle ζ above horizon. Effective sampling radius r_s is H$\tan\zeta$, where H is instrument height. Let $\zeta = 80°$ and desired radius =140 m. Then H~25 m.
Surface diffuse plus direct irradiance	scale not reported	275 x 704 m	~ 1 km(?)	Contributions at point dependent on solar zenith angle, and extent of multiple reflections between sky and ground, which depend on surface reflectance and sky turbidity.

6.7 EVALUATION OF MISR CALIBRATION, AEROSOL, SURFACE ALGORITHMS AND PRODUCTS

The goals of ground-based validation for MISR are: (1) to provide independent pathways for radiometric calibration of MISR on orbit using the so-called vicarious (reflectance-based) method and a radiance-based method with AirMISR as a well-calibrated radiometer, (2) to provide ground values of the spectral irradiance to compare with values generated by MISR aerosol and surface retrieval algorithms as intermediate products, (3) to provide values for important aerosol model parameters (size, refractive index, phase function, single scattering albedo) from ground measurements using mostly well-known inversion procedures operating on direct solar irradiance sky radiance and surface irradiance measurements, (4) to provide values of the local surface BRF for comparison with the MISR-retrieved values. For ground-based work each of these retrievals is accompanied by an analysis of the standard errors present, in is the subject of a continuing search for systematic errors (or biases) present. This section describes use of ground and aircraft values in evaluation of MISR products.

6.7.1 Radiometric calibration of MISR

Both vicarious and radiance methods and the radiance-based method with AirMISR are intended to supply TOA or near TOA radiances at all nine MISR observing angles for comparison with MISR radiances produced using pre-launch and, in-flight, the on-board calibrator results.

6.7.1.1 Reflectance-based.

The first of these calibrations will provide directly values of the MISR instrument response functions for a few MISR pixels at any given overpass. Statistical hypothesis testing to decide on significance of differences in coefficients will be carried out. A set of new values of the MISR calibration coefficients will be obtained by combining the ground-based and on-board calibration coefficients with weighting according to the standard errors present in each observation.

The calibration coefficients for each MISR camera so obtained, if differing statistically from original values, will be used to rederive MISR aerosol and surface parameters and irradiance values for a target area not involved in the vicarious calibration, to assess differences obtained and to assess improvements or degradations arising from the changes. These latter steps may be termed *validation of the calibration adjustments*. If significant improvements are found from a number of such intercomparisons, the decision may be required by the Principal Investigator to examine alteration of the calibration status of MISR in accordance with findings of the Calibration/Validation team.

6.7.1.2 Radiance-based.

The second of these calibrations, the radiance-based calibration, relies on the absolute radiometric calibration of AirMISR, which itself is based upon a preflight laboratory calibration, updates provided for a few pixels from vicarious ground-based calibration, and finally, possible use of the AirMISR PIN-diode on-board calibrator. The determination also depends upon timing and orientation of the AirMISR overpass to correspond precisely with that of MISR itself. AirMISR then provides radiances for 1504 pixels in its image array for four wavelengths and nine angles spanning a footprint on the ground of about 9 km transverse to the flight direction. The nine-km swath thus provides increased coverage of the MISR detector array and for calibration directly of the off-nadir camera angles.

The calibration coefficients for each MISR camera obtained from the radiance-based method depend upon the errors in the calibration coefficients derived from any vicarious and on-board calibration steps. Use of the vicarious method for AirMISR links the calibrations of AirMISR and MISR through the ground-based step. The on-board calibrator step is independent of all procedures connected with the vicarious calibration, and will be of great value, once its FOV is lowered to correspond to a potential surface target within which the FOV's of all nine angles can be encompassed.

We expect that radiance values reported by AirMISR will be accurate to $\pm$ 3%.

Statistical hypothesis testing to decide on significance of differences in coefficients obtained by these independent pathways will be carried out. The various independent determinations of MISR calibration coefficients, if found differing statistically as a result of these tests, will be combined, weighted by standard errors present in each step, to provide new radiance-based determinations. These coefficients too must be tested to verify or reject changes found from MISR on-board or pre-flight laboratory values. This step will involve comparisons of MISR-derived aerosol, surface and radiation parameters with surface-measured values.

6.7.1.3 Radiance propagation method

Application of the radiance propagation method will similar to the two methods just enumerated. This method produces TOA radiances whose values depend upon errors in the atmospheric model and in the calibration of PARABOLA. Statistical hypothesis tests will be used to determine if these calibration coefficients differ significantly from coefficients of the previous two methods, and combined with the other two weighting by uncertainties present. These coefficients must be tested to verify or reject changes found based on recalculation of MISR retrievals and comparison with ground-based values.

6.7.2 Spectral irradiance at the surface

Every successful MISR aerosol (and surface) retrieval produces a surface spectral irradiance from the SMART data set corresponding to the chosen best fit aerosol model and the derived surface HDRF (or BRF). The ground-based irradiance values are provided by measurements with MFRSR's at the ISIS stations. with measurements by an MFRSR and by PARABOLA at specific ground stations occupied as part of MISR algorithm validation or product validation exercises.

Although surface irradiances play an important role in ground-based aerosol model retrieval, the comparison of irradiances described here is an indicator flag primarily that differences between measured irradiances and those provided by application of the local MISR aerosol model do or do not exist. These observations can be used with modified MISR calibration coefficient determinations to check on possible improvements provided by updates, if any, to the on-orbit calibration coefficient values.

Reported values of the MISR irradiance over a local mode site at the surface at ~250 m resolution over a 17.6 km (on a side) area surrounding a given station will be obtained for these comparisons of irradiances. The pixel value corresponding to the actual station will be compared with the MISR retrieved value. The standard deviation of values over these areas will be used as a measure of the local scatter. The values of the actual measured surface irradiance may be possible using arrays of MFRSR's on occasions when cooperative experiments with specific investigators can be arranged.

We expect, based on calibration reports of the MFRSR manufacturer (Yankee Engineering), The measured irradiances from MFRSR will be accurate to ± 1% for newly calibrated instruments. Deviations between MISR-derived and surface-measured irradiance values greater than ±1% will be thought of as in disagreement. Statistical hypothesis testing to decide on significance of differences in measurements obtained will be carried out. An assessment of areal variability not measured by single ground stations will be required.

6.7.3 Aerosol models

Successful MISR aerosol retrieval report aerosol optical depth and adopted aerosol model properties at an areal scale of 17.6 km. The aerosol model includes specifying the log-normal and/or power law size distribution parameters and a compositional indicator (complex refractive index), the derived single scattering phase function, single scattering albedo computed according to Mie theory or according to a theory for nonspherical (*e.g.*,spheroidal) particles *[53]*.

For ground-based retrievals, the direct solar irradiance, solar aureole, sky radiance, and surface irradiance are (currently) combined to generate size and compositional estimates using a modified method of Nakajima *et al. [58]*. The JPL method of recovery *[M-7]* is being developed

further as a reparameterization in terms of single scattering phase function and single scattering albedo. This will avoid explicit introduction of the Mie theory and therefore the assumption of spherical homogeneous particles. Specification of an equivalent refractive index and size distribution will be dealt with as a separate retrieval problem. The generated ground-based aerosol model will be closed with respect to comparisons of radiances and irradiances calculated from the RTC employed and those measured at the surface and also with the upwelling directional radiances at AirMISR or AVIRIS, when aircraft measurements are available.

Differences between ground-based and MISR retrievals greater than the standard error present in each will be characterized as disagreements. Attempt to understand disagreements, if necessary, will begin by examination of the time variation of aerosol properties at the surface assuming that this variation reflects spatial variation of aerosol load, not simply in situ generation of particles (also possible). An alternative procedure will be to supply direct measurement through a network of Reagan radiometer or MFRSR stations.

Scaling of the local ground-based retrievals in a closer approximation to the 17.6 km area reported by MISR will require intervention of AirMISR. This chain of recoveries begins first with an intercomparison of local values from the ground study compared with local retrievals in the same site from AirMISR. AirMISR is then used to provide an estimate at the 9 x 10 km scale. Surface HDRF and BRF.

6.7.4 Surface HDRF and BRF

The surface HDRF is retrieved after a MISR aerosol recovery and subsequent to this the BRF. The HDRF/BRF is reported at a surface scale of 1.1 km.

The MISR HDRF is based on interpretation of the multiangle radiances in two azimuths, e.g., heading of about 190° and 10° for northern mid-latitude targets, for a single solar zenith angle. The accumulation of additional solar zenith angles for the site depends upon seasonal measurements. The MISR BRF is model dependent, arising from a fit of the observations to a specific BRF model involving three parameters *[M-5]*, namely the Rahman-Pinty-Verstraete model *[68]*.

The ground-based retrieval on the other hand employes the entire sky and ground hemispheres in 5° increments and is developed from all possible sun incidence directions for the local site. This implements the procedure described by Martonchik *[49]*.

Expected errors in the BRF recovery from PARABOLA measurements on homogeneous targets are on the order of 3%, including those of instrument calibration origin and algorithm errors arising with numerical solution of the governing integral equation.

The intercomparison between MISR retrievals and ground-retrievals based on PARABOLA thus can proceed either on basis of comparison of radiances from a combined atmosphere-surface model to retrieve on-orbit radiances, or by comparison of values of the model parameters from the surface PARABOLA observations fitted with the RPV model, with the MISR-derived parameters. The fitting of the PARABOLA-derive RPV model parameters will itself involve errors in the fit that are outside of uncertainties in deriving the BRF itself. A chi-square intercomparison of surface and AirMISR retrievals and local MODE MISR BRF retrievals will be sought. This is subject of ongoing investigation.

A principal source of differences seen is likely to arise in differences in surface area sampled by ground and by MISR observations. The area sampled by PARABOLA is proportional to instrument height above surface, and in practice is limited to circles of dimensions *O*(few hundred meters in diameter) To recover average values for areas as small as one MISR pixel (704 x 275 m) thus requires potentially many surface sampling stations. Intervention of AirMISR is essential. The chain of measurement is first, the BRF of a few AirMISR pixels will be determined to evaluate MISR like retrievals from aircraft height. Subsequently the measurement is extended to the 1.1 km scale using AirMISR.

6.8 DATA QUALITY

Prior to conducting postlaunch field campaigns, activities will be coordinated with EOSDIS to ensure the highest quality data stream during the time(s) of MISR overflight. Quality indicators planned for Level 2 data products are described in *[M-14]* and *[32]*. When these data products are retrieved for validation purposes, the corresponding quality indicators will be examined as part of the retrieval comparison procedure. In addition, the science validation team will participate in the selection and evaluation of these indicators.

Similar types of checks (*e.g.* instrument performance, physical constraints etc.) will be made on field experiment data as part of the reduction process, however, due to the much smaller volumes of data involved, this process will only be automated on an “as needed” basis. Intercalibration of field instruments will provide an additional measure of data quality.

7. INSTRUMENTS

7.1 APPROACH

Table 16 gives a summary description of the ground and aircraft based instruments used in MISR validation field campaigns together with their unique characteristics. The most frequently used instruments are listed ahead of those used less often. The following sections provide more details about these instruments.

7.2 MISR AIRCRAFT SIMULATORS

7.2.1 AirMISR

A description of AirMISR is given in Chapter 3 of this Science Data Validation Plan.

7.3 ANCILLARY AIRCRAFT INSTRUMENTS

7.3.1 RC-10 Aerial Mapping Cameras

Object height determination using photogrammetric techniques on stereo pairs of aerial photographs is a well-developed methodology. The principal means of validating cloud height retrieval algorithms that employ machine vision techniques, will be photogrammetric analysis of stereo aerial photography. Small scale stereoscopic aerial photographs (about 1/65,000), many with clouds, have been routinely acquired over the years aboard the ER-2 aircraft platform, in support of mapping projects for NASA as well as other government agencies. These data are routinely archived as part of large data bases at Ames Research Center and EROS Data Center, and can be accessed by reference to geographic coordinates and on basis of fractional cloud cover.

The principal aerial mapping camera used here will be the Wild-Heerbrug RC-10. The camera can be operated at focal lengths of 6”(152.33 mm) or 12” (304.66 mm) with film size of 9” x 9” format. Mounted on the ER-2 aircraft platform and operating at an altitude of 20 km, vertical photographs are acquired at an approximate scale of 1/130,000 or 1/65,000. The angular image field of view is ±20.5° about nadir, producing a square footprint on the ground 225 km^2 in area with ground spatial resolution under clear atmospheric conditions of a few meters. Acquisition of one photograph every 29 seconds at an aircraft ground speed of 400 knots (205 m/sec) generates stereophotographic pairs with about 50% overlap with photo centers spaced nearly 6000 meters apart.

Table 16: MISR Science Data Validation Instruments

Instrument	Description	Spectral Range	Characteristics/Uses
AIRCRAFT			
AirMISR	Airborne MISR Simulator. Flies on ER-2.	446, 558, 672, 866 nm	Produces calibrated, multi-angle, spectral imagery from ER-2 platform operating at 20 km altitude (close to top-of-atmosphere) over MISR angular range +70.5° forward, -70.5° aftward
AVIRIS	Airborne Visible/Infrared Imaging Spectrometer. Flies on ER-2.	224 channels; 400 - 2500 nm	Produces 20 m resolution multispectral images and near TOA calibrated radiance measurements
Wild-Heerbrug RC-10	Aerial camera mounted on ER-2. Takes stereophotographic images from 20 km altitude with resolution of a few meters (clear atmosphere)	VIR	Provides stereo aerial photos for validation of cloud height retrieval algorithms using conventional stereophotogrammetric methods.
MAS	MODIS Airborne Simulator, flies with CALS, SSFR on ER-2	50 channels, 547-14170 nm	Utilized for estimation of cloud top pressure (height) from CO_2 split window technique and cloud water phase other thermal infrared channels *[43]*.
CALS	Cloud and Aerosol Lidar System, flies with MAS and SSFR on ER-2	532 nm	Polarization Lidar. Determination of vertical distance between cloud tops and sensor, cloud top structure, cloud microphysics and dynamics *[64]*,*[76]*.
SSFR	Solar Spectral Flux Radiometer on ER-2 platform	250-2500 nm, $\Delta\lambda$ = 5-10 nm	Calibrated instrument measures simultaneously solar spectral irradiance and spectral radiant exitance over downward and upward hemispheres from which local spectral albedo is obtained. By integration over spectrum, determines total spectral irradiance, radiant exitance, and albedo (250-2500 nm)

Table 16: MISR Science Data Validation Instruments

Instrument	Description	Spectral Range	Characteristics/Uses
GROUND			
Reagan #1	Auto-tracking, auto-recording sunphotometer	10 channels; 380 - 1028 nm	Measures direct solar irradiance for determination of aerosol spectral optical depth, ozone optical depth, column abundance of water and particle size distribution
Reagan #2	Auto-tracking sunphotometer	10 channels; 380 - 1028 nm	“
Reagan #3	Manual sunphotometer	10 channels; 380 - 1028 nm	“
Reagan #4	Manual sunphotometer	10 channels; 380 - 1028 nm	“
MFRSR	Multifilter Rotating Shadowband Radiometer	6 channels + 1 broadband; 414 - 931 nm	Independent determination of downwelling total irradiance and separation into sky and direct solar components. Used with models to retrieve surface albedo and imaginary part of the aerosol refractive index. Irradiance data for comparison with MISR retrieved values at the surface.
PARABOLA III	Portable Apparatus for Rapid Acquisition of Bidirectional Observations of the Land and Atmosphere. Sphere-scanning multispectral radiometer	8 channels; 443 - 1650 nm	Measures downwelling irradiance incident at the surface in 5° FOV’s over upward hemisphere. Measures surface reflected radiance in 5° FOV’s over lower hemisphere.
CIMEL	Sunphotometer and sky radiometer with polarization	9 channels; 340 - 1020 nm	Measures direct solar irradiance for aerosol optical depth, radiance in solar almucantar and in principal plane for aerosol size distribution and single scattering phase function

Table 16: MISR Science Data Validation Instruments

Instrument	Description	Spectral Range	Characteristics/Uses
GROUND (cont.)			
ASD	Analytical Spectral Devices Field Spectrometer. Portable, light weight, battery powered instrument for taking rapid spectra of ground targets	350 - 1000 nm 900 - 1800 nm 1700- 2500 nm	Rapid acquisition of spectra allows quick determination of average spectral bidirectional reflectance of large natural target areas over extended spectral range.
Whole sky/ ground cameras	A pair of Nikon N8008 SLR autofocusing film cameras with 180° fisheye lenses	Visible	Monitors cloud cover, determination of cloud top/bottom height from stereo views, cloud speed from image sequences.
Davis Weather Monitor II	Weather station	N/A	Continuous measurement, at ground level, of air temperature, wind speed and direction, atmospheric pressure, relative humidity and rainfall
Magellan GPS	NAV 5000 PRO GPS unit.	N/A	Determines geographic location within ~50 m (stand-alone) or within ~1 m if used in a differential mode
Albdeometer	Kipp and Zonen Model CM 7B	300-3000 nm,	Measures global (diffuse + direct) total irradiance and radiant exitance at the surface, 2%
GER	Geophysical Environmental Research Corporation Spectrometer	programmable intervals; 400 - 2500 nm	Makes moderate resolution measurements of spectral bidirectional reflectance of surface targets, spectral optical depth of atmosphere
Cloud sounding radar (94 GHz), SGP ARM site	Ground-based radar operating at 94 GHz (3 mm). 3 dB beam width of about 0.24°.	94 GHz (3 mm)	Used for determination of cloud tops, cloud bottoms and internal cloud structure (reflections from multiple cloud layers) from ground.

7.3.2 AVIRIS

The Airborne Visible/Infrared Imaging Spectrometer (AVIRIS) is a whiskbroom imaging spectrometer that produces images of spectral radiance in 224 channels (each approximately gaussian and 10 nm FWHM) between 400 and 2500 nm. The instrument flies aboard the ER-2 aircraft platform at an altitude of 20 km above terrain. At this flight altitude the side to side angular field-of-view of ±15° about nadir generates an image swath approximately 11 km in width with pixel size of 20 m. The areal coverage rate determined by ER-2 ground speed is approximately 12 image lines/s (110 km^2 in 40 s).

AVIRIS is used for rapid mapping to atmospheric precipitable water distributions using the 940 nm water vapor absorption band, and for determination of calibrated TOA radiances. With respect to the latter, the whiskbroom nature of this scanner determines that the vicarious calibration method using ground targets can be used with surface reflectance measurements on just a few 20 m size pixels to place a radiometric calibration on the instrument. This calibration is independent of both on-board and laboratory pre-or post-flight calibrations. This determines that near-TOA radiances are known from all pixels over the approximate 11 km image swath of AVIRIS. When co-flown with AirMISR, this facilitates calibration of the entire AirMISR sensor array which otherwise would require measurements on a target of 10 km linear dimension for a stand-alone calibration by the vicarious method. For this purpose the calibration of AVIRIS is checked by independent vicarious calibration in circumstances where AirMISR and AVIRIS are co-flown.

7.3.3 MODIS Airborne Simulator

The MODIS Airborne Simulator (MAS) is a 50 channel cross-track scanning spectrometer consisting of four spectrometers and detector assemblies with linear array detectors, covering the wavelength range 547-14170 nm *[43]*. Nineteen of the 50 channels correspond to those of MODIS, including near and thermal infrared bands that provide information about cloud properties and temperature. MAS flies aboard the ER-2 platform and is designed to scan through nadir in a plane perpendicular to the direction of motion of the aircraft with maximum scan angle extending to ± 43 ° (side to side) of nadir. From the 20 km operational altitude of the ER-2 this corresponds to a total swath width of about 37 km. Each pixel (total of 716 Earth-viewing) has an IFOV of 2.5 mrad that represents spatial resolution of 50 m at nadir.

MAS will be utilized for estimation of cloud top pressure (height) and cloud water phase from CO_2 split window technique and other thermal infrared channels *[31]*.

7.4 FIELD RADIOMETERS AND SPECTROMETERS

7.4.1 Reagan Solar Radiometer

These instruments are used for determination of atmospheric aerosol spectral optical depth,

estimation of ozone optical depth (ozone column abundance), and the column abundance of atmospheric precipitable water. The so-called Reagan radiometers are manufactured by J.A. Reagan, and associates at University of Arizona. The instruments are portable (battery powered) and automatic sun-tracking. They contain 10 spectral bands with typical filter wavelengths ranging from 380 nm to 1028 nm with full-width-half-maximum (FWHM) filter bandwidths of 7 to 17 nm. Four such instruments are available (two manual, two automated tracking). Automated Sun tracking is implemented using a four element "quad" detector mounted in a tracking telescope that is coaxially aligned with the optical system of the radiometer head. Tracking accuracy is ±0.05°. Altitude and azimuth movements of the radiometer head telescope are carried out by stepper motors with a 0.025°step angle. The larger FOV tracking system maintains solar tracking even in the presence of occasional small cloud interference. The automated data acquisition system is microprocessor controlled. The instrument noise level is less than the quantization error or one part in 65,536. Data collection is possible for a maximum single period of one day (sunrise to sunset) at time intervals adjustable from a minimum of 10 seconds to several minutes.

7.4.2 PARABOLA III

The Portable Apparatus for Rapid Acquisition of Bidirectional Observation of the Land and Atmosphere (PARABOLA) is a sphere-scanning multispectral radiometer system that generates radiance measurements from a transportable platform mount over complete downward (ground) and upward (sky) looking hemispheres. The instrument contains eight channels distributed four each on two scanning heads. The channels are 440, 550, 650, 860, 940, 1030 and 1665 nm each 10-20 nm in width, plus a PAR sensor (400-700 nm). The sensor field of view is 5° with partial vignetted field extending to 8° full angle. A complete scan of the head over 4π Sr. requires 3.3 minutes including off loading of the scan data to files on a microprocessor memory. The microprocessor can be programmed to scan repetitively. The dynamic range is 2^{20} so that, for example, direct solar irradiance and dark vegetation or water targets can be encompassed within a single scan without need for gain changes.

Radiometric calibration of PARABOLA is carried out in the laboratory using the MISR integrating sphere, in the field using the Langley method, and also by placing neutral density filters over the instrument apertures to get instrument response over six orders of magnitude light intensity.

PARABOLA III observations will be utilized to calculate BRF's of surface targets, and by spatial integration the hemispherical directional and bihemispherical reflectances (HDR and BHR respectively) plus the downwelling total and diffuse irradiances at the surface.

7.4.3 CIMEL Sun and Sky Radiometer System

The CIMEL CE 318-3 (CIMEL Electronique, Paris, France) Sun/sky radiometer system is a

fully automated weather-resistant, battery and solar panel-powered instrument capable of long-term independent operation for measurement of direct solar irradiance and sky radiances used for determination of atmospheric optical depth and aerosol scattering and absorption properties by the use of certain inversion techniques described below. It is the principal instrument of the AERONET network (Holben, *et al*., *[30]*) Two 33 cm collimators on the sensor head feed two detectors for measurement of direct sun, and aureole and sky radiance. The full-angle field of view is 1°, with stray light rejection in the collimated beams of 10^{-5}. Eight interference filters, each having a 10 nm bandwidth, are contained in a filter wheel. These are located at wavelengths of 300, 340, 380, 440, 670, 870, 940, and 1020 nm. Polarizing filters are provided to give skylight polarization at 870 nm in vibration directions of 0°, 60°, and 120° to the principal plane of sun incidence. Detector temperatures are monitored with thermistors to compensate for temperature variations.

The sensor head is attached to a robotic mechanism that carries out direct beam solar measurements as well as sky radiance measurements in the solar almucantar and in the solar principal plane. The head is moved by direct drive stepper motors with pointing accuracy of ± 0.05°. A microprocessor contains a solar ephemeris that computes the position of the sun to within about 1°; subsequent precise solar location and tracking are carried out by quadrant detector. During inactive or wet periods the head is returned to a downward pointing parked position to protect the optics from dust, pollen, soot, ash, and moisture etc.

7.4.4 MFRSR

Independent determination of the downwelling sky irradiance will be obtained with a Multi-Filter Rotating Shadow Band Radiometer (MFRSR), manufactured by Yankee Environmental Systems Inc. The MFRSR is a portable instrument that determines nearly simultaneously global, diffuse, and direct components of the solar spectral irradiance. From these measurements it is possible to estimate imaginary part of the aerosol refractive index as well as an average surface Lambertian reflectance by the so-called diffuse-direct method.

MFRSR uses independent interference filter-photodiode combinations that are mounted in a temperature-controlled enclosure for measurement of spectral irradiance at six wavelengths and one broad channel. Observations at 616 nm and 931 nm also give determinations of ozone and water vapor optical depths and column abundances as a function of time.

The MFRSR uses an automated rotating shadowband to make measurements of the global and diffuse solar irradiance components. The shadowband is a strip of metal formed into a circular arc and mounted along a celestial meridian with the instrument entrance aperture at the center of the arc. The shadow band blocks a strip of sky with 3.3° umbral angle which is sufficiently wide to occult the direct solar beam plus adjacent aureole components. Two additional observations 6° to either side of the Sun are made to correct for excess sky that is blocked during the Sun occultation measurement. An entire measurement sequence (four measurements) is completed in 15 sec-

onds and can be programmed by the controlling microprocessor to occur up to two times/minute. At each measurement cycle the shadowband is positioned for solar occultation by computing the sun's position using an approximation to the solar ephemeris contained in the microprocessor. This latter function requires accurate orientation of the instrument to level and with respect to north.

This instrument is calibrated by the manufacturer using an integrating sphere whose irradiance is traceable to NIST standards. Newly calibrated, the instrument is said to provide measurements to 1 percent absolute

7.4.5 GER field spectrometer

The Geophysical Environmental Research Corporation Spectrometer (GER) field spectrometers are employed to place the spectrally widely placed spectral measurements of MISR's channels for aerosol optical depth and surface spectral reflectance within a broader spectral context. A moderate resolution field instrument, the GER is a self-contained portable single beam grating spectrometer system designed for observations of light levels typical of terrestrial land surfaces. The spectrometer covers the wavelength region 350-2700 nm with spectral resolution ~1.5 to 12.0 nm. Data acquisition and recording are microprocessor-controlled. The output signal is sampled in wavelength every ~0.5 to 6.0 nm and converted to 12 bit digital data in the microcomputer. The wavelength scan interval as well as other functions are programmable. A complete spectral scan 400 to 2500 nm requires about 40 s.

The GER spectrometer is employed in the field to provide moderate resolution measurements of spectral bidirectional reflectance of surface targets and to carry out moderate spectral resolution measurements of atmospheric transmittance using a specially designed sun-tracking mount. These measurements are useful in their own right, first providing moderate resolution optical depth determinations, and second intercomparisons with determinations from the sunphotometers. Since the GER is a grating instrument it is not subject to the same degradation of the dispersing element from solar radiation as are interference filters. Thus systematic changes between responses of the two types of instruments may help to pinpoint otherwise difficult-to-detect changes in sunphotometer performance.

7.4.6 ASD field spectrometer

The Analytical Spectral Devices (Boulder, Colorado) Field Spectrometer (ASD) is a portable, light weight, battery powered instrument that uses a trifurcated fiber-optic cable to sample the light field being measured. Inside the instrument the supplying fiber-optic bundle within the cable is divided into three bundles. Each of these delivers the collected radiation to the entrance slit of one of three spectrometers. Technically the instrument provides measurement of the surface spectral HDRF at normal viewing, when output is compared to Spectralon field reflectance standards and corrections made for reflectance of Spectralon. The ASD spectrometer analyses radiation in

the spectral range 350-2500 nm using three spectrometers (I, II, III). Spectrometer I uses a 512 element silicon photodiode array coated with an order separation filter and covers the wavelength region 350-1000 nm (VNIR) with sampling interval 1.4 nm. The VNIR spectrometer has spectral resolution (FWHM) of approximately 3 nm. The short-wave infrared (SWIR /NIR) portion of the spectrum is covered by two scanning spectrometers. Both employ light dispersal with holographic concave gratings and thermoelectrically cooled InGaAs detectors. The first of these spectrometer (II) covers the interval 900 nm to 1800 nm and the second (III) from 1700 nm to 2500 nm. The spectral sampling interval is 2 nm and spectral resolution 10-11 nm. The fiber optic cable has a full view angle of 25 ,with special attachments allowing restriction to 8 .The total spectral acquisition time is rapid on the order of a few seconds to accumulate averages of 10 spectra, but depending in detail on integration time options chosen, making the instrument very useful for rapid acquisition of large numbers of ground spectra that may be coadded, and which therefore can be used to form average HDRF reflectances of large natural target areas. Rapid measurement of one or two km length targets is required for in-flight calibration of the pushbroom ASAS sensor, for example and areas of this order and larger are contemplated for vicarious calibration of MISR. The instrument in particular is useful for calibration of nadir-viewing sensors and for gaining measures of the variation of reflectance from place to place to form statistical pictures of the variability.

7.5 ANCILLARY FIELD INSTRUMENTS

7.5.1 Air Research Corporation balloon-borne tropospheric sounder

The Air Research Corporation balloon tropospheric sounding system is used to determine the distribution of relative and absolute humidity through the boundary layer. The system consists of the Airsonde balloon-borne instrument package and a ground station known as the Atmospheric Data Acquisition System (ADAS). The Airsonde package transmits measurements of each sensor it contains by RF telemetry at a frequency of about 400 MHz to the ADAS. The basic Airsonde sounder package makes measurement of atmospheric pressure, as well as hygristor sensors to determine relative humidity. ADAS calculates relative humidity, records elapsed time and sends the data to a laptop computer. ADAS can be operated stand-alone with internal or external battery power for operations remote from line power. The atmospheric data received by the station are displayed in real time every 5-6 seconds for manual recording if necessary. No tracking of balloon ascent is done apart from independent measurements by theodolite. Balloon altitude is inferred from atmospheric pressure. Pressure altitudes of about 100 mb have been achieved. The relative humidity recorded by the package at the surface prior to launch is used to correlate readings with those from an automated surface weather station, described below.

7.5.2 Whole-sky and whole-ground camera system

Routine monitoring and recording of ground shadow patterns and sky and cloud cover conditions will be carried out to support PARABOLA III and sunphotometer observations using a pair of Nikon N8008 single lens reflex autofocusing film cameras. In addition, image sequences gath-

ered automatically with pairs of cameras at selected time intervals will be used to estimate cloud motions and cloud base (and top) heights. These cameras are equipped with 8 mm f/2.8 Fisheye-Nikkor lenses and Nikon MF-21 Multi-control databacks. The fisheye lenses records every object in a full 180° hemisphere and produces a circular photographic image 23 mm in diameter on film.

7.5.3 Davis Weather Monitor II

We employ a Davis Weather Monitor II™ weather station to determine local surface meteorological variables on a continuous basis during field experiments. The system components include weather computer, temperature, wind speed and direction, atmospheric pressure and relative humidity and rainfall amount sensors. Time and date are automatically recorded. The data can be fed via a standard serial port to laptop computer for permanent storage and display.

7.5.4 Magellan Global Positioning System

To determine geographic position we use a Magellan Systems Corporation NAV 5000 PRO GPS unit. The NAV 5000 PRO uses up to five channels working simultaneously to locate and collect data from the GPS satellites. Rapid processing by the unit allows computation of current position, altitude, velocity, and navigation data in less than one minute. Updates are produced every second. The instrument calculates altitude as either height above the ellipsoid of choice or elevation above mean sea level. The unit is generally capable of 50 m (RMS) horizontal accuracy in stand-alone operations. The instrument can store up to 1500 position fixes, which can be downloaded to a PC for monitoring of position changes which may be important during observations while under way at sea.

Differential GPS techniques afford better than 1 meter accuracy when two units are used (one at a known location). This technique will be used to measure the relative placement of experiment site features and the geographic locations of MISR pixels at all viewing angles. This will allow efficient and rapid locations for delineation of ground measurement areas. Most detailed features especially on uniform targets (dry lake beds) are not readily discernible from topographic maps alone or possibly even aerial photography unless the sites happen to be marked, such as by colored tarpaulins.

7.5.5 Kipp and Zonen Albedometer

The Kipp and Zonen Albedometer Model CM 7B is a precision instrument that measures independently global (direct plus diffuse) total solar irradiance, coupled with total radiant exitance at the surface. The two observations combined as the ratio irradiance/radiant exitance yield the surface albedo. The spectral response is 300 to 3000 nm with a resolution of 2 W/m^2. The azimuthally independent cosine response is known better than 1% for zenith angles less than 75°, and 2% between 75 °and 90°. The instrument is ruggedized for field use but may be operated under both field and laboratory conditions.

The principal uses of pyranometer measurements are to provide direct connections between the spectral values of the downwelling irradiance measured by the sunphotometers and other field instruments (MFRSR, PARABOLA III) and the total solar irradiance incident at a site. The instrument will also allow inference of the presence of clouds by departures from expected clear sky irradiances, an important factor in interpretation of MFRSR data for the direct normal incident radiation. The total albedo (*e.g.*, *[82]*) is a quantity of importance to radiation balance studies is a function of solar zenith angle and cloud cover, and will provide important connections to measurements in the SURFRAD network *[28]*, and in relation to CERES validation *[9]*.

8. RADIATION NETWORKS, LONG TERM SITES, AND ARCHIVES

8.1 INTRODUCTION

Achievement of the long term global product validation goals of MISR depends upon the existence of networks and special sites that provide continuous well-calibrated surface and other atmospheric observations relevant to MISR's products, and upon special sites that offer unique infrastructure to study surface cover. Two radiation networks, AERONET and ISIS, the ARM CART site, and the BOREAS experiment site, together with other special vegetation sites are described in this chapter. The BOREAS experiment area has been used for a MISR algorithm validation experiment over a dense dark vegetation (DDV) canopy.

There are pre-launch and post launch uses of the networks planned for validation, both of which have the same goal, comparison of ground-based retrievals from the networks using well established algorithms, with retrievals using MISR algorithms via AirMISR or MISR observations for intermediate radiation quantities (surface radiances and irradiances), aerosol properties. and possibly BHR. at selected stations. The following pertains mostly to aerosol retrievals.

In pre-launch time overflights of AirMISR are planned at selected stations to provide point comparisons in time of the remote retrievals with the ground-based retrieval time series.

In post-launch time the ground-based time series from many widespread stations, representing the maximum range of aerosol types and concentrations and environmental conditions, will be correlated with an accumulating time sequence of MISR retrievals.

Both pre- and post-launch types of intercomparisons will be accompanied by estimates of the uncertainties involved in each pathway. The point intercomparisons plus associated error budgets will constitute the basis for validation of the MISR products and will hopefully lead to better understanding of scaling issues between the ground-based validation path and the MISR retrieval path.

8.2 GROUND RADIATION NETWORKS

8.2.1 AERONET

A network (Holben, *et al*., *[30]*) of 50-60 weather-resistant fully automated CIMEL sun/sky photometers accumulating observations at seven wavelengths (including water vapor) between 340 and 1030 nm is under development and deployment over five continents and a few marine sites by investigators at NASA/GSFC. The purpose is to assess long term time-dependent aerosol concentrations and properties at remote sites. The system transmits data from individual solar radiometers using the Geostationary Data Collection System. Real time inversions of both direct solar and sky radiance observations generate time-dependent aerosol optical depth, size distribution, phase

function, and atmospheric column water vapor content at each site and perform an assessment of instrument calibration and health. The Sun/sky radiometer data are accumulated in a data base to provide a long term continuous climatology of aerosol concentrations and properties over the network. The network will provide a direct means of near real-time validations of atmospheric aerosol abundance and property retrievals derived from analysis of MODIS and MISR top-of-atmosphere radiance measurements in a diverse series of important globally-distributed aerosol environments.

The MISR validation team will use our own CIMEL instrument to derive intercomparison data sets with a few of these network instruments, as a basis for mapping CIMEL aerosol values onto those derived by MISR. We will further maintain a local CIMEL station contributing to the database as part of the network as a further basis for judging MISR data quality. An ever present issue is relevance of a point aerosol measurement relative to a MISR value (250 m minimum areal size). Networks of a few MISR solar radiometer stations locally (~km spacing), plus correlated time dependent records from each, will be used to estimate areal variability of aerosol load and how good an estimator the record from a single station is in mapping variability of larger tropospheric air volumes.

In the pre-launch phase of MISR aerosol algorithm validation the principal objective will be to intercompare retrievals of aerosol optical depths, size distributions and phase functions achieved with the CIMEL instruments and associated inversion software with aerosol loadings and properties derived from inversion of measurements with the Reagan sunphotometers, our CIMEL instrument, PARABOLA III direct and sky radiance measurements, and the MFRSR.

Distribution of CIMEL radiometers in AERONET - The current GSFC operational network of automated sunphotometer stations is described in *[30]*. Locations of some of these stations and the dominant aerosol type expected, are given in Table 17. A map showing the distribution of both

Table 17: Compilation of long- and short-duration automated sunphotometer (CIMEL) sites and expected average aerosol types

Network Station Location	Aerosol Type
Brazil	biomass burning, background continental
Central Canada (BOREAS)	high latitude continental, biomass burning
Europe	sulfate, background continental
Long Term Ecological Reserve (LTER)	desert, eastern continental, high-latitude continental, maritime
West Africa	eolian dust, background continental
Oceanic Islands	marine/oceanic
Short Term Moveable	industrial pollution, sulfate, forest fire smoke, background continental, desert, oceanic

seasonal and permanent stations and corresponding to MISR local mode sites is shown in the Appendix, Figure A-1.

8.2.2 ISIS

NOAA Integrated Surface Irradiance Study (ISIS) is a surface radiation monitoring network in the United States recording continuously the diffuse and hemispheric solar spectral irradiance at a group of stations using a seven channel shadow band radiometer, MFRSR. The instrument array was selected to conform with recommendations of both the WMO, Baseline Solar Radiation Network (BSRN) sponsors and U.S. scientists. The network is carefully maintained and calibrated. The ISIS stations will be a network independent of AERONET supplying optical depth measurements on a continuous basis for comparison with MISR retrievals. In addition, values for the downwelling (and upwelling) irradiance at the surface will be used to compare with the incident irradiance calculated from the MISR retrievals. We will use our own MFRSR instrument to derive intercomparison data sets between a few of these network instruments as a basis for mapping MFRSR aerosol values and irradiances into those derived by MISR and for study of problems of instantaneous aerosol variations. See the Appendix, Figure A-2, for locations of the stations.

8.2.3 IMPROVE Network

The Interagency Monitoring of Protected Visual Environments (IMPROVE) network consists of 30 original monitoring sites used to monitor and protect Class I visibility areas, national parks and national wilderness areas larger than about 20 square kilometers in size. See Eldred *et al., [17]*; Malm *et al., [48]*. Optical monitoring with transmissometers and nephelometers is now being conducted at 18 sites. In addition monitoring of particulate size and composition is carried out on a twice weekly basis to establish connections between visibility degradation and the responsible particulate agents. Some of the IMPROVE network sites will be monitored as part of MISR local mode retrievals to examine connections between MISR aerosol retrievals, local visibility of the atmosphere and size and chemistry of the particulate agents involved.

8.3 LONG TERM SITES

8.3.1 ARM CART

The Atmospheric Radiation Measurement (ARM) program focuses on atmospheric measurement and modelling, emphasizing tests of parameterizations of cloud and radiative processes used in atmospheric models *[78]*. The Cloud and Radiation Test Bed (CART), Lamont, Oklahoma, is the facility providing continuous observations for the testing of models. In addition to the ARM CART site, Oklahoma, two additional sites are planned, a Tropical Western Pacific location and a site on the North slope of Alaska. These taken together provide coverage under virtually all relevant climatic conditions. Of special importance to long term MISR validation goals are the following instruments and measured quantities:

(1) Multifilter upward and downward-looking radiometers mounted on 10 m and 25 m towers -bihemispherical reflectance estimate as function of solar zenith angle.

(2) Belfort Laser Ceilometer - cloud height, extinction coefficient, cloud layers.

(3) Multi-Filter Rotating Shadowband Radiometer (MFRSR) - direct normal, diffuse horizontal and total horizontal solar irradiances, derivation of atmospheric multispectral optical depth, column ozone abundance, column water vapor abundance, column aerosol optical depth. Two of these instruments are co-located, one mounted on a 10 m tower, downward looking, the other at the surface, upward looking, provide estimates of surface bihemispherical reflectance.

(4) Whole sky imager (WSI) - cloud field and cloud field dynamics over upper hemisphere.

(5) Aerosol Facility - aerosol optical absorption, multispectral integrating nephelometry, optical particle counter, condensation particle counter, tropospheric ozone monitoring.

(6) Wind, temperature and humidity sounding systems - Balloon-borne sounding system, Radio Acoustic Sounding System (wind profilers), Multifilter Rotating Shadowband Radiometer (MFRSR) network.

8.3.2 BOREAS

The Boreal Ecosystem-Atmosphere Study (BOREAS) was a major deployment of US and Canadian scientific resources. US efforts were sponsored and coordinated by NASA. The BOREAS experiment site in central Saskatchewan is included here because of the significant tower infrastructure present suitable to MISR validation needs in boreal forest canopies, and because of the possibility (resources permitting) that the site may be revisited for measurement of BRF in the post-launch time frame. A summary of results from the 1994 field campaign is given in *[72]*.

The principal focus of BOREAS is on biological and physical characterization of major and minor forest canopy components and upon measurement of fluxes of CO_2, methane, and other trace gases, latent and sensible heat between canopy and atmosphere. Precipitation, soil, atmospheric and runoff water measurements are also made. Accurate mass and energy flux measurements are provided at three so-called flux tower sites located in homogeneous areas of Old Aspen (OA), Old Black Spruce (OBS), and Old Jack Pine (OJP) forest cover. The PARABOLA instruments were deployed at each of these sites suspended 15 m above as well as within each canopy near the surface, both on cable tramways. The in-canopy measurements will be used to estimate FPAR for these canopies. The above-canopy observations provide downwelling directional sky radiance as well as canopy-reflected radiance as a function of solar zenith angle. The PARABOLA, mounted on its tower to tower tramway infrastructure, provides an average representation of average forest canopy reflecting properties over the horizontal span of 70 meters.covered b the tramway. Such tower facilities enable measurements on canopies of such large stature (about 15 m tree height).

8.3.3 MISR Local Mode Sites

MISR Local Mode sites are sites that will be acquired post-launch on a regular basis at the full MISR spatial resolution of 275 m and along-track length of at least 17.6 km Such sites have special uses such as support of the vicarious calibration of MISR, as well as aerosol, surface, and TOA/Cloud scientific product retrievals. For example, potential local mode MISR sites for aerosol, surface, and radiation product retrievals include stations of the AERONET, the ISIS network, and the SGP ARM site. An additional local mode site for which long term aerosol, surface irradiance, and reflectance observations are planned at the surface is the Jet Propulsion Laboratory (site coordinates are Lat. 34°11′54″;Long. 118°10′20″). This site will be instrumented with CIMEL, MFRSR, and PARABOLA and a meteorological station recording surface wind speed, direction, atmospheric pressure, temperature, and relative humidity. All of these instruments are outfitted to record long term observations with at least 30 sec sampling interval or longer. Nearby at JPL (*e.g.*, *[52]*), a ground-based CO_2 lidar is operated on a weekly to twice-weekly daytime basis and provides long term altitude- dependence and range of variability of aerosol backscatter profiles over the Pasadena site. These lidar data will be available for interpretation and intercomparison with our on-going accumulations of aerosol abundances and microphysical properties.

8.3.4 Wind River Canopy Crane

The Wind River Canopy Crane research facility is a forest system observatory managed by the University of Washington College of Forest Resources, USDA Forest Service Pacific Northwest Research Station and Gifford Pinchot National Forest. The crane itself is 250 ft tall and has a load jib that is 280 feet long. The gondola can rise 225 feet into the air or be lowered in almost any location in a 550 foot circle, giving access to more than 2.4 hectares of old growth canopy consisting of Douglas Fir and Hemlock.

The crane provides a site for long-term monitoring of canopy BRF and easy access vertically through the canopy to perform light attenuation measurements. The crane facility will be used as a long-term local mode site for monitoring of canopy reflectance and correlation studies of biophysical parameters.

8.4 ARCHIVES

8.4.1 Global Energy Balance Archive

The objective of the Global Energy Balance Archive (GEBA) (*[59]*, *[60]*) is to organize instrumentally measured energy fluxes from stations distributed over the globe and representing contributions from greater than 800 stations among which were more than 130 stations (1988) with more than one year's net radiation measurements. This number is expected to be substantially greater at the present time. The main sources of data are periodicals, monographs, data reports and unpublished sources, which has led to unevenness in quality control, but a major effort has been

instigated to upgrade quality of all observations selected for the database. Among the uses that have been made of the Archive are validations of radiation calculations by GCM models *[22]*, and in studies of discrepancies between models and observations in the disposition of solar energy within the Earth's climate system *[88]*.

Among the recorded data are direct solar radiation and diffuse sky radiation which are of principal interest to post-launch MISR validation activities at stations represented in the Archive. The predominance of these stations from around the world are in addition to those presently represented in the ISIS and AERONET networks.

9. FIELD EXPERIMENTS

9.1 APPROACH

Definition - A *field experiment* is a coordinated group of activities carried out under chosen atmospheric and surface conditions designed to provide data for comparison of two geophysical parameter retrievals based on independent measurements and techniques. The retrievals are those of the ground-based and the MISR-based paths. The focus here is: (1) to test MISR retrieval algorithms (pre-launch) or data products (post-launch) for differences present between ground-based and MISR-based approaches, (2) to provide periodic on-orbit (vicarious) calibrations of MISR using natural ground targets, surface, atmospheric and radiation measurements.

Definition - A *field campaign* is an activity that involves conducting one or more field experiments.

The purpose and methods employed for each of these experiments are defined as follows: Section 9.2 describes calibration and intercalibration of ground based field instruments; Section 9.3 discusses field calibration of MISR simulator and other aircraft instruments. The methods used here are closely related to those to be used for vicarious calibration of MISR itself in flight; Section 9.4 discusses TOA radiance intercomparisons; and finally, both algorithm validation and product validation are covered in Section 9.5, since such experiments will typically be performed simultaneously during post-launch campaigns.

9.2 CALIBRATION AND INTERCALIBRATION OF FIELD INSTRUMENTS

9.2.1 Purpose

Calibration provides the constants for conversion of instrument response to radiance or irradiance (SI) units. Establishing and maintaining the calibration of field instruments is crucial for retrieval of accurate time-series of atmospheric optical depths and aerosol properties that may be: (1) intercompared from one time to another, or (2) intercompared between geographically separated stations.

The previously described methods (Section 3) for retrieval of aerosol microphysical models and surface reflectance depend upon the use of multiple field instruments. Hence knowing the relationship between instrument responses in terms of radiance and irradiance units is necessary.

9.2.2 Methods

Calibration for the JPL field instruments described here, constitutes: (1) radiometric determination of V_0,the zero airmass instrument response, (2) determining spectral response functions of individual channels, (3) determining cosine response of the MFRSR, (4) providing for traceabil-

ity of radiometric calibrations to NIST standards that provide SI units.

Instrument and method intercomparison campaigns constitute exercises among different EOS instrument groups (for example, MISR, MODIS, ASTER) for intercomparison of atmospheric optical depth retrievals, measurements of surface spectral reflectance, intercomparison of radiative transfer codes leading to intercomparison of TOA radiance determinations. Preliminary results from one such campaign have been reported by Thome, *et al. [85]*.

9.2.2.1 Determination of radiometric instrument calibration: laboratory and field

Radiometric calibration is carried out in the laboratory using NIST- traceable standard lamp observations or observations with the MISR integrating sphere used to provide pre-launch laboratory radiometric calibration for MISR. The laboratory calibration of MISR and characterization of the calibration sphere is described in *[M-11, M-12]*. The MISR integrating sphere itself contains 25 independent lamps capable of covering the solar reflectance range of 0.0 -1.0. Thirty radiance levels are used to characterize behavior of field instruments with its use. The laboratory calibration is carried out to capture accurately the low radiance level instrument response, especially for PARABOLA III (which has a total dynamic range of 2^{20}) to encompass targets of low reflectance (water, vegetation) as well as the direct solar beam. The PARABOLA detectors display slight non-linear behavior over surface -> solar irradiance range so that both laboratory and Langley-based field calibrations are needed to characterize the complete range. The laboratory calibration provides source stability seldom enjoyed by field determinations, and is useful for characterization of inherent instrument noise levels independent of atmospheric fluctuations. A laboratory determination of instrument V_0, either relative to that of a nearby channel which has been determined in the field, or absolutely from a standard lamp, is essential for the 940 nm water vapor channel of all solar radiometers. This is because of the inherent unsuitability of the Langley method for this purpose due to the usual water vapor fluctuations in the sky.

In the field the so-called Langley method is used for determination of V_0 for Reagan, CIMEL, MFRSR and PARABOLA using the Sun as a source. The Langley method is well-known and straightforward to use, but must be applied with caution. The method depends upon determination of slope and intercept by least square methods of scatter plots of logarithm of instrument response vs. airmass. The zero airmass intercept together with standard error of its determination may be made without regard to calibration of the instrument in terms of SI units, which requires specification of the exoatmospheric solar irradiance over channel bandpasses. The slope and its standard error constitute an estimate of average τ over the observation period with uncertainties. Stable skies are required for use of the Langley method of calibration. Strictly, even for clear skies, this is in general not the case. *i.e.*, there is instability and possibly secular variation in the abundance of aerosol scatterers present. Since instantaneous optical depth retrievals (two-point determinations) are especially sensitive to uncertainty in V_0, the field calibration of solar radiometers is of special concern. An analysis of this field calibration problem was carried out by Bruegge *et*

al.[6] at FIFE (see also *[27]*). Experience there found local calibrations, as opposed to calibrations from high mountain sites, to be preferable.

To help guard against introduction of bias into retrieval of V_0 because of secular changes in airmass characteristics, the temporal spans of observations used for its calculation are limited to a specific air mass range, for example, 5.5 to 1.5. On calibration days at ordinary field sites, the time history of residuals of instantaneous optical depth compared to the long term average, and is inspected for systematic trends. Days with random variation of residuals about the mean optical depth are sought. Days with pronounced systematic trends are discarded for calibration purposes. Examination of optical depth retrievals around solar noon will isolate changes in τ as opposed to solar zenith angle A collection of three to five daily records of such stability are averaged to obtain a local value of the calibration. Measurements of the Sun are also taken at high altitude mountain sites under stable homogeneous atmospheric conditions Such calibrations are repeated at regular intervals (every six months) to establish variations in the calibration over time.

9.2.2.2 Spectral response functions

The spectral response functions of individual solar/sky radiometer channels give the combined effect of filter function, spectral response of the detector plus electronic system influences. These functions are determined at a spectral resolution of about 1 nm using collimated light sources from a well-calibrated monochromator, provided by the JPL standards and calibration laboratory. The low energy incident on the instrument aperture usually requires synchronous detection of the resulting radiometer signal, which is then analyzed to provide an estimate of system response. The results are normalized to the maximum response in each channel. Mostly these response functions can be approximated adequately by a Gaussian curve shape, but there are exceptions. For example, the spectral response function at 940 nm for the Reagan radiometers is not Gaussian-shaped. Details of the shape are required to obtain accurate rules for retrieval of response to water vapor column abundance via water vapor transmission spectra contained in the MODTRAN III atmospheric transmittance code.

9.2.2.3 MFRSR calibration and characterization of the cosine response functions

The MFRSR diffuse/direct radiometer radiometric calibration is provided both by the manufacturer (Yankee Environmental Systems [YES]) and in the field through application of the Langley method to the derived direct beam instrument response. The manufacturer calibration is carried out on the total response using a well-calibrated integrating sphere traceable to NIST.

In addition to determination of instrument V_0, YES also performs a detailed spectral determination of the azimuthal and zenith angle dependence of the receiver response to correct for non-Lambertian performance of the receiver. These are supplied with the instrument as part of standard software reduction for adjustment of direct solar irradiance determinations. and are updated with

each refurbishment of the instrument by the manufacturer.

9.2.2.4 Traceability or verification by NIST standards

Calibration of the MISR integrating sphere with respect to the Goddard Spaceflight Center integrating sphere, the Optical Sciences Center, University of Arizona, integrating sphere, and Optical Technology Division, NIST, have been carried out using transfer radiometers as part of a round-robin intercalibration of these calibration standards. NIST has verified radiance calibration of the MISR integrating sphere to within ±3%.

9.2.2.5 Intercalibration campaigns involving EOS and other experiment groups

An integral part of sky and ground measurement campaigns involving diverse instruments and EOS groups are instrument intercalibration exercises. Intercalibration campaigns between groups from differing facilities face problems of differences in methods of data reduction as well as differences in instruments and field reflectance standards used. Intercalibration between (multiple) instruments is carried out by simultaneous observations of the Sun or for reflectance, the ground, at the same site and at the same time. Intercalibration establishes the difference in instrument response expected for the same conditions and provides a basis for mapping of determined optical depth and surface reflectance from one solar radiometer to another and from one portable spectrometer to another.

Such campaigns have so far been carried out at high altitude or desert sites that are expected to be used for vicarious calibrations. We expect to participate whenever possible with other EOS groups in such intercalibration activities. Two such intercomparisons at Mt Lemmon, Arizona have been carried out in 1994 and 1996, and two at Lunar Lake, Nevada, 1994 and 1997. The latter lead to intercomparisons of optical depths, surface reflectance and RTCs leading to intercomparisons of TOA radiances among four groups (see Thome, *et al.[85]*).

The 1997 field campaign was preceded by intercalibration sessions at Optical sciences Center, University of Arizona, to characterize reflectance standards using NIST traceable standard sources.

9.2.2.6 AERONET and ISIS calibrations.

The estimation of calibration coefficients for CIMEL radiometers at field sites in the AERONET network is carried out by the Langley method, examining the airmass-dependent output of each instrument to judge quality of the atmospheric and cloud conditions and to eliminate obviously aberrant data points. The calibration coefficients so obtained from the edited data sets are accumulated as a record of possible changes over time in instrument response.

Since it is not feasible to remove each instrument of the network to a high altitude site for independent calibration, an alternative method is *in situ* comparison of the response with a well-calibrated standard instrument, with the transfer solar radiometer calibrated at a known site of excellent sky characteristics such as Mauna Loa Observatory, Hawaii.

Similar procedures are followed for MFRSR radiometers that comprise the ISIS network. These comprise one component of the NOAA/ARL Surface Radiation Research Branch (SURFRAD). Operation of this network includes much effort in the yearly calibration and characterization of the radiation measurements provided by the MFRSRs.

Adoption of the optical depth and other aerosol property retrievals supplied by the CIMEL or ISIS networks for post-launch MISR data product validations means that connections between these retrievals and ground-based retrievals accompanying algorithm validation field campaigns with AirMISR must be established. Intercalibration campaigns will be implemented through simultaneous field observations involving the MISR validation instrumentation and CIMEL instruments.

9.2.2.7 Validation of ozone and water vapor retrievals

Corrections of residual optical depths (total minus Rayleigh component) for ozone and water vapor absorptions, are required to isolate the aerosol component. It is important to derive estimates of column ozone abundance and column water vapor amount on a time dependent (instantaneous) basis from the sunphotometer data themselves because the instantaneous aerosol optical depth values are required to compare with overflights. We will validate/calibrate the procedures employed for the gas and water vapor extractions (Flittner *et al* method for ozone, MODTRAN III law for water vapor), and compare them to values from methods used by others. The column abundances obtained from the solar radiometry will be validated with column amounts derived from analysis of single gas absorption lines using JPL's Mk IV interferometer at JPL and by intercomparisons with standard ozone measuring instruments at other sites.

An example of the use of the latter for ozone is supplied by comparisons carried out between ozone column abundances from Brewer spectrophotometer observations with those obtained from reduction of Reagan data using the Flittner method. The(standard) Brewer observations have been verified to the 1-2 percent level by intercomparisons with ozone sonde and other measurements, so we can be assured of the column abundances obtained are well established.Retrievals of ozone column abundance using the Flittner method and Reagan observations at a CAPMON station (Saturna Island), have shown good agreement between standard and Reagan values. In fact the Reagan retrievals of column ozone prove sensitive to the calibration constants V0. This suggests the possibility of using such intercomparisons to secure V0 values on a secure basis independent of the usual Langley method, which has been criticized in the past for its dependence on optical depth invariance through the calibration period.

9.2.3 Exoatmospheric solar irradiance spectrum adopted

Wherever the conversion of V_0s of our field instruments to irradiance units is required, we have adopted the World Radiation Center (WRC) exoatmospheric solar irradiance spectrum *[86]* for this transformation.

9.3 VICARIOUS CALIBRATION OF AIRBORNE INSTRUMENTS AND MISR

9.3.1 Purpose

Field calibration experiments involving the MISR simulators (either ASAS or AirMISR) or AVIRIS will include an inflight calibration of the sensor. Inflight calibration, also termed vicarious calibration, means development of transformation formulas between the instrument spectral response and a calculated upwelling spectral radiance at the sensor. Inflight calibration is required because laboratory based calibrations may not apply under flight circumstances because of changes in sensor characteristics. The vicarious method will be used to provide an independent pathway for the inflight calibration of MISR itself.

9.3.2 Methods

Three methods of vicarious calibration will be employed. Then an outline of a strategy for use of AirMISR as a well-calibrated instrument for radiance-based work is outlined.:

9.3.2.1 Reflectance-based

The reflectance-based method employs a bright homogeneous natural target that encompasses pixels in the sensor ground footprint. The target (non-Lambertian) reflectance and atmospheric properties are measured and used to constrain a radiative transfer code (RTC). The RTC is used to calculate upwelling radiance at the sensor (TOA radiance) which consists of the path radiance plus direct and diffusely transmitted components reflected from the surface. The spectral response function of the sensor is established by comparing the calculated spectral radiance pixel by pixel with the instrument response over the target.

A significant difference between conventional applications of the vicarious method to calibration of (essentially) nadir-viewing sensors as Landsat or AVIRIS, and application to MISR is the need for radiance determinations in nine upwelling directions for nine separate MISR cameras with view angles ranging over 70.6°, including nadir. This requires specification for the RTC of an aerosol scattering model, which in practice, will be estimated from and constrained by other measurements and retrievals using methods outlined in Chapter 5. Most important, application of the method also requires accurate determination of the surface BRF with PARABOLA III,

The smaller footprint sizes of AirMISR pixels at all angles of view presents less of a problem

for sampling of the surface BRF than that posed by MISR. (see below)

9.3.2.2 Diffuse/direct measurement substitution at surface

A second method by Biggar *et al*. *[4]* for calculation of TOA radiance is to use measurements of the ratio diffuse irradiance/direct irradiance at the surface to eliminate a function describing diffusely transmitted flux in the TOA radiance equation. The atmospheric optical depth and surface reflectance must be measured. The path radiance, together with the bihemispherical backscatter function of the atmosphere must be calculated from the RTC for assumed or measured atmospheric scattering properties. The additional measurements (carried out in practice with MFRSR) reduce the number of functions that require calculation from the RTC. The original method of *[4]* must be modified for MISR application to allow for non-Lambertian surface reflectance. It is easier for this modification to constrain the aerosol model by forcing agreement between the calculated and measured downwelling irradiances at the surface after incorporating the measured BRDF.

9.3.2.3 Method of propagation of surface-leaving radiance through atmosphere

A third method is available if measurements of the surface-reflected radiance (carried out in practice with PARABOLA) are available together with the optical depth. Since the surface reflected radiance is measured directly, TOA radiance may be calculated by propagating the surface-reflected component through the atmosphere using the governing integral equation of radiative transfer. The TOA emergent radiance is thus obtained without calculation of the surface BRDF. The RTC is required to calculate the path radiance and the diffuse atmospheric transmittance, both from the best-determined aerosol model

9.3.2.4 Radiance-based calibration of AirMISR

A fourth method involves a radiometrically well-calibrated instrument aloft. The main goal here is to use AirMISR itself as a multiangle radiometer. The imaging spectrometer AVIRIS co-flown with AirMISR will act initially as a presumed well-calibrated auxiliary radiometer for viewing directions close to normal to the surface.

Once the calculation of multiangle monochromatic spectral TOA radiances is possible based on field data, the inflight vicarious radiometric calibration of AirMISR becomes possible. This will enable the spectral output of the single gimballed camera of that instrument, for all nine camera positions and all spectral bands, to be interpreted in terms of the incident radiance at AirMISR. Together with on-board PIN and HQE diode readouts, the AirMISR will approach a well calibrated radiometer permitting radiance based calibrations of MISR. These studies on radiometric calibration of AirMISR inflight are planned at one or more desert sites as well as other locations.

9.3.2.5 Use of AVIRIS for radiance-based comparison of nadir AirMISR views

As a whiskbroom sensor with pixel size of about 20 m, the entire AVIRIS detector array can be calibrated from field measurements by a target of 20 pixels or so, that is 200 by 40 m in dimension. Through the use of on-board calibration systems and the ground-based calibration, AVIRIS provides near nadir (±20° about nadir) of surface scenes at 20 m spatial resolution, with an absolute accuracy of about 3% *[27]*. The observed ground swath of AVIRIS scenes is about 10 km, and thus covers the entire AirMISR scene at the nadir view. Thus AVIRIS can provide a means of checking the calibration of AirMISR over the entire detector array at nadir, for comparison with a calibration obtained by the ground-based method.

9.3.2.6 Extension to MISR

The on-orbit vicarious calibration plan for MISR will involve the four approaches mentioned previously. Two will be discussed here: (1) reflectance-based, and (2) radiance based using AirMISR with AVIRIS as a supporting spectral radiometer

A complete in-flight reflectance-based calibration of a pushbroom detector array requires a ground target of linear dimensions equivalent to the projected length of the spatial dimension of the (pushbroom) detector array at the surface. For ASAS as an example, this has required a homogeneous target one-two km in length, but only a few tens of meters in width. For AirMISR the nadir the swath width is near 10 km with IFOV about 7-8 m in the nadir and 7-8 m by 18 m along track for Df and Da views. For MISR the swath width is near 350 km with pixels about 215 m along track and 275 m across track at nadir, extending to 704 m along track and 275 m across at Df and Da position of ±70°.

(1) Reflectance based

The footprint sizes for MISR pixels vary with view direction from 214 m (along track) by 275 m (across track) in the An view, to 704 m (along track) to 275 m (across track) in Da and Df views.

The large footprint size of MISR especially at Da and Df angles presents problems in sampling the surface BRF, and a parsimonious method of surface sampling must be adopted. At least two strategies are possible: (1) sampling of areas many times the pixel size around overflight to ensure capture of at least one MISR pixel at all angles, (2) precise location of each pixel center, with its location error, after the overflight, and construction of the imaged area based on these locations together with the known ground-projected geometry of the unresampled pixels.

The construction of average BRF values for the surface areas chosen by either strategy require multiple sets of PARABOLA observations, since the PARABOLA sampling area is ordinarily only part of a single pixel area. A promising method of averaging employs the ASD spectrometer to assess large area uniformity in terms of normal incidence HDRF, and to scale the PARAB-

OLA determinations based on local HDRF values assuming that BRF characteristics are independent of the HDRF. Measure reflectance of a few MISR pixels covering nadir and all off -nadir views after these pixels and their positions have been identified in the Level 1B1 image processing. Because of the large size of full ground pixels, several days with correct sun angle may be required to measure the required target area. However, carry out atmospheric measurements concurrent with MISR overpass to establish ambient sky turbidity and aerosol model at time of overflight.

(2) Radiance-based

The radiance-based plan employs AirMISR as a well-calibrated radiometer acquiring a complete multiangle data set with its one camera plus calibration data along a ground track coincident with the MISR overpass and timed to arrive at the target area simultaneously with the calculated overpass time. The burden of calculating multiangle radiances from ground-based observations is placed on direct measurement by one AirMISR camera over all required angles of view.

To aid in the rapid acquisition of spectral reflectance measurements for this purpose we use a field spectrometer (ASD) that acquires a complete spectrum between 390-2500 nm at 10 nm sampling interval in a few seconds. Many such spectra at measurement stations along the target are used to establish point by point the reflectance values and variations. The rapid acquisition allows a complete survey with minimal variation of sun angle.

The radiance based approach with AirMISR will be implemented with that instrument aboard the ER-2 platform, which operates at an altitude of about 20 km above terrain. At this altitude about 50 mb of atmosphere are above the aircraft, plus most of the stratospheric ozone. We will proceed to evaluate the atmospheric contribution by assuming it to be comprised of molecular scattering with magnitude governed by pressure measured on board the aircraft inflight, and will rely on our ground-based determination to estimate the ozone absorption.

Vicarious calibration of MISR is also discussed in *[M-12]*.

9.4 EOS INSTRUMENT TOA RADIANCE INTERCOMPARISON

9.4.1 Purpose

This section summarizes the purpose and methods of the plan to intercompare between EOS groups atmospheric and surface measurements and radiative transfer models to calculate TOA radiances. The MISR-related experiment objectives include:

(1) Calibration and intercomparison of sunphotometers and other instruments from JPL and other participating EOS instrument groups.

(2) Intercomparison the determined atmospheric parameters (principally optical depth and aerosol model, e.g., size distribution and complex refractive), employing comparisons between calculated and MFRSR-measured surface irradiance to improve the aerosol and size models (simplified closure experiment lacking direct determinations of aerosol model).

(3) Intercomparison of surface HDRF determined as functions of solar zenith angle and relations to PARABOLA III-derived BRDF.

(4) Intercomparison of calculated TOA and near-TOA radiances from various radiative transfer codes for three solar zenith angle conditions corresponding to sun incidence angles for the equinox and summer and winter solstices.

(5) Provide inflight calibration of AirMISR at all nine viewing angles for overflights at the MISR overpass azimuth (heading about 190° true) and overpass time for the local latitude (about 10:15 AM LST).

(6) Provide inflight calibration for AVIRIS using reflectance-based and other methods described in Section 7.3.2.

(7) Validate inflight calibration of AVIRIS using reflectance determinations derived from AVIRIS measurements for ground targets not involved in inflight calibration.

(8) Intercompare calculated TOA and near TOA radiances obtained by various EOS instrument groups involving independent reduction methods for the reflectance conditions corresponding to equinox and solstice viewing and illumination geometry.

(9) Compare calculated TOA radiances with radiances measured by AirMISR (9 angles) and AVIRIS (nadir view)

9.4.2 Methods

Locations of field targets have been established for the intercomparison campaigns. The current site for TOA radiance intercomparisons is Lunar Lake, Nevada, elevation 5700 feet (1740 m), which is a uniform dry lake bed, roughly oval in shape, and about 3 by 5 km in dimension. with long axis trending NE. Optical determinations of atmospheric properties will be carried out using solar radiometric measurements at times coordinated between instrument groups. For calibration validation purposes, ground measurements will be carried out at two sites, Lunar Lake playa (for

calibration) and Railroad Valley playa, elevation 4900 feet [1500 m]. An additional set of atmospheric and surface reflectance measurements will be carried out at targets to be selected in Railroad Valley, which will act as sites for prediction of aerosol optical depth and BRF from AirMISR and HDRF for AVIRIS, and hence comparison with ground-measured values

9.5 ALGORITHM AND PRODUCT VALIDATION EXPERIMENTS

9.5.1 Purpose

The purpose of an algorithm or product validation experiment is to find out if the aerosol and surface parameters generated by ground-based and MISR aircraft simulator or MISR pathways agree or disagree within experimental error. A wide range of environmental conditions and model types are sought to explore robustness of the algorithms.

9.5.2 Methods

Experiments involving the MISR simulator instrument, ASAS and AirMISR, together with a simultaneous field observational campaign will constitute the core of the MISR *algorithm* validation program. Each validation field experiment focuses on accumulating aircraft simulator data over a selected target under the best experimental conditions available. The ground-based atmospheric and surface measurements to be employed are listed below. These focus on providing as realistic a picture as possible of equivalent aerosol, atmospheric and surface properties that are valid during experiment time.

Field atmospheric and optical measurements at field sites are used to:

(1) Establish meteorological conditions, at the surface using conventional weather instruments, and aloft with balloon-borne sonde packages.

(2) Establish atmospheric diffuse and direct radiation fields at the surface.

(3) Characterize column equivalent aerosol abundances, size distributions, and optical properties.

(4) Measure the surface bidirectional reflectance function (BRF) of target areas in PARABOLA bands plus the spectral HDRF from 400-2500 nm.

(5) For marine targets, establish surface winds and wave characteristics to fix or estimate water surface BRF via Cox-Munk model. Exclude actual *in situ* radiation measurements.

(6) For marine targets measure the diffuse sky and direct solar irradiance components. Determine atmospheric total optical depth and aerosol component plus diffuse irradiance at surface.

9.5.3 Criteria for site selection

A matrix of aerosol types and surface reflectance boundary conditions that can be used as a guide to experiment types, together with some generic experiment sites, both within and outside of the U.S., where the listed aerosol types are highly likely to occur, are given in Table 18. In practice the choice of sites must be much more modest in keeping with budget constraints and aircraft flight and deployment schedules. Examples of actual site choices are described later.

Table 18: SMART DATASET AEROSOL AND SURFACE REFLECTANCE TYPES WITH SOME CHARACTERISTIC SITES AND FIELD EXPERIMENTS

AEROSOL \ SURFACE	DUST	INDUSTRIAL/ SULFATE	CLEAN MARITIME	BIO-BURN	SOOT	CONT INENTAL;
MARITIME	West Africa, Canary Islands, ACE II (1) DryTortugas in Florida Keys	Coastal Eastern US in summer TARFOX(2)	Ocean sites off S. and Central Calif., Monterey Bay, San Nicholas Island EOPACE (3)	SCAR-B (4), South Africa	Coastal Eastern US in winter	Great Lakes, Great Salt Lake
DDV	Caribbean Islands	Eastern United States, Central Pennsylvania	Coastal Washington, Oregon, Puget Sound	SCAR-B, Central CA, Western US in summer	Poland, Russia, Germany	BOREAS, Prince Albert, Sask. ARM site, Lamont, Oklahoma
HETEROGENEOUS	Desert Environments, Western United States, West Africa	Eastern/Western PA, Nashville, Tenn., Brown Creek, TX, NGS, AZ	Oceanic Islands or Islands offshore S. CA	Brazil, China, Central America in Spring	India, Central and Eastern Europe	ARM site, Oklahoma

(1) Aerosol Characterization Experiment (North Atlantic Region)
(2) Tropospheric Aerosol Radiative Forcing Observational Experiment
(3) Electro-optic Propagation Assessment in Coastal Environments (NRaD)
(4) Smoke, Clouds, and Radiation-Brazil

Validation site selection is a major step in experiment planning; the process is under constant evaluation and review and therefore continues to the present. The following general guidelines have been exercised for selection of MISR algorithm and product validation sites, past, present and in future:

(1) Identify general locations where given aerosol types might be found against surface reflectance backgrounds that approximate elements of the MISR aerosol climatology-surface reflectance data matrix (Table 18.)

(2) Co-locate algorithm and product validation experiments where possible with other major surface and/or atmospheric experiments to take advantage of resources and infrastructure present and make possible the sharing of scientific data. Examples of these in the past have included BOREAS and SCAR-C.

(3) Emphasize logistic convenience for surface and aircraft observations to minimize field access problems as well as aircraft deployment, flight hour and other field costs. Sites may be occupied on a repeated basis over a period of years. Sites in North America and continental United States plus adjacent ocean waters have thus been favored whenever possible, except where significant advantages are thought possible by joining forces with experiment groups elsewhere.

(4) Availability of records of seasonal conditions to optimize chances for choices of clear sky opportunities for aerosol and surface reflectance studies.

(5) Sites should be capable of characterization by simply designed field observations. For surface reflectance targets, this suggests flat homogeneous or simple heterogeneous terrain and low or no topographic relief. MISR FOV conditions suggest minimum homogeneous areal dimensions of 250 m by 250 m and larger targets of minimum 1 km by 1 km dimensions. These target specifications are also needed for PARABOLA III retrievals. The presence of towers, roads, electrical power, bucket or gondola hoists, other infrastructure can be very helpful.

(6) Availability of long time series records of surface and sky conditions, *e.g.*, (a) solar/sky radiometer network data for optical depth, aerosol optical properties, such as AERONET, (b) direct observations of aerosol particle properties, vertical distributions, and composition such as the ARM CART site, Oklahoma, (c) radiation network data for irradiance and BHR time series such as the SURFRAD/ ISIS network and the ARM CART site, (d) at sea, instrumented moorings with wind direction and speed, wave heights and spectra, surface relative humidity and temperature records, (e) records of cloud cover, and cloud top and bottom height measurements from surface networks, such as at the ARM site.

(7) For marine targets it is useful to pick sites at offshore moorings, such as the NOAA National Data Buoy Center (NDCB) buoys, where wind speed and direction and wave data sets are continuously recorded. This helps to assure that ocean surface roughness conditions locally can be constrained and used for estimation of ocean glitter pattern, white cap and foam estimation.

9.5.3.1 Desired observing conditions

All of the MISR aerosol and surface product algorithms have been developed from radiative transfer theory assuming laterally homogeneous and cloud-free atmospheric conditions. Aerosol populations are assumed to fall off exponentially with height, scale height 2 km. Atmospheric pressure giving rise to Rayleigh scattering is exponentially height dependent with scale height 8 km. The surface reflectance is allowed to be a detailed function of position. So-called adjacency effects due to aerosol scattering are ignored. The surface is assumed flat, without microrelief arising from vegetation canopies, dunes, etc. To simplify problems of interpretation, uniform cloud-free atmospheric observing conditions on essentially flat ground are sought for aerosol and surface validation experiments, although the cloud free restriction is not necessary for recovery of BRDF provided that the direction to the Sun remain unobscured by cloud during the observation periods.

To achieve target and atmosphere viewing conditions comparable to those of MISR in-flight, AirMISR overflight times will be made to coincide with anticipated overflight times of MISR on the EOS platform, and to coincide in azimuth with the anticipated ground track (direction) of MISR overpass. For example at 34° N latitude, the overpass time would be approximately 10:20 AM at an azimuth of 188°, a zero heading being geographic north. Two additional aircraft flight lines, one in the solar principal plane and another bisecting the first two lines, will also be sought routinely to secure additional constraints on azimuthal dependence of the aerosol light scattering, and reflection by the surface cover. The solar principal plane coverage assures capture of portions of the so-called hotspot or enhanced retroreflection due to self-shadowing in the surface.

In addition to the idealized target geometry specified earlier, analysis of MISR and field data for hilly surfaces and partial cloudy skies will also be carried out to assess the effects on surface retrievals of departures from the idealistic conditions where the MISR algorithms apply. These conditions can be expected to occur during some field exercises in some areas, but these studies are a low priority compared to clear sky opportunities.

9.5.3.2 Field measurements

AirMISR overflights are closely coordinated with the following ground-based observations:

(1) Location of surface targets using (differential) GPS, aerial photo and map techniques.

(2) Surface BRF of target areas using PARABOLA III. Spectral HDRF determination of target areas using ASD field spectrometer. The BRF and HDRF determinations may, if necessary, be carried out on successive days not coincident with overpass at similar Sun incidence directions. This may be required for large target characterization.

(3) Multispectral sky radiance, and direct solar irradiance observations with the PARABOLA, CIMEL (eventually complete analysis of sky radiance polarization at 870 nm) and Reagan radiometers, diffuse and direct irradiance measurements with the MFRSR. These observations are combined to secure estimates of atmospheric optical depth, determination of aerosol scattering and absorption properties including size distribution, scattering phase function, and refractive index according to methods of Section 3. Additional (instantaneous) determinations of atmospheric path water vapor and ozone are provided. These measurements will be supplemented with moderate spectral resolution (e.g. 2 nm sampling, 10 nm resolution, 390-2500 nm) determinations of optical depth obtained using GER field spectrometer. The GER data yield the spectral extinction variation over the extended spectral range, further details of the size distribution and extended limits of the size retrieval range.

(4) Vertical soundings of temperature and relative humidity using a balloon borne (Airsonde) instrument package.

(5) Surface pressure and temperature, relative humidity (RH), wind speed and wind direction are continuously monitored using a Davis Meteorological Instrument package at the surface.

(6) Two conventional fish-eye lens camera systems will be deployed along a measured baseline to record cloud cover, cloud motion and cloud base and top heights.

9.5.3.3 Additional airborne and surface measurements

Direct measurements of aerosol microphysical and optical properties by aircraft-borne sensors or ground-based instrumentation will be carried out as opportunities permit. The following additional airborne/surface observations are desirable.

(1) Vertical optical depth profiles such as those obtained by the ARC Airborne Tracking Sunphotometer (ATS) to measure stratospheric and upper tropospheric extinction above the aircraft platform elevation, plus profiles of aerosol optical depth from surface through the scattering layers. These data together with ground-based sunphotometry will be combined to isolate total atmospheric attenuation to that arising below the observing platform, *e.g.*, to isolate the predominantly tropospheric contribution. The structure of the aerosol scattering layer will be correlated with RH and absolute humidity profiles obtained from balloon sounder data.

(2) Direct measurements of aerosol abundances and microphysical properties as functions of elevation above the target site utilizing an aircraft sampling and analysis platform, such as that of University of Washington C-131A. Measurement of actual aerosol property profiles through the scattering layer would then be possible.

(3) Additional sources of information on aerosol microphysical properties at ground level are sampling and optical measurements such as those now on line at the ARM CART, and IMPROVE network sites or urban air quality monitoring stations.

(4) For selected sites such the ARM CART, JPL, and selected field sites, correlation of column equivalent aerosol properties with aerosol backscattering profiles from lidar observations together with compositional estimates (ARM CART) will be possible on a more or less routine basis. The lidar systems of Langley Research Center (R.A. Ferrare, NASA NRA-97-MTPE-03) will also be employed.

9.5.3.4 Land surface product validation; local networks and tower measurements

A series of site-specific product validation campaigns independent of the inflight calibration program will be carried out. For large area average optical depth determinations as required for validation of the reported MISR Level 2 aerosol parameters (17.6 km global) we will deploy small (few km spacing say) networks of solar radiometers to assess average optical depth properties and variations with time over the sampled areas. The scaling issues have been described in Section 4. The assessment of BRF over large areas with time (seasonally, say) is much more difficult. Determination of surface BRF variations at km size surface areas will require intervention of AirMISR aircraft measurements. To afford traceability to direct measurements at the surface, such overflights will be coordinated with ground measurement campaigns in homogeneous or quasi-homogeneous areas situated directly along MISR ground tracks, wherein local measurement field instruments such as PARABOLA III are moved from site to site and the large scale properties (1-2 km) determined by averaging. Such averaging campaigns will probably be possible without elaborate infrastructure only in areas where stature and inhomogeniety of the surface cover is not too great, e.g., desert scrub vegetation on gentle alluvial slopes, grassy prairies (e.g., FIFE, Niobrara, Nebraska, or Tallgrass, OK sites) etc. Representative sampling of larger stature forest covers, such as those at BOREAS, was possible because of the existence of tower structures and tramways erected by investigators within the project for that specific intent. Such structures will continue to be required if the time series of BRF for that type of domain is to be maintained. One additional site has been mentioned, Canopy Crane in Wind River National Forest, WA. Since the BOREAS tower sites represent DDV cover types in the MISR surface retrieval methodology, we suggest specifically utilizing the BOREAS sites, reoccupying them periodically during accessible seasons to assess DDV BRF and possible changes seasonally or more closely spaced in time.

In addition to sites used for the FIFE and BOREAS experiments, the selection of additional homogeneous large-area surface targets with minimal topographic relief should be taken from existing land surface classifications where these have been validated by detailed vegetation and soil surveys. Such selections are under study. Other areas where considerable site characterization has been implemented are the Long Term Ecological Research (LTER) sites. One such candidate in central Oregon is H.J. Andrews Experimental Forest. The usefulness of these sites for BRF determinations and intercomparisons depends upon detailed site surveys. The field validation activities at specific sites in cooperation with the MODIS BRDF/Albedo and Land Surface Cover Change groups are also being planned. The proposed target areas listed in these documents need to be specifically defined and evaluated for relevance to MISR validation goals. This includes foreign campaigns such as SAFARI 2000.

9.5.3.5 Logistics of experiments in marine areas

Offshore marine aerosol and ocean surface validation efforts are important because 70% of Earth's surface is ocean that generates marine aerosol and because MISR retrievals over water are the simplest types carried out. Land-derived mineral dust components over ocean waters are also widespread. Methods of obtaining observations at sea extending perhaps over periods of months or more have been studied. These will require installations on offshore platforms (Southern California Bight) or island locations (San Nicholas, Island, for example) dominated by marine aerosols. Solar radiometers such as the CIMEL instruments, capable of operating largely unattended for extended periods would be required. The Southern California coast, has oil production platforms and small isolated islands exist in proximity to NOAA buoys that record wind speed, wind direction, an wave statistics on a routine high frequency basis. Offshore platforms have been successfully used for long term verification of TOPEX/Poseidon ocean topographic data *[10]*. Use of these platfoms is difficult because of problems of access. San Nicholas Island is a site where regular Rawinsonde balloon launches are made, and where a CIMEL instrument part of AERONET is located. Aerosol sampling is carried out by NRaD (ONR) and the local Los Angeles Air Quality Management District. In addition buoy measurements are available for ocean surface state about 8 km to the east during summer months. The island lies within the Pacific Missile Test Range and is therefore difficult to use for validation studies with aircraft, but San Nicholas is suitable for post-launch product validations not involving aircraft.

9.5.3.6 Connections with AERONET

MISR validation of aerosol optical properties and abundances on a local scale for continental stations will be linked directly to aerosol determinations by the CIMEL sunphotometers that make up the GSFC network. MISR aerosol observations can also be checked against future data from anticipated local observations and networks forming the International Global Aerosol Program (IGAP), but detailed intercomparisons will depend upon our ability to intercalibrate instruments.

9.5.3.7 Connections with networks of MFRSR instruments

Another network of shadowband radiometers (MFRSR) of considerable use to MISR is available. It is reported that the USDA has deployed 20 such instruments and the DOE through ARM experiment approximately 100, in stations around the country. Radiometric calibrations are in process of being updated. In addition to providing frequent automatic measurements of atmospheric optical depth at six wavelengths (400-940 nm), these instruments measure diffuse downwelling sky radiance concurrently and in some instances are believed to determine water vapor column abundance as well. The spectral downward diffuse light at the surface is needed in the MISR retrieval strategy for recovery of surface reflectance properties and is calculated from the aerosol model specified by comparisons with the SMART data set. Thus, the MFRSR network observations can provide an important additional constraint on MISR radiometric/algorithm performance

and will be so employed. One such instrument has been operating for several years at the ARM site, Oklahoma. Additional major ARM facilities for long term measurement campaigns are planned for the Tropical Western Pacific Ocean, North Slope of Alaska, Eastern North Pacific (or Atlantic) Ocean and the Gulf Stream.

9.6 GROUND CAMPAIGNS COORDINATED WITH DIRECT AEROSOL SAMPLING BY GROUND STATIONS AND AIRCRAFT

9.6.1 Purpose

Coordinated campaigns of remote determination of aerosol properties using optical methods and direct measurements of aerosol microphysical properties are a means of establishing actual physical significance of remotely determined aerosol properties.

9.6.2 Methods

Optical measurements using sunphotometers, sky radiometers and diffuse-direct irradiance radiometers will be carried out at sites collocated with aerosol measuring facilities and/or with direct aircraft observations. Column equivalent aerosol microphysical properties and compositional information, inferred by inversion of the optical measurements, will be compared with such properties deduced from direct sampling throughout the aerosol column (by aircraft) and approximately by comparisons with in situ ground level sampling stations.

9.7 EXPERIMENT PROTOCOLS

9.7.1 Summary of Experiment Types and Intercomparisons

In previous chapters two types of experiments have been defined corresponding to the pre-launch algorithm validation phase of the mission and to the post-launch algorithm + product validation phase. The pre-launch phase relies on individual field campaigns coordinated with MISR simulator overflights timed to duplicate MISR on-orbit observing conditions. Ground-derived and MISR derived geophysical parameters and surface radiance and irradiance are compared and uncertainties by each path assessed on an individual experiment basis. Post-launch activities rely heavily on intercomparisons of MISR retrievals at specific sites with retrievals from the network stations. The object is to build time series of MISR retrievals for comparison with the independent ground data. During both prelaunch and post launch times individual MISR ground campaigns will be mounted to intercompare network derived geophysical parameters, radiances and irradiances with those of MISR. A second activity is vicarious calibration of AirMISR (prelaunch and post launch) and MISR (post-launch) using ground targets. Also AirMISR, if well calibrated, provides a radiance based calibration of MISR. This section provides protocols and data flows for field experiments for (1) vicarious calibration, (3) surface radiation, and (3) aerosol/surface retrievals, and indicates the MISR data flow required to complement the field operation data output. A complete ground-based experiment is one where surface and atmospheric measurements coupled with

AirMISR radiance measurements, secure a combined aerosol and surface model that brings radiative closure with the field and aircraft measurements; the aerosol/surface model used in a radiative transfer code

The following deletes any reference to use of albedometry, although these measurements are made routinely to monitor surface albedo and related broad-band surface irradiance conditions.

9.7.2 Experiment Plan for Vicarious Calibration, Radiance/Irradiance, and Aerosol/ Surface Retrievals

9.7.2.1 Vicarious Calibration ground-based experiment pathway

(1) *Goal of Experiment:* Provide ground-based TOA radiances at all nine MISR view directions and for all MISR spectral bands for comparison with values measured by MISR for target area using laboratory and on-board calibration coefficients.

(2) *Experiment timing:* Vicarious calibration attempt at first post-launch opportunity after degassing, instrument checkout and onboard calibration attempts (about one month). For a particular experiment, time the principal field atmospheric and surface measurement campaigns to correspond to the expected time of MISR overpass (see below)

(3) *Site Selection:* Utilize large uniform dry lake beds at high altitude in dry desert areas to optimize chances for clear cloud-free conditions, and homogeneous target reflectance. Present primary target: Lunar Lake, Nevada; present backup targets Ivanpah Playa, CA or Rogers Dry Lake, CA.

(4) *Compilation of Solar and Platform Ephemeris and MISR Pixel Location Data*:

(a) Field - For selected geographic targets and times of year, provide solar and EOS platform ephemerides, namely Sun azimuth and zenith angle at site for platform overpass, sunrise and sunset,

(b) Platform/MISR - expected timing and path orientation (together with orbit number and other image and pixel identifying data) plus expected pixel locations (with uncertainties due to camera model and platform jitter) for all nine angles and all wavelengths throughout selected calibration target area.

(5) *Check of Instrument Calibrations and Field Reflectance Standards* - Routine field calibration experiment at Table Mountain Observatory. Determine spectral response functions at JPL calibration facility, check field reflectance standards at JPL Spectralon BRF calibration facility

(6) *Post-overpass actual target location (if needed)*- Locate actual MISR pixels together with uncertainty ellipses after the actual overflight from Level 1B2 imagery (unresampled) for each wavelength, each angle, utilizing locations reported by MISR GEOCAL team. Use GPS instrumentation and reference to actual landmarks visible in images to cross-check and verify these locations (should be possible with differential GPS to ~ 1 m)

(7) *Coordination with AirMISR*: AirMISR to be scheduled for overflight during field experiment at multiple azimuths: AirMISR to have three to five overpasses in MISR azimuth, with middle overpass timed for coincidence with MISR observation schedule of target area. Alternate coordination plan for AirMISR (1) along MISR track, (2) in principal plane of the Sun, (3) line bisecting paths (1) and (2). Overpass time to be that of MISR for the local site latitude.

(8) *Observational conditions*: Clear sky, cloud-free conditions meeting cloud screening conditions of MISR, minimum aerosol and water vapor burdens dry stable target surface

(9) *Field Instruments*

(a) Atmosphere and sky: Reagan, CIMEL, MFRSR, PARABOLA III, All-sky cameras.

(b) Meteorology (wind speed, direction, RH, pressure and temperature, surface and aloft): Davis Instrument, Airsonde (one-half hour before overpass, pressure, temperature, RH aloft through ABL), AirResearch barometer

(c) Surface BRF: PARABOLA III and ASD for spectral coverage and rapid large area sampling.

(10) *Measurement Protocol*: Instrument clocks synchronized at UT to nearest second. Geographic north determined by compass or by shadow orientation measurements at solar meridian transit.

(a) Atmosphere and Sky - Direct solar and sky radiation, irradiance and radiant exitance measurements from sunrise to (minimum) one hour past solar noon, each day. All sky camera operation at 10 min intervals throughout measurement period from two stations spaced 1 km apart centered cross track.

(b) Meteorology and Airsonde - Continuous operation of Davis instrument station throughout field measurement periods. Airsonde launches timed for one-half hour before expected overpass to assure passage through boundary layer.

(c) Surface irradiance and radiant exitance with PARABOLA e.g., BRF and HDRF (with ASD) - Objective is to determine BRF over at least one MISR pixel for all view angles. Radiant exitance to be sampled at one identifiable (nadir) pixel location at time of overpass

(11) *Surface sampling strategy:* Ground sampling for MISR pixels involves large areas that increase in size (per pixel) to more than 0.7 km along track and 0.275 m across track at the most oblique viewing directions. The nominal sampling size for PARABOLA is ~20 m and probably ~100 m circular diameter in the limit. Full recovery of BRF with PARABOLA requires observations over complete range of Sun incidence angles. Thus adequate sampling of target areas will take a number of days, to be determined based on determined surface sampling conditions.

(a) Optimal situation - MISR pixels found to be accurately located, except for expected color displacements in raw radiance images, at all view angles. Strategy is to sample largest pixel target area systematically over required number of days, assuming that surface properties remain invariant from day to day (excludes rain/snow damage, initial or developed wet or damp surfaces, any conditions that are obvious by quick surface inspection). Use initial PARABOLA location on nadir pixel as base station for reflectance measurement, re-occupy station periodically to check on repeatability of BRF or HDRF retrievals. Use ASD as adjunct instrument to assess repeatability of measurements from day to day, and also spatial variability over target areas and to provide spectral continuity over the MISR range of measurement

(b) Non-optimal conditions - MISR pixels found to be scattered or displaced along track because of platform jitter or other factors related to MISR camera model, leading to reduced area common to all view directions. This circumstance requires location of individual pixels and sampling one by one over successive days.

(12) *Data reduction and flow:* The TOA radiance calculation requires determination of: (i) Rayleigh scattering, ozone, and aerosol optical depths from the total optical depth measurements by the solar radiometers, (ii) specification of an aerosol scattering model from the combined CIMEL, REAGAN, MFRSR and PARABOLA observations, *and* either: (a) determination of the complete average surface BRF from combination of numbers of observations over large target areas taken throughout adjacent days of the campaign, or (b) use of reflected surface radiance measured by PARABOLA at the time of platform overflight from a single subarea in the MISR sampling pattern. For strategy (b), use of radiance measurements from a single small area is an approximation whose seriousness will be evaluated for the extant conditions.

(a) Total Instantaneous Optical Depth - The total instantaneous optical depth is retrieved from the Reagan data sampled at 30 second intervals using locally derived instrument calibration coefficients. The values are averaged (short term) over the ~ seven minute MISR sampling period and the variation about the mean used as a measure optical depth variability. The (long term) average obtained from total temporal record is used as a first approximation to regional variability.

(b) Aerosol optical depth retrieval - The aerosol instantaneous optical depth is derived from the residual optical depth obtained from Reagan total optical depths by subtracting the Rayleigh component based on instantaneous pressure variation. The aerosol and ozone optical depths are retrieved together using constrained second-derivative (Flittner) method. Short term averages constructed from overpass period with scatter about mean as indicator of variability. Long term records to estimate a regional variability.

(c) Aerosol model retrieval - The CIMEL, MFRSR, PARABOLA, and Reagan observations are combined to produce an aerosol model (size distribution and composition on homogeneous spherical particles) that is radiatively consistent with calculated and measured downwelling sky radiance (and irradiance) distributions, and upwelling multiangle radiance measures as provided by AirMISR.

(d) Surface BRF retrieval from PARABOLA- The multitemporal PARABOLA observations are combined to provide the local surface BRF using iterative solution to direct + diffuse integral equation representation of reflectance boundary condition. Multiple measures representing differing surface areas of multiangle target pixels are averaged (up to seven in nominal case) to obtain representations of BRF for each view angle.

(e) Surface HDRF retrieval from ASD - Areal variability of surface HDRF at normal incidence is calculated from rapid sampling ASD observations taken over subpixel sampling grid. Frequent Spectralon observations used to correct for instrument instabilities. Laboratory measured Spectralon BRF together with downwelling radiancemeaures with PARABOLA used to correct local HDRF to Lambertian perfect reflector basis.

(13) *Data Import from MISR*: Calibrated but unresampled radiance data for vicarious calibration site. Isolate along- and across- track pixels corresponding to calibration target from unresampled radiance data using MISR-provided geographic coordinates for each pixel together with fit of image data to recognizable geographic features of known location.

(14) *Safety checks:* Prior to each field day, battery voltages of buffer storage batteries and computer batteries are checked and maintained at or near full charge. Field data checked at end of each day to assure actual records exits. For cases where data are found missing or unreadable, and where repeat observations are possible, *e.g*., surface reflectance, observations, these are repeated at next available opportunity to replace those data missing.

(15) *Archiving of Field Data*: All raw observations of sky, solar, surface radiance quantities, meteorological data, downloaded to laptop computers together with location, time, weather data, other descriptions of activities pertinent to field record. At JPL field data and descriptions are transferred to Unix system for archival and data reduction. Key parameters of the archival system are experiment site, instrument designation, date (yymmdd) and time (hhmmss). All descriptive data are entered as header files to a particular experiment campaign.

9.7.2.2 MISR calculated irradiance and radiance validation experiments

The following assumes that field observations of surface irradiance or downwelling radiance are available at one instrumented ground site only, *e.g.,* no network of surface instruments such as MFRSR available. The experiments take place mainly in the post-lanch time frame

(1) *Goal of Experiments*: Provide comparisons of surface irradiance and radiance values calculated as part of MISR aerosol/surface retrievals with values measured by surface stations (MFRSR, CIMEL, and PARABOLA).

(2) *Experiment timing*: Measurements coordinated around time of MISR overpass

(3) *Site selection:* Two types of sites are utilized: (a) Fixed station at JPL for long time series development, (b) side-by-side intercomparison of ISIS and JPL instruments at ISIS sites (one or two).

(4) *Compilation of Solar and Platform Ephemeris and MISR Pixel Location Data*:

   (a) Field - For the geographic targets (JPL or ISIS stations) and times of year, provide solar and EOS platform ephemerides, *e.g.*, Sun azimuth and zenith angle at site for platform overpass, sunrise and sunset times,

   (b) Platform/MISR - expected timing and path orientation (together with orbit number and other image and pixel identifying data) plus expected pixel locations (with uncertainties due to camera model and platform jitter) for all nine angles and all wavelengths throughout selected surface station target area.

(5) *Check of Instrument Calibrations:* Routine field calibration experiment at Table Mountain Observatory for MFRSR, PARABOLA, CIMEL, Reagan instruments, and at manufacturer (YES for MFRSR). Redetermine cosine response functions as needed.

(6) *Post-overpass actual target location:* Locate actual MISR pixels together with uncertainty ellipses after the actual overflight from unresampled imagery for each wavelength, each angle, utilizing locations reported by MISR GEOCAL team. Use GPS instrumentation and reference to actual landmarks visible in images to cross-check and verify these locations.

(7) *Coordination with AirMISR:* Not sought for long time series comparisons.

(8) *Observational conditions*: Clear sky, largely cloud-free conditions meeting cloud screening criteria of MISR, ambient aerosol and water vapor burdens, ambient surface reflectance condition at time of overflight.

(9) *Field Instruments:*

   (a) Atmosphere and sky- MFRSR, PARABOLA, Reagan, CIMEL, all-sky cameras

   (b) Meteorology - Davis Weather Station, AirResearch Barometer

   (c) Surface BRF - MFRSR and PARABOLA

(10) *Measurement protocol*:

(a) Atmosphere and sky radiation - Begin sky radiance (PARABOLA) and surface irradiance (MFRSR) observations, Reagan and CIMEL solar radiometer observations at sunrise, continue until (minimum) one hour after solar noon.

(b) Meteorology - Continuous observations with Davis Weather Station throughout measurement period.

(c) Surface BRF - Depending on siting of network instrument, derive surface BRF for immediate area from PARABOLA observations taken throughout the measurement period.

(11) *Surface Sampling Strategy*: Set up all sky and surface radiation instruments at fixed location in close proximity to each other and to network station.

(12) *Field Data reduction and flow*: The BOA irradiance determination requires calibrated MFRSR observations; the BOA sky radiance determination requires incident sky radiance over hemisphere measured by PARABOLA particularly at the time of platform overflight within the single subarea in the MISR sampling pattern corresponding to location of the surface station.

(13) *Data Import from MISR:* Calibrated but unresampled radiance data for irradiance/radiance calibration site. MISR aerosol model parameters or calculated surface irradiance and downwelling radiance values at comparison site. Isolate along and across track pixels corresponding to irradiance intercomparison target from unresampled radiance data using MISR provided geographic coordinates for each pixel and according to recognizable geographic features in imagery. Use local (pixel-by-pixel) retrievals of MISR irradiance model over 1.1 km x 1.1 km area to establish scatter of calculated values. Use local retrieved aerosol model together with validation RTC to supply downwelling radiances at site for comparison with PARABOLA-measured values.

(14) *Safety checks*: See Section 9.7.2.1, subitem 14.

(15) *Archiving of Field data*: See Section 9.7.2.1, subitem 15.

9.7.2.3 Aerosol optical depth validation experiments

The following assumes that field observations for aerosol optical depth retrieval are available at one fully instrumented ground site only, *e.g.*, no large scale network of surface instruments such as Reagan, PARABOLA, CIMEL or MFRSR are available. These experiments take place mainly in the post-launch time frame.

(1) *Goal of Experiments:* Provide comparisons of aerosol optical depths calculated from MISR multiangle radiance data according to MISR algorithms with values measured by surface stations by CIMEL and Reagan radiometers.

(2) *Experiment timing*: Measurements coordinated around time of MISR overpasses.

(3) *Site selection and Inspection*: Two types of sites are utilized: (a) Fixed station at JPL for long time series of comparisons, (b) side-by-side intercomparisons of AERONET and JPL instruments at AERONET stations (one or two). AERONET Stations TBD. To extent possible inspect chosen sites to meet uniform cover, low topographic relief criteria.

(4) *Compilation of Solar and Platform Ephemeris and MISR Pixel Location Data*:

(a) Field - For the geographic targets (JPL or AERONET stations) and times of year, provide solar and EOS platform ephemerides, *e.g.*, Sun azimuth and zenith angle at site for platform overpass, sunrise and sunset times.

(b) Platform/MISR - expected timing and path orientation (together with orbit number and other image and pixel identifying data) plus expected pixel locations with uncertainties due to camera model and platform jitter for all nine angles and all wavelengths throughout selected surface station target area.

(5) *Check of Instrument Calibrations:* Routine field calibration experiment at Table Mountain Observatory for MFRSR, PARABOLA, CIMEL, Reagan instruments, and at manufacturer (YES for MFRSR). Redetermine cosine response functions of MFRSR as needed.

(6) *Post-overpass actual target location:* Locate actual MISR pixels together with uncertainty ellipses after the actual overflight from unresampled imagery for each wavelength, each angle, utilizing locations reported by MISR GEOCAL team. Use GPS instrumentation and reference to actual landmarks visible in images to cross-check and verify these locations.

(7) *Coordination with AirMISR*: Selected opportunities coordinated with MISR overpasses. Not sought for long time series comparisons.

(8) *Observational conditions*: Clear sky, cloud-free conditions, ambient aerosol and water vapor burdens, ambient surface reflectance condition at times of MISR overpasses.

(9) *Field Instruments:*

(a) Atmosphere and sky- MFRSR, PARABOLA, Reagan, CIMEL, all-sky cameras

(b) Meteorology - Davis Weather Station, AirResearch barometer, AirSonde radiosonde system.

(c) Surface Lambertian Equivalent Reflectance (via diffuse/direct) - MFRSR

(10) *Measurement protocol*:

(a) Atmosphere and sky radiation - Begin sky radiance (PARABOLA) and surface irradiance (MFRSR) observations, Reagan and CIMEL solar radiometer observations at sunrise, continue until (at a minimum) one hour after solar noon.

(b) Meteorology - Continuous observations with Davis Weather Station throughout measurement periods.

(c) Surface Equivalent Lambertian Reflectance - Depending on siting of network instrument, derive surface Lambertian Equivalent Reflectance from MFRSR observations, or BRF for immediate surrounding area from PARABOLA observations taken throughout the measurement period.

(11) *Surface Sampling Strategy*: Set up all sky and surface radiation instruments at fixed location in close proximity to each other and to network station, either JPL or AERONET.

(12) *Field Data reduction and flow:* Pathway for analysis of the BOA radiance and irradiance observations leading to recovery of an aerosol model, together with radiance/irradiance closure, has been described in Section 9.7.2.1, subitem 12.

(13) *Data Import from MISR:* Calibrated unresampled radiance data for aerosol validation site. Local MISR aerosol model parameters and retrieved aerosol optical depths pixel by pixel for the 17.6 km x 17.6 km areas. Isolate along and across track pixels corresponding to local aerosol intercomparison target from MISR radiance data using MISR-provided geographic coordinates for each pixel and according to recognizable geographic features in imagery. Use local (pixel-by-pixel) retrievals to establish scatter of calculated values. Use local retrieved aerosol model together with validation RTC to supply downwelling radiances at site for comparison with PARABOLA-measured values, and AirMISR-measured upwelling radiance values (latter if available).

(14) *Safety checks*: See Section 9.7.2.1, subitem 14.

(15) *Archiving of Field and MISR data*: See Section 9.7.2.1, subitem 15.

9.7.2.4 BRF validation experiments

The following describes the general nature of a MISR BRF validation experiment. Unlike aerosol and irradiance, no long-term network of surface stations is yet available for monitoring of possible BRF trends with season or within seasons. Potential long term BRF sites are TBD, although some promising possibilities are mentioned. It may prove possible to utilize one or more AERONET, ISIS or EOS core validation sites*[81]*for long-term characterization. For MISR purposes, PARABOLA retrievals of BRF are taken as an “absolute” standard. It is to be realized that no standard target has yet been defined against which MISR-based or ground-based BRF retrievals can be compared as an “absolute” standard.

(1) *Goal of Experiments:* Provide BRF’s of bare surfaces, grass and vegetation canopies both homogeneous and heterogeneous, that serve to compare with BRF retrievals from MISR multiangle observations. Surface categories to be chosen in accordance with accordance with major types identified in previous studies *[M-5], [35], [36], [37]*. Use AirMISR to scale local BRF observations to larger scale, e.g., 1.1 km by 1.1 km. Coordinate MISR field observations with surface determinations of biophysical parameters (LAI, fAPAR).

(2) *Experiment timing*: Field measurements coordinated around precise timing of MISR overpass, seasonally, and intraseasonally where possible.

(3) *Site Selection:* Local TBD. Criteria include flat homogeneous canopies or bare surfaces over MISR retrieval areas (1.1 km x 1.1 km). Towers or cranes present to deal with taller canopies such as needle or broadleaf forests. Examples include BOREAS OJP, OA and OBS sites, Boardman poplar-cottonwood tree farms, OR, Wind River Canopy Crane (old growth needle forest) WA, grasslands (Niobrara, NE or Tallgrass, OK).

(4) *Compilation of Solar and Platform Ephemeris and MISR Pixel Location Data*:

(a) Field - For the geographic targets and times of year, provide solar and EOS platform ephimerides, *e.g.*, Sun azimuth and zenith angle at site for platform overpass, sunrise and sunset times.

(b) Platform/MISR - expected timing and path orientation (together with orbit number and other image and pixel identifying data) plus expected pixel locations with uncertainties due to camera model and platform jitter for all nine angles and all wavelengths throughout selected surface target area.

(5) *Check of Instrument Calibrations*: Routine field calibration experiment at Table Mountain Observatory for MFRSR, PARABOLA, CIMEL, Reagan instruments, and at manufacturer (YES for MFRSR). Redetermine cosine response functions of MFRSR as needed.

(6) *Post-overpass actual target location*: Locate actual MISR pixels together with uncertainty ellipses after the actual overflight from unresampled imagery for each wavelength, each angle, utilizing locations reported by MISR GEOCAL team. Use GPS instrumentation and reference to actual landmarks visible in images to cross-check and verify these locations.

(7) *Coordination with MISR and AirMISR:* Selected opportunities are to be coordinated with MISR overpasses. and especially with selected groundbased campaigns. AirMISR to be used as scaling tool to bridge gap between PARABOLA scale observations (~ 100 m maximum diameter), and MISR retrievals (minimum ~ 250 m, maximum 1.1 km).

(8) *Observational conditions*: Clear sky, cloud-free conditions, ambient aerosol and water vapor burdens, ambient surface reflectance condition at times of MISR overpasses.

(9) *Field Instruments:*

(a) Atmosphere and sky- MFRSR, PARABOLA, Reagan, CIMEL, all-sky cameras

(b) Meteorology - Davis Weather Station, AirResearch barometer, AirSonde radiosonde system

(c) Surface Lambertian Equivalent Reflectance (via diffuse/direct) - MFRSR

(d) Surface BRF - PARABOLA in conjunction with locally available infrastructure, tower, cherry picker, crane, local single pier stand

(10) *Measurement protocol*:

(a) Atmosphere and sky radiation - Begin sky radiance (PARABOLA) and surface irradiance (MFRSR) observations, Reagan and CIMEL solar radiometer observations at sunrise, continue until (at a minimum) one hour after solar noon.

(b) Meteorology - Continuous observations with Davis Weather Station throughout measurement periods.

(c) Surface Equivalent Lambertian Reflectance - Depending on siting of network instrument, derive surface Lambertian Equivalent Reflectance from MFRSR observations, or BRF for immediate surrounding area from PARABOLA observations taken throughout the measurement period.

(d) Surface BRF - see (a) above

(11) *Surface Sampling Strategy*: Set up sky and surface radiation instruments adjacent to PARABOLA measurement sites (few hundred meters limit). Set up PARABOLA at sited dictated by available infrastructure, or at typical site within canopy. Repeat PARABOLA observations at chosen site on two successive days throughout measurement period to judge reproducibility. Move PARABOLA to either: (a) grid- or line traverse- controlled or (b) random locations to assess scatter of BRF retrievals over sampling area. Sampling areas to be located with reference to MISR image coordinates using methods described in subitem 4 of present subsection. Mark surface target edges with tarps, or place them at recognizable landmarks visible in AirMISR imagery.

(12) *Field Data reduction and flow*: Pathway for analysis of the BOA downwelling radiance and irradiance observations leading to recovery of BRF together with fitting of RPV model to the array recoveries, follows *[49]*. First, edit raw PARABOLA data acquired to delete and interpolate across gaps due to shadows not inherent in actual target, those due to reflectance standards, or dropped pixels. For location and misregistration anomalies, apply solar ephemeris to Sun elevation and azimuth position on individual frames to correct orientation. Utilize corrected imagery together with direct beam calibration equations to provide BOA direct-beam solar irradiance for use in reductions to BRF.

(13) *Data Import from MISR*: Calibrated unresampled radiance data for BRF validation site. Local MISR BRF model parameters and retrieved BRF model parameters pixel by pixel for an intended 1.1 x 1.1 MISR recovery area. Isolate along and across track pixels corresponding to local BRF intercomparison target from MISR radiance data using MISR-provided geographic coordinates for each pixel and according to recognizable geographic features in imagery. Use local (pixel-by-pixel) retrievals to establish scatter of MISR calculated values. Use local retrieved aerosol model together with validation RTC to supply downwelling radiances at site for comparison with PARABOLA-measured values, and AirMISR-measured upwelling radiance values (latter if available). Compare direct measurement of solar irradiance by PARABOLA with calculated values using imported MISR aerosol model together with Reagan (plus other) optical depths and adopted exoatmospheric solar irradiance model *[86]*.

(14) *Safety checks*: See Section 9.7.2.1, subitem 14

(15) *Archiving of Field and MISR data*: See Section 9.7.2.1, subitem 15

9.8 LIMITATIONS OF FIELD/AIRCRAFT OBSERVATIONS AND ANALYSIS

The limitations of our field experiment program are as follows:

(1) Apart from direct measurements of aerosol properties by ancillary measurement schemes, such as aircraft sampling, no attempt is made to interpret aerosol refractive indices in terms of mixture models other than those used for construction of the SMART Dataset.

(2) A logical part of aerosol algorithm validation campaigns is the direct measurement of aerosol microphysical properties by ground-based or aircraft sampling. Direct field sampling of aerosols and associated analysis is not a direct part of the MISR validation activity. To the extent permitted by budgetary and logistical constraints we will seek to join field campaigns possibly organized by other agencies where sampling activities are scheduled to occur. Requests to involve others (budget constraints permitting) who can provide direct aerosol light scattering measurements from ground based instruments, *e.g.*, integrating nephelometers will be made.

(3) Equivalent column aerosol properties are reported.

(4) Experimental sites will be (initially) chosen on flat ground, hence topographic effects are included only for regional estimates of the (Lambertian) surface reflectance.

(5) No explicit attempt made to "verify" the Cox-Munk wave-facet model as part of any marine aerosol validation exercise carried out under MISR auspices.

(6) Limitations of aircraft scale on areal averages obtainable: (a) for ASAS, the maximum areal field of view available is about 1 km $\times$ 1 km for determination of either aerosol, surface or TOA/Cloud products, (b) for AirMISR the available FOV depends upon look angle. For nadir views the field is about 9 km $\times$ 10 km, and increases to (approximately) 25 km $\times$ 32 km at 70°. The common FOV for all look angles is thus limited to about 9 km $\times$ 10 km.

(7) Limitations of field observations themselves:

   (a) Aerosol optical depth - sunphotometer observations are essentially point measurements of attenuation (optical thickness) through a slant path in the atmosphere. To calculate an optical depth it is assumed that the atmosphere is homogeneous. Some idea of horizontal atmospheric variability may be achieved by using the time-dependent fluctuations of optical thickness. Alternatively, and in addition, we will employ local networks of 3 or 4 sunphotometers to assess areal variability of the atmosphere,

(b) Surface HDR and BHR - (i) local direct determination of HDRF requires use of PARABOLA and determinations of hemispherical directional properties over the complete range of sun zenith angles from 90° to 0°. This range of sun angles can only be achieved (seasonally below latitudes of 23° (northern hemisphere). All other measurement sets will be incomplete, with requirement that missing measurements be included by interpolation or model. (ii) The local measurement area is estimated to be on the order of 250 - 1000 m, but ultimately depends upon flatness of the terrain at a field site, horizon conditions, height of instrument above the ground, and the instantaneous instrument field of view*(e.g.*, mixed pixels of sky and ground will be different for an instrument FOV of 5° as opposed to 2°, and disregarding mixed target contributions resulting from vignetting).

(8) Inherent differences between ground-based and MISR observations

Note is made of limitations in retrievals based on differences in airmass (or atmospheric volume) sampled near the same times by ground instruments and by MISR. The differences pointed out here disappear for homogeneous stable skies and homogeneous ground targets.

(a) MISR passes overhead in about 7.3 minutes in its orbit sweeping out with multi-angle views an airmass volume of curved trapezoidal cross-section symmetrically disposed about a point surface target as base. During this time the sun has moved approximately 1.8°.

(b) Solar radiometers sample a direct nearly instantaneous optical path through the mid-morning (eastern) sky to the sun over the ~7 minute MISR overpass interval.

(c) The CIMEL almucantar and principal plane observations sample both the eastern sky for morning observation (direct beam) and western skies (sky radiance).

(d) The PARABOLA III instrument samples radiance from the entire upward hemisphere for each incident sun angle.

(e) Adjacency effects in aircraft and MISR data are not generally important.

9.9 OTHER NASA-SPONSORED EOS VALIDATION EFFORTS

The Workshop for Atmospheric Validation in EOS-AM1 and SAGE III (WAVES) was held at Hampton University, Virginia in October, 1997. See *http://asd-www.larc.nasa.gov/WAVES/home.html#new_valid* for a complete list and summaries of the investigations. Some WAVES Principal Investigators and their investigations pertinent to MISR is given in Table 18.

Table 19: Some WAVES Investigations Pertinent to MISR Validation

PI	Investigation Title
Dutton, Ellsworth	EOS/CERES Surface Radiation Validation at NOAA Climate Monitoring and Diagnostics Laboratory Field Sites
Ferrare, Richard	EOS Validation of Aerosol and Water Vapor Profiles by Raman Lidar
Liang, Shunlin	Validating MODIS/MISR Land Surface Reflectance and Albedo Products
Mace, Gerald	Cloud Property and Surface Radiation Observations and Diagnostics in Support of EOS, CERES, MODIS, and MISR Validation Efforts
Meyer, David	Validating MODIS Surface Reflectance, FAPAR and LAI Products OVER the North American Grasslands
Myers, Daryl	Application of Saudi Arabian Surface Radiation Flux Measurements for Validation of Satellite Remote Sensing Systems
Nolin, Anne	Validation Studies and Sensitivity Analyses for Retrievals of Snow Albedo from EOS AM-1 Instruments
Porter, John	Aircraft Radiation and Aerosol Measurements near Hawaii: Satellite Validation at the Moby and Hot Sites
Privette, Jeffrey	Southern Africa Validation of EOS (SAVE): Coordinated Augmentation of Existing Networks

10. REFERENCES

[1] Anderson, G.P., H.S. Muench, R.E. Good, C.R. Philbrick, and W. Swider(1985), in (Jursa, A.S. editor), *Handbook of geophysics and the space environment*, Air Force Geophysics Laboratory, Air Force Systems Command, United States Air Force, 21-30,21-34.

[2] Anderson, G. P., J. Wang and J. H. Chetwynd, 1995, MODTRAN 3: An update and recent validations against high resolution measurements, in *Summaries of the Fifth Annual JPL Airborne Earth Science Workshop, Jan 23-26* (1995), vol. I, AVIRIS Workshop, 5-8.

[3] Biggar, S.F., D.I. Gellman, and P.N. Slater (1990), Improved evaluation of optical depth components from Langley plot data, *Remote Sens. Environ.*, **32(2-3)**, 91-101.

[4] Biggar, S.F., R.P. Santer, and P.N. Slater (1990), Irradiance-based calibration of imaging sensors, *Proceedings of IGARSS 90*, **1**, 507-510.

[5] BOX, M.A., and A. Deepak (1979), Atmospheric scattering corrections to solar radiometry, *Appl. Opt.*, **18(12**), 1941-1949.

[6] Bruegge, C.J., R.N. Halthore, B. Markham, M. Spanner, and R. Wrigley (1992), Aerosol optical depth retrievals over the Konza Prairie, *J. Geophys. Res*., **97(D17**), 18743-18758.

[7] Bruegge, C.J., J. E. Conel, R.O. Green, J.S. Margolis, R.G. Holm, and G. Toon (1992), Water vapor column abundance retrievals during FIFE, *J. Geophys Res*., **97 (F17)**, 18759-18786.

[8] Buchholz, A (1995) Rayleigh-scattering calculations for the terrestrial atmosphere, *Appl. Opt*., **34 (15)**, 2765-2773.

[9] Charlock, T.P. (1996), Clouds and the Earth's radiant energy system (CERES) validation document.

[10] Christensen, E.J., B.J. Haines, S.J. Keihm, C.S. Morris, R.A. Norman, G.H. Purcell, B.G. Williams, B.D. Wilson, G.H. Born, M.E. Parke, S.K. Gill, C.K, Shum, B.D. Tapley, R. Kolenkiewicz, and R.S. Norem (1994), Calibration of TOPEX/POSEIDON at Platform Harvest, J. *Geophys. Res*., **99 (C12)**, 24465-24485

[11] Clothieaux, E.E., M.A. Miller, B.A. Albrecht, T. P. Ackerman, J. Verlinde, D.M. Babb, R.M. Peters, and W.J. Syrett, An evaluation of a 94-GHz radar for remote sensing of cloud properties (1995), *J. Atmos. Oceanic Technol.*, **12(2)**, 201-229.

[12] Cox, C. and W. Munk (1954). Measurements of the roughness of the sea surface from photographs of the Sun's glitter. *Jour. Opt. Soc. of Am.* **44**, 838.

[13] Davies, R. (1984), Reflected solar radiances from broken cloud scenes and the interpretation of scanner measurements, *J. Geophys. Res.*, **89(D1)**, 1259-1266.

[14] Deer, W.A., R.A. Howie, and J. Zussman (1966), *An Introduction To The Rock-forming Minerals*, John Wiley and Sons, Inc., New York, New York, 528pp.

[15] Diner, D.J., L.M. Barge, C.J. Bruegge, T. G. Chrien, J.E. Conel, M.L. Eastwood, J.D. Garcia, M.A. Hernandez, C.G. Kurzweil, W.C. Ledeboer, N.D. Pignatano, C.M. Sarture, and B.G. Smith (1998), The Airborne Multi-angle Imaging SpectroRadiometer (AirMISR): Instrument description and first results, *IEEE Trans. Geosci. Remote Sensing*, **36 (4)**, 1339-1349.

[16] Ehsani, A.R. (1992), Design of a microprocessor-based auto sun-tracking and multi-channel solar radiometer system, M.S. Thesis, Department of Electrical and Computer Engineering, The University of Arizona, 130 pp.

[17] Eldred, R.A., T.A. Cahill, K. Wilkinson, P.J. Feeney, J.C. Chow, and W.C. Malm (1990), Measurement of fine particles and their chemical components in the IMPROVE/NPS networks, in *Visibility and Fine Particles*, v. 17, *A&WMA Transactions Ser.*, edited by C.V. Mathai, A&WMA, Pittsburg, Pa., 187-196.

[18] Engelsen, O., B.D. Pinty, and M.M. Verstraete, and J.V. Martonchik (1996), Parametric bidirectional reflectance factor models: Evaluation, Improvements and Applications, Internal report, Institute for Remote Sensing Applications, Joint Research Centre, Italy, 114 pp.

[19] Erxleben, W.H., and J.A. Reagan (1998), An approach for obtaining best estimates of spectral optical depths and calibration intercepts from temporally variable solar radiometer data, submitted to *IEEE Transactions on Geoscience and Remote Sensing*.

[20] Flittner, D.E., B.M. Herman, K.J. Thome, and J.M. Simpson (1993), Total ozone and aerosol optical depths inferred from radiometric measurements in the Chappuis absorption band, *J. Atmos. Sci.*, **50(8)**, 1113-1121.

[21] Froidevaux, L., W.G. Read, T.A. Lungu, R.E. Cofield, E.F. Fishbein, D.A. Flower, R.F. Jarnot, B.P. Ridenoure, Z. Shippony, J.W. Waters, J.J. Margitan, I.S. McDermid, R.A. Stachnik, G.E. Peckham, B. Braathen, T. Deshler, J. Fishman, D.J. Hofmann, and S.J. Oltmans (1996), Validation of UARS MLS ozone measurements, submitted to *J. Geophys Res.* special issue on UARS data validation.

[22] Garratt, J.R. (1994), Incoming shortwave fluxes at the surface- A comparison of GCM results with observations, *J. Climate*, **7**, 72-80.

[23] Good, R.E., in Jursa, A.S. (Editor) (1985), *Handbook of Geophysics and the Space Environment*, Air Force Geophysics Laboratory Air Force Systems Command, United States Air Force, Ch. 21.2.

[24] Grant, I.P., and G.E. Hunt (1968), Solution of radiative transfer problems using the invariant S_n method, *Mon. Not. R. astr. Soc*., **141**, 27-41.

[25] Hansen, J.E., and Travis, L.D.,(1974), Light scattering in planetary atmospheres, *Space Science Reviews*, **16**, 527-610.

[26] Harrison, L., and J. Michalsky (1994), Objective algorithms for the retrieval of optical depths from ground-based measurements, *Appl. Opt*., **33(22)**, 5126-5132.

[27] Harrison L., J. Michalsky, and J. Berndt (1994), Automated multifilter rotating shadow-band radiometer: an instrument for optical depth and radiation measurements, *Appl. Opt*., **33 (22)**, 5118-5125.

[28] Hicks, B.B., J.J. DeLuisi, and D.R. Matt (1996), The NOAA integrated surface irradiance study (ISIS) - a new surface radiation monitoring program, *Bull. Am. Meteorol. Soc.* (submitted).

[29] Hofman, D, P. Bonasone, M. De Maziere, F. Evangelisti, G. Giovanelli, A. Goldman, F. Goutail, J. Harder, R. Jakoubek, P. Johnston, J. Kerr, W.A. Matthews, T. McElroy, R. McKenzie, G. Mount, U. Platt, J.-P. Pommereau, A. Sarkissian, P. Simon, S. Solomon, J. Stutz, A. Thomas, M. Van Roozendael, and E, Wu, Intercomparison of UV/VIsible spectrometers for measurements of stratospheric NO_2 for the Network for the Detection of Stratospheric Change, *J. Geophys Res.*, **100 (D8)**, 16765-16791.

[30] Holben, B.N., T.F. Eck, I. Slutsker, D. Tanre, J.P. Buis, A. Setzer, E. Vermote, J.A. Reagan, Y.J. Kaufman, T. Nakajima, F. Lavenu, and I. Jankowiak (1998), Automatic Sun-and sky-scanning radiometer system for network aerosol monitoring, *Remote Sens. Environ.* (in press).

[31] Irons, J.R., K.J. Ranson, D.L. Williams, R.R. Irish, and F.G. Huegel (1991), An off-nadir imaging spectroradiometer for terrestrial ecosystem studies, *IEEE Trans. Geosci. Remote Sensing*, **29**, 66-74.

[32] Kahn *et al*., "Quality Assessment for MISR Level 2 Data", *The Earth Observer*, **8**, 19-21.

[33] Kaufman, Y., and C. Sendra (1988), Algorithm for automatic atmospheric corrections to visible and near-IR satellite imagery, *Int. J. Remote Sensing*, **9(8)**, 1357-1381, Table 1.

[34] Kaufman, Y.J., A. Gitelson, A.Karnieli, E. Ganor, R.R. Fraser, T. Nakajima, S. Mattoo, and B.N. Holben(1994), Size distribution and scattering phase function of aerosol particles retrieved from sky brightness measurements, *J. Geophys. Res*., **99(D5)**, 10341-10356.

[35] Kimes, D.S.(1983), Dynamics of directional reflectance factor distributions for vegetation canopies, *Remote Sens. Environ*., **34**, 75-91.

[36] Kimes D.S., W.W. Newcomb, R.F. Nelson, and J.B. Schutt (1985a), Directional reflectance distributions of a hardwood and pine forest canopy, *IEEE Trans. Geosci. Remote Sens*., **GE-24,** 281-293.

[37] Kimes, D.S., W.W. Newcomb, C.J. Tucker, *et al.* (1985b), Directional reflectance factor distributions for cover types of Norther Africa in NOAA 7/8 AVHRR Bands 1 and 2, *Remote, Sens. Environ.*, **18**, 1-19.

[38] King, M.D.(1982), Sensitivity of constrained linear inversions to the selection of the Lagrange multiplier, *J. Atmos. Sci.*, **39**, 1356-1369.

[39] King, M.D., and D.M. Byrne (1976), A method for inferring total ozone content from the spectral variation of total optical depth obtained with a solar radiometer, *J. Atmos. Sc*i., **33,** 2242-2251.

[40] King, M.D., D.M. Byrne, B.M. Herman, and J.A. Reagan (1978), Aerosol size distribution obtained by inversion of spectral optical depth measurements, *J. Atmos. Sci*., **35**, 2153-2167.

[41] King, M.D., and B. M. Herman (1979), Determination of the ground albedo and the index of absorption of atmospheric particulates by remote sensing. Part I: Theory, *J. Atmos. Sci*., **36,** 163-173.

[42] King, M.D.(1979), Determination of the ground albedo and the index of absorption of atmospheric particulates by remote sensing. Part II: Application, *J. Atmos. Sci.***,** **36**, 1072-1083.

[43] King, M.D., W. P. Menzel, P.S. Grant, J.S. Meyers, G.T. Arnold, S.E. Platnick, L.E. Gumley, Si-Chee Tsay, C.C. Moeller, M. Fitzgerald, K.S. Brown, and F.G. Osterwisch (1996), Airborne scanning spectrometer for remote sensing of cloud, aerosol, water vapor and surface properties, *J. Atmos. Ocean Technol.* **13(4)**, 777-794.

[44] Koepke, P. (1984), Effective reflectance of oceanic whitecaps. *Appl. Opt.* **23**, 1816.

[45] Koepke, P., and M. Hess (1988), Scattering functions of tropospheric aerosols: the effects of nonspherical particles, *Appl. Opt.*, **27 (12)**, 2422-2430.

[46] Loveland, T.R., J.W. Merchant, D.O. Ohlen, and J.F. Brown (1991), Development of a land cover characteristic data base for the coterminous U.S., *Photogram. Eng. and Remote Sens*., **57**, 1453-1463.

[47] Malm, W.C., J.F. Sisler, D. Huffman, R.A. Eldred, and T.A. Cahill (1994), Spatial and seasonal trends in particle concentration and optical extinction in the United States, *J. Geophys. Res.*, **99**, 1347-1370.

[48] Malm, W.C., J.V. Molenar, R.A. Eldred, and J.F. Sisler (1996), Examining the relationship among atmospheric aerosols and light scattering and extinction in the Grand Canyon area, *J. Geophys. Res*., **101**, 19251-19265.

[49] Martonchik, J.V. (1994), Retrieval of surface directional reflectance properties using ground level multiangle measurements, *Remote Sens. Environ.*, **50**, 303-316.

[50] Martonchik, J.V. (1997), Determination of aerosol optical depth and land surface directional reflectances using multiangle imagery, *J. Geophys. Res*., **102,** 17015-17022.

[51] Martonchik, J.V., D.J. Diner, B. Pinty, M.M. Verstraete, R. B. Myneni, Y. Knyazikhin, and H.R. Gordon (1998), Determination of land and ocean reflective, radiative, and biophysical properties using multiangle imaging, *IEEE Trans. Geosci. Remote Sensing*, **36(4)**, 1266-1281.

[52] Menzies, R.T., and D.M. Tratt (1995), Evidence of seasonally dependent stratosphere-troposphere exchange and purging of lower stratospheric aerosol from a multiyear lidar data set, *J. Geophys. Res*., **100 (D2)**, 3139-3148.

[53] Mishchenko, M.L., and L.D. Travis (1994), Light scattering by polydisperse, rotationally symmetric nonspherical particles: Linear polarization, *J. Quant. Spectrosc. Radiat. Transfer*, **51**, 759-778.

[54] Monahan, E. C. and I. G. O'Muircheartaigh (1980). Optimal power-law description of oceanic whitecap coverage dependence on wind speed. *J. Phys. Oceanogr.* **10**, 2094.

[55] Muller, P., personal communication, 1996

[56] Nakajima, T, M. Tanaka, and T. Yamauchi (1983), Retrieval of the optical properties of aerosols from aureole and extinction data, *Appl. Opt*., **22 (19)**, 2951-2959.

[57] Nakajima, T., M. Tanaka, M. Yamano, M. Shiobara, K. Arao, and Y. Nakanishi (1989), Aerosol optical characteristics in the yellow sand events observed in May, 1982 in Nagasaki - Part II, models, *J. Meterol. Soc. Jpn*., **67**, 297-291.

[58] Nakajima, T., G. Tonna, R. Rao, P. Boi, Y. Kaufman, and B. Holben(1996), Use of sky brightness measurements from ground for remote sensing of particulate polydispersions, *Appl. Opt.*, **35(15)**, 2672-2686.

[59] Ohmura, A., and H. Gilgen (1991), Global Energy Balance Archive (GEBA), World Climate Program-Water Project A7, Report 2: The GEBA Database: Interactive Applications, Retrieving Data, Heft 44, Geographisches Institut, ETH Zurich, 66 pp.

[60] Ohmura, A., H. Gilgen and M. Wild (1989),Global Energy Balance Archive (GEBA), World Climate Program-Water Project A7, Report 1:Introduction, Heft 34, Geographisches Institut, ETH Zurich, 62 pp.

[61] O'Neill, N.T., and J.R. Miller (1984a), Combined solar aureole and solar beam extinction measurements. 1: Calibration considerations, *Appl. Opt*., **23(20)**, 3691-3696.

[62] O'Neill, N.T., and J.R. Miller (1984), Combined solar aureole and solar beam extinction measurements. 2: Studies of the inferred aerosol size distribution, *Appl. Opt.*, **23 (20)**, 3697-3704.

[63] Pilewskie, P., and F.P.J. Valero (1995), Direct observations of excess solar absorption by clouds, *Science*, **267**, 1626-1629.

[64] P. Pilewskie (1996), Personal Communication

[65] Pilnis, C.(1989), Numerical simulation of visibility degradation due to particulate matter: model development and evaluation, *J. Geophys. Res.*, **94(D7)**, 9937-9946.

[66] Platt, C.M.R., J.D. Spinhirne, and W.D. Hart (1989), Optical and microphysical evidence of a cold cirrus cloud: Evidence for regions of small ice particles, *J. Geophys. Res*., **94(D8)**, 11151-11164.

[67] Pollack, J.B., and J.N. Cuzzi (1980), Scattering by nonspherical particles of size comparable to a wavelength: A new semi-empirical theory and its application to tropospheric aerosols, *J. Atmos. Sci.*, **37**, 868-881.

[68] Raman, H., B. Pinty, and M.M. Verstraete (1993), Coupled surface-atmosphere reflectance (CSAR) model 2. Semiempirical surface model usable with NOAA Advanced Very High Resolution Radiometer data, *J. Geophys. Res*., **98**, 20971-20801.

[69] Reagan, J.A., K.J. Thome, and B.M. Herman (1992), A simple instrument and technique for measuring columnar water vapor via near-IR differential solar transmission measurements, *IEEE Trans. Geoscience and Remote Sensing*, **30(4)**, 825-831.

[70] Russell, P.B., and G.E. Shaw (1995), Comments on "The Precision and Accuracy of Volz Sunphotometry", *J. Appl. Meteo*r., **14**, 1206-1217.

[71] Russell, P.B., J.M. Livingston, E.G.Dutton, R.F. Pueschel, J.A. Reagan, T.E. Defoor, M.A. Box, D. Allen, P. Pilewskie, B.M. Herman, S.A. Kinne, and D.J. Hofman (1993),Pinatubo and pre-Pinatubo optical-depth spectra: Mauna Loa measurements, comparisons, inferred particle size distributions, radiative effects an relationship to lidar data, *J. Geophys. Res*, **98(D12)**, 22969-22985.

[72] Sellers, P.J., F. Hall, H. Margolis, R. Kelly, D. Baldocchi, G. den Hartog, J. Chilar, M.G. Ryan, B. Goodison, P. Crill, K.J. Ranson, D. Lettenmaier, and D.E. Wickland (1995), The Boreal Ecosystem-Atmosphere Study (BOREAS): An overview and early results from the 1994 field year, *Bull. Amer. Meteor. Soc*., **76(9)**, 1549-1577.

[73] Shaw, G.E. (1976), Error analysis of multi-wavelength sun photometry, *Pageoph.*, **114**, 1-14.

[74] Shiobara, M., T. Hayasaka, T. Nakajima, and M. Tanaka 1991, Aerosol monitoring using a scanning spectral radiometer in Sendai, Japan, *J. Meteor. Soc. Jpn*., **69 (1)**, 57-70 (esp app).

[75] Smart, W.M. (1958),*Combination of Observations*, Cambridge, Chapter 2.

[76] Smith, W.L., and C.M.R.Platt (1978), Comparison of satellite-deduced cloud heights with indications from radiosonde and ground-based laser measurements, *J. Appl. Meteor*., **17**, 1796-1802.

[77] Spinhirne, J.D., M.Z. Hansen, and J. Simpson (1983), The structure and phase of cloud tops as observed by polarization lidar, *J. Climate Appl. Meteor*., **22(8)**, 1319-1331.

[78] Stokes, G.M., and S.E. Schwartz (1994), The Atmospheric Radiation Measurement (ARM) program: Programmatic background and design of the Cloud and Radiation Test Bed, *Bull. Amer. Meteor. Soc*., **48,** 1160-1189.

[79] Strabala, K.I., S.A. Ackerman, and W.P. Menze (1994), Cloud properties inferred from 8-12 μm data, *J. Appl. Meteor*., **33**, 212-229.

[80] Stull, R.B.(1991), *An Introduction to Boundary Layer Meteorology*, Klewer Academic Publishers, Boston, 5-6.

[81] Suttles, T., C. Justice, D. Wickland, and D. Starr (1996), Summary report of the EOS Test Sites meeting - March 18-19, 1996, *The Earth Observer*, **8(2)**, 32-40

[82] Suttles, J.T., and G. Ohring (eds.) (1986), Surface radiation budget for climate applications, *NASA Reference Publication 1169*, 132 pp.

[83] Tanaka, M., T. Nakajima, and T. Takamura (1982), Simultaneous determination of complex refractive index and size distribution of airborne and water-suspended particles from light scattering measurements, *J. Meteorol. Soc. Jpn*., **60**, 1259-1272.

[84] Thomason, L.W., B.M. Herman, R.M. Shotland, and J.A. Reagan (1982), Extraterrestrial solar flux measurement limitations due to a Beers's law assumption and uncertainty in local time, *Appl. Opt.*, **21 (7)**, 1191-1195.

[85] Thome, K, S. Schiller, J. Conel, K. Arai, and S. Tsuchida (1998), Results of the 1996 joint EOS vicarious calibration campaign to Lunar Lake, Nevada, submitted to *Metrologia.*

[86] Wehrli, C (1986), World Climate Research Programme (WCRP) Publication Series No. 7 WMO ITD No. 149, 119-126.

[87] Wendisch, M., and W. von Hoyningen-Huene (1992), Optically equivalent refractive index of atmospheric aerosol particles, *Beitr. Phys. Atmosph.*, **65 (4)**, 293-308.

[88] Wild, M., A. Ohmura, H. Gilgen and E. Roeckner (1995), Validation of general circulation model radiative fluxes using surface observations, *J. Climate***, 8**, 1309 -1324.

[89] Wylie, D.P., W.P. Menzel, H.M. Woolf, and K.I. Strabala (1994), Four years of global cirrus cloud statistics using HIRS, *J. Climate*, **7**, 1972-1986.

Science Data Validation Plan

Part III: TOA/Cloud Algorithms and Products

Thomas P. Ackerman
Roger Marchand
Eugene Clothiaux
Pennsylvania State University

11. VALIDATION CRITERIA

11.1 OVERALL APPROACH

The goal of the MISR cloud validation plan is to determine and document the accuracy, limitations and uncertainties of the MISR cloud products. By validation, we mean comparison of MISR-derived results with those obtained from *independent* sources. That is, we are differentiating validation from what might be termed algorithm development activities and data quality assurance. This goal will be achieved through three main approaches:

(1) **EOS-AM1 Instrument Assessments** - comparison and analysis of common cloud products, such as cloud masks, between MODIS, CERES, ASTER and MISR;

(2) **Long-term Assessments** - analysis obtained by way of comparisons with long term measurements at fixed sites. These comparisons will be, at least partially, statistical in nature and are expected to test algorithms under a robust set of conditions;

(3) **Short-term Assessments** - analysis via comparisons with independent observations obtained as part of specific field campaigns. These comparisons, which are essentially case studies, will be conducted for two reasons. First, they can be conducted at locations not used in longer term assessments and hence broaden the range of climatic conditions. However, their primary purpose is to augment the long-term activities by providing periods with a more complete, and hopefully more redundant, data set, in essence enabling us to gain a better understanding of the accuracy and limitations of the independent data sources.

The primary long term ground-based remote sensing sites used in support of MISR validation will be the Department of Energy (DOE) Atmospheric Radiation Measurement (ARM) program sites. These sites are critical to the validation effort. The DOE ARM sites continually operate a substantial array of equipment including radiometers, sun photometers, lidars, wind profiling radars and millimeter cloud radars. As described further below, other long term data sets such as those provided by the Baseline Surface Radiation Network (BSRN) and the Surface Radiation Budget Network (SURFRAD) may be used, but only the ARM sites contain the full complement of instrumentation which is needed.

Activities associated with the short-term assessments will involve comparisons of cloud or surface properties obtained from MISR (or a “MISR-like” instrument) with those inferred from ground-based, airborne and possibly other satellite-based sensors. In particular, the Airborne MISR simulator (AirMISR) will be used whenever possible. Of course, because AirMISR flies much closer to the surface than the EOS-AM1 platform, the AirMISR ground resolution is greater than that of the MISR instrument and the swath width is correspondingly smaller. More information on AirMISR can be found in Part I of this Science Data Validation Plan.

11.2 SAMPLING REQUIREMENTS AND TRADE-OFFS

The EOS-AM1 platform will complete its orbital cycle once every 16 days. During this period every part of the Earth is imaged, but not equally. Regions near the poles are observed more frequently than those regions near the equator. For example, Barrow, Alaska (one of the ARM sites) will be imaged 6 times every 16 days, while Nauru Island (another ARM site) in the tropical western Pacific will be imaged 2 times every 16 days. Given the sporadic nature of cloud coverage, several years of data will have to be collected before the long term assessments activities can be completed. During the early stages, the validation efforts will focus more strongly on the EOS-AM1 instrument and short-term assessment activities.

11.3 MEASURES OF SUCCESS

Ultimately, MISR cloud products will be considered valid, or a success, if they produces results which are accurate and consistent in both the long term and short term with measurements from independent data sources. This not only means that any given MISR-based results should fall within some precision of an independent measurement, but also that the various data sources should yield parameters with similar statistical properties. Situations which produce dissimilar results will be carefully studied to isolate the cause and determine if the problem is an inherent limitation in one of the data sources or if corrective action can be taken.

12. PRE-LAUNCH ACTIVITIES

In the pre-launch time period, AirMISR data will be used as a proxy for MISR data, while in the post-launch time period this data will generally be used as an independent source of radiance data for validation and vicarious calibration. From the validation point of view, the purpose of the pre-launch activities is primarily to:

(1) assess the expected accuracy of the MISR algorithms; and

(2) establish the infrastructure (e.g, software tools) and understanding required to compare MISR data with data obtained from other instruments.

12.1 FIELD EXPERIMENTS AND STUDIES

Although a number of pre-launch field experiments were planned, many of these exercises have been cancelled due to problems with the AirMISR instrument. However, AirMISR did participate in the FIRE Arctic Cloud Experiment (ACE), which is described in the following subsection. Much of the data collected during this experiment is currently being processed at JPL and will be analyzed by several of the MISR science team members over the coming months. In addition to the FIRE experiment, the MISR validation team is also considering (resources permitting) an experiment targeting marine stratus clouds in spring or summer of 1999. Some details of this experiment are described below.

12.1.1 FIRE ACE

From May 18 through June 6 of 1998, AirMISR participated in the FIRE Arctic Cloud Experiment. The overall objective of this experiment is to produce an integrated data set that (1) supports the analysis and interpretation of physical processes that couple clouds, radiation, chemistry and the atmospheric boundary layer, (2) provides in situ data for testing satellite, aircraft and surface-based remote sensing analyses; and (3) provides initial data, boundary conditions, forcing functions, and test data to support cloud modeling efforts. Aircraft observations were made over surface measurements sites provided by FIRE, SHEBA (Surface Heat Budget of the Arctic Ocean), and ARM communities. SHEBA, which is sponsored by the National Science Foundation (NSF) and the Office of Naval Research (ONR), is a research program designed to document and understand the physical processes that couple the atmosphere, ice, and ocean in the Arctic. It is currently completing a year-long extensive set of measurements directly on, under, and above the sea ice in the Beaufort sea, using the Canadian Coast Guard ice breaker Des Groseilliers as a permanent ice station. The ARM program is sponsored by the Department of Energy to resolve scientific uncertainties about global climate change with a specific focus on improving the performance of general circulation models used for climate research and prediction. ARM is providing a number of key surface-based remote sensing instruments specifically designed for the measurements of clouds and radiation at the SHEBA ice station. ARM is also operating instruments at Barrow, Alaska, as part of a decade-long program to measure the clouds and radiation in the Arctic Basin.

During the spring operations phase of FIRE ACE, AirMISR successfully acquired data during a variety of arctic cloud conditions. Cloud types observed include thin and thick, high, low and multilayered clouds. Data were also acquired over land, ice, and on one occasion a large area of open water. In combination with data from other airborne instruments (e.g., MAS, SSFR, and CLS) and ground-based instruments (e.g., lidar, radar and downwelling radiation), this data set will provide a rich resource members of the MISR science team to examine MISR cloud products. In particular, this data should prove valuable in testing the albedo and cloud masking algorithms and, in a few instances, to test the stereo-matching algorithms for cloud top height retrieval. More information regarding the FIRE ACE experiment can be obtained via the world wide web at http://eosweb.larc.nasa.gov/ACEDOCS/index.html.

12.1.2 California Coast Marine Stratus Experiment

In this mission, under review for implementation in spring or summer 1999, multiple pass measurements over a marine stratus cloud field will be made using AirMISR and the Solar Spectral Flux Radiometer (SSFR). Other instrumentation includes two 94 GHz Cloud Radars. The purpose of this experiment will be to examine variations in the cloud structure and their effects on the scattering dependence in several azimuthal planes. The ER-2 measurements will be coordinated with a combined ground-based and aircraft-based cloud radar experiment being planned by Dr. Bruce Albrecht at the University of Miami.

12.2 OPERATIONAL SURFACE NETWORKS

The primary ground-based remote sensing sites used in support of MISR validation will be the Department of Energy Atmospheric Radiation Measurement program sites. The development and testing of algorithms to ingest and analyze data from the ARM sites is being developed [Marchand, 1998]. Important aspects of the ground-based validation effort (such as how compare narrow field of view radar measurements with larger satellite views) are being studied.

13. POST-LAUNCH ACTIVITIES

Many of the MISR algorithms depend on threshold values which have not been and can not be well established prior to launch. Many of these thresholds are designed to be updated based on a statistical analysis of the MISR radiance measurements themselves. Because of this updating process and a general need to evaluate the uncertainty and limitations of the cloud products under a robust set of conditions, a large body of comparable measurements is required. A validation program of this type has the potential to be costly unless significant use is made of existing facilities. Fortunately, much of the infrastructure needed already exists. Involvement of this validation effort with existing research programs and field campaigns is a key aspect of this plan.

13.1 PLANNED FIELD ACTIVITIES AND STUDIES

Because of the variable types and quality of data that are available from preexisting ground-based sites, more intensive short-term assessment activities, where airborne measurements can be incorporated, will remain important in the post-launch validation effort. Data will be gathered and analyzed from non-EOS missions, such as the yearly intensive operational periods (IOPs) held by the ARM Clouds Working Group. The MISR science team will also take advantage of field measurements conducted by other EOS validation science teams. In terms of cloud products this includes plans by the MODIS team to conduct field campaigns targeted at cirrus cloud near Hawaii and in the Gulf of Mexico (1999 and 2000), as well as marine stratocumulus clouds and valley fog in California (2000).

13.2 NEW EOS-TARGETED COORDINATED FIELD CAMPAIGNS

The sites and timing for some MISR organized short-term validation activities will be identified in the future based on detected problems, that is, situations where MISR-based retrievals do not agree with those from other instruments. At this time, the MISR validation team anticipates conducting the following post-launch targeted exercises, but recognize that more or different needs may be identified in the future:

(1) **Cumulus / broken cloud fields** - Spring or Summer 2000;

(2) **Single layered cirrus clouds and cirrus clouds over lower cloud fields** - late 2000 or Spring 2001;

(3) **Continental stratus clouds over heterogeneous terrain** - Coordinated with ARM Clouds Working Group - late 1999 or 2000.

Participation of the airborne MISR simulator (AirMISR) is of major importance to the success of these activities. The MISR validation team anticipates having approximately 10 hours of ER-2 flight time and the necessary support to analyze this data each year. Additional measurements from airborne cloud radar, MAS (MODIS Airborne Simulator), SSFR (Solar Spectral Flux Radi-

ometer), CLS (Cloud Lidar System) and lower-flying radiometrically equipped aircraft are also highly desirable. However no funding exists to directly support this need, and so cooperation with other EOS and non-EOS field programs will be used to acquire this additional data.

13.3 NEEDS FOR OTHER SATELLITE DATA

Common cloud data products between MISR and other EOS-AM1 instruments (ASTER, CERES, and MODIS) will be compared. These data sources have the distinct advantage of being collected continuously over the same locations and at nearly same time. There are no plans at this time to compare MISR cloud products with those obtained from current satellites-based programs, as part of the validation effort. However, Dr. Jan-Peter Muller (University College London) does plan to evaluate MISR stereo derived cloud tops with IR temperature-based retrievals from ESA (European Space Agency) satellites (primarily ATSR). Furthermore, the MISR radiance-based cloud detection algorithm is currently being compared with a "MODIS-like" algorithm using global AVHRR LAC data.

13.4 MEASUREMENT NEEDS AT VALIDATION SITES

The ARM sites are the primary validation sites which will be used by in the MISR cloud validation effort. The ARM sites include (1) the Southern Great Plains (SGP) site in Oklahoma, (2) the Tropical Western Pacific (TWP) with sites on Nauru island and at Manus Island, Papua New Guinea, and (3) the North Slope of Alaska (NSA) site at Point Barrow. All of these sites are equipped (or soon will be) with vertically pointing millimeter cloud radars, as well as lidars which can be used to detect clouds and determine their vertical structure, including cloud top height. The ARM sites are equipped with hemispherical viewing instrumentation, e.g., whole sky imagers, which can be used to infer the spatial cloud fraction. Finally, these sites have routine rawinsonde releases (and in the case of the SGP a radar wind profiler) which will be used to examine cloud velocity retrievals.

Several universities also currently operate systems which the MISR science team will take advantage of as the opportunity permits. These organizations include:

(1) The University of Massachusetts, which operates a dual frequency 35/95 GHz co-aligned radar system that is well calibrated and can be scanned.

(2) The University of Utah, which operates a 94 GHz radar and an advanced polarization lidar, both of which can be scanned.

(3) University College London, which operates a stereo all-sky camera system. This group is also collecting data from the Chilbolton radar facility.

(4) The University of Miami, which operates and 94 GHz radar and an AERI (Atmospheric Emitted Radiance Interferometer).

(5) The Pennsylvania State University, which currently operates two 94 GHz cloud radars, as well as a lidar system.

More limited observations from other long term projects will also be analyzed. These sites contain at a minimum broadband downwelling solar total and diffuse irradiance measurements, which can be used to estimate the local cloud fraction [Long 1996]. The correlation between vertically pointing narrow field of view cloud fractions, hemispherical sky imager cloud fractions, and diffuse field inferred cloud fractions are currently being studied. Among these sites are:

(1) The Baseline Surface Radiation Network (BSRN) - Because of the important role radiation plays in the climate system, in 1990 the World Climate Research Programme (WCRP) proposed the establishment of a worldwide network to continuously measure radiative fluxes (upward and downward solar and infrared broadband irradiance) at the Earth's surface. BSRN is part of the WCRP Global Energy and Water Cycle Experiment (GEWEX) and they currently plan to have more than 30 sites. Many of these stations began operation in 1992 and each year more are added to the network. The data are archived at the World Radiation Monitoring Center (WRMC), in Zurich, Switzerland.

(2) The Integrated Surface Irradiance Study (ISIS) is a continuation of earlier NOAA surface-based solar monitoring programs in the visible and ultraviolet. ISIS provides basic surface radiation data with a stated accuracy, based on reference standards, to better than 1%. The Air Resources Laboratory (ARL) operates the this network. ISIS operates at two levels: Level 1 monitors incoming radiation only, and Level 2 (i.e., SURFRAD sites) focuses on the surface radiation balance.

(3) The Surface Radiation Budget Network (SURFRAD) was established in 1993 through the support of NOAA's Office of Global Programs. The SURFRAD mission is to support climate research with continuous, long-term measurements of the surface radiation budget over the United States. Currently there are five SURFRAD stations, which are located in Pennsylvania, Montana, Colorado, Illinois, and Mississippi. The upwelling and downwelling solar and infrared are the primary measurements; ancillary observations include direct and diffuse solar, photosynthetically active radiation, UVB, and meteorological parameters. Currently, consideration is also being given to the addition of lidar systems. Data are downloaded, quality controlled, and processed into daily files that are distributed in near real time by anonymous FTP and the World Wide Web (http://www.srrb.noaa.gov).

14. SPECIFIC VALIDATION PLANS FOR MISR CLOUD PRODUCTS

In the following subsections, a summary of MISR cloud data products is given, concentrating on those features important to the validation effort, along with a general description of how these products will be validated. For the purposes of this document, the cloud products are divided into three categories: (1) cloud top altitude and velocity, (2) cloud masks and cloud fractions, and (3) albedo products.

14.1 CLOUD TOP ALTITUDE AND VELOCITY: OVERVIEW

Using MISR multiple angle imagery, stereo-photogrammetric techniques can be applied to determine cloud direction and speed as well as cloud height. The basic idea is to identify the same cloud features, or scenes, at several MISR view angles. Because the MISR images of the same target are displaced in time by up to several minutes, by observing the apparent displacement of these features, cloud height and motion can be simultaneously determined. Detailed procedures by which cloud features are identified and the height and velocity are determined are given in the MISR Level 2 Cloud Detection and Classification Algorithm Theoretical Basis Document.

The essential approach used by MISR is to first determine the cloud motion using 3 MISR view angles. Nominally, the calculation is done using the Df/Bf/An views and the Da/Ba/An views (both at the 672 nm wavelength). Once the velocity is determined, a parameter referred to as the Reflecting Level Reference Altitude (RLRA) is then retrieved using two closely spaced view angles. Nominally, either the Af/An views or the Aa/An views are used to obtain the RLRA, depending on which pair views more forward-scattered light. Simulations at the University of Arizona have demonstrated that the more forward-scattering pair gives smaller systematic errors.

14.1.1 Reflecting Level Reference Altitude (RLRA)

In determining the RLRA, a combination of area- and feature-matching algorithms is used such that 1.1 km x 1.1 km areas in one view angle are identified at a second view angle. Given (1) the satellite orbit, (2) the apparent shift in position of matched areas, and (3) the scene velocity, the altitude of the matched areas can be determined. Of course, the height of clouds can vary significantly within the 1.1 km resolution. Therefore, the calculated height does not necessarily correspond to the top of an individual cloud, but will be typical of the main reflecting level. Typically, the RLRA will be near the tops of bright clouds, or at the surface under clear sky or thin cloud conditions. The calculation of the retrieved height is based on image disparity measurements to which several quality metrics are applied in order to specify the retrieval confidence.

14.1.2 Cloud Velocity

In order to determine the RLRA as described above, it is assumed that the cloud motion was known. As mentioned earlier, MISR uses one set of view angles to obtain the cloud velocity field and another set to determine the RLRA. This approach is used in order to increase the impact of cloud motion when determining the cloud velocity and minimize the effects of the cloud motion in determining the RLRA. In the MISR algorithm, the cloud velocity is taken to be given by one of two values within each 70.4 km x 70.4 km region. In general, clouds at different altitudes move at different velocities, and the general solution requires a continuum of altitudes and velocities. Over mesoscale domains, however, the MISR algorithms approximate this complexity by using only the two most common cloud velocities. In the case of partially cloud-free regions, one of the two most common velocities may be a value close to zero, owing to matches obtained from the surface. In this case the two velocities will correspond to a layer comprised of the surface terrain and a layer containing all of the clouds. In other situations, the two velocities may correspond to two distinct cloud layers.

14.1.3 Overview of the RLRA and Cloud Velocity Validation

During pre-launch validation, AirMISR data will be used to calculate cloud RLRAs. These results will be compared with those from ground-based measurements, as well as MAS, CLS, and airborne cloud radar to the degree such data can be obtained through cooperative field exercises.

In the post-launch time frame, regular comparisons between MODIS and MISR estimates of cloud top altitude will be examined, and compared with nearby ground-based measurements. Areas or situations where the MISR and MODIS cloud heights disagree will be further investigated using additional airborne measurements as necessary.

In regards to ground systems, both surface-based lidars and radars can be used to determine the altitude of cloud tops. Of course, ground-based lidars require clear sky or optically thin cloud conditions at low altitudes to detect high altitude cirrus clouds and in the case of optically thick clouds can generally only detect the altitude of the cloud base. Although not as sensitive to cirrus clouds as lidar systems, ground-based cloud radars can penetrate low optically thick clouds and can often measure cirrus clouds even through thick low clouds. Since cloud velocity is generally close to wind velocity, radar wind profilers and rawinsondes will be used to evaluate MISR calculations of the cloud velocity.

14.2 CLOUD MASKS AND CLOUD FRACTIONS

The MISR standard cloud products consist of three cloud masks and a number of measures of the cloud coverage over 17.6 km x 17.6 km areas (i.e., cloud fractions).

14.2.1 RCCM

The Radiometric Camera-by-camera Cloud Mask (RCCM) is a filter which identifies which samples in the image for each MISR camera are cloud covered and which pixels are clear. More specifically, the RCCM identifies each 1.1 km x 1.1 km area as cloudy with either high confidence or low confidence or clear with either high confidence or low confidence.

The RCCM is determined by examining the intensity and spatial variability of image pixels in the MISR 3rd and 4th spectral bands (i.e., at 672 and 866 nm, respectively). The processing details are given in the Level 1 Cloud Detection Algorithm Theoretical Basis Document. The basic idea is that there is expected to be a distinguishable difference between the image intensity and variability for cloud cover and for the underlying surface at these two wavelengths. A threshold test can therefore be applied to classify the scene as cloud covered or as clear. The required thresholds are a function of the surface type [as specified in the Cloud Screen Surface Classification (CSSC) data set], solar angle and view angle. Although a set of default threshold values will be used at launch, the thresholds will be modified using measured results via an ongoing automated statistical analysis. This threshold approach is expected to work well over most surfaces. Much like clouds, however, snow covered surfaces are highly reflective at both wavelengths. A RCCM quality flag which specifies what algorithmic tests were used in constructing the mask is also stored in the standard TOA/Cloud data set.

14.2.2 SDCM

The stereoscopically retrieved height field that is used as input to generating the RLRA is also used to construct a cloud mask, known as the Stereoscopically-Derived Cloud Mask (SDCM). Each successful stereo height retrieval is designated as either Near or Above the surface and rated with high confidence (HC) or low confidence (LC). The confidence ratings are based on algorithm metrics associated with the disparity and height retrieval process. The SDCM is derived from this height/confidence designator and the RCCM mask for the reference camera, nominally the nadir camera. The SDCM can take on one of five values: CloudHC, CloudLC, NearSurface, Clear, and No Retrieval. Clear indicates that the RCCM indicated clear conditions and the height retrieval has been set to the known terrain height. An RCCM result of clear with high confidences always overrides the stereo-derived height confidence designator. An RCCM result of clear with low confidence overrides the stereo-derived height retrieval designator, unless the stereo height designator specifies cloud with high confidence. Thus, CloudHC means that the height retrieval found clouds above the surface with high confidence and this result was not overridden by the RCCM. NearSur-

face indicates that a the height retrieval found the reflecting level near the surface, but the RCCM still indicated the presence of clouds. CloudLC means either (1) that the height retrieval failed and the RCCM indicates the presence of clouds or (2) the height retrieval indicated the presence of clouds with low confidence and the RCCM is missing or also supports the existence of clouds. No Retrieval occurs only when no result was obtain for both the height retrieval and the RCCM.

14.2.3 ASCM

Optically thin, high-altitude cirrus clouds will often not be detected by the RCCM thresholds. To detect cirrus clouds, a technique known as Band-Differenced Angular Signature (BDAS) [Di Girolamo 1992, Di Girolamo and Davies 1994] is employed using MISR's 70.5° and 60° view angles. The resulting detections are then projected to a climatological cirrus-cloud altitude, and the resulting mask is known as the Angular Signature Cloud Mask (ASCM). The BDAS technique uses the difference in measured radiances between either the 866 nm and 446 nm channels or between the 672 nm and 446 nm channels, depending on surface type (generally water or land respectively). Especially for these large viewing angles, the measured radiances are sensitive to the contribution of Rayleigh scattering, which has a strong wavelength dependence, and this dependency provides the basis of the technique. Quantitatively, the 866 nm and 446 nm wavelengths differ by almost a factor of 15 in their sensitivity to Rayleigh scattering, while the 672 nm and 446 nm wavelengths differ by more than a factor of 5. Since the contribution of Rayleigh scattering decreases in the presence of high clouds, the difference in the measured radiances can be used to identify the presence of cirrus clouds. The 672 to 446 difference is used over land targets to reduce the impact of land surface spectral variations.

Simulations using LOWTRAN 7 indicate that the BDAS technique is expected to work best over ocean and, interestingly, over snow surfaces (where most other satellite cloud detection techniques experience difficulties). Over most land surfaces, the BDAS technique is generally expected to offer poor cloud detection capability due to the large variability in land reflectance.

Lastly, it should be mentioned that the BDAS technique used to determine the presence of thin cirrus clouds does not provide any independent information on the cloud height; making it difficult to determine the exact location of these clouds relative to other cloud masks.

14.2.4 Cloud Fractions

For scene classification purposes, the stereoscopically derived cloud altitudes and the associated RCCM, SDCM and ASCM are used to generate regional altitude-binned cloud coverage fractions over 17.6 x 17.6 km regions. The regional scene classifiers consist of the following parameters:

(1) $f^{k}_{m,\,l}$, an altitude-binned classifier in which *k* represents one of five altitude classes: surface, low cloud, mid-level cloud, high cloud, and no retrieval; *m* represents one of the three masks (feature-projected RCCM, ASCM, SDCM); and *l* represents the clear/cloud or surface/cloud and confidence designations associated with each mask. The altitude binning is referenced to the surface terrain.

(2) F_{CloudHC}, the fractional area of the region that is classified, with high confidence, as consisting of any type of cloud, and F_{ClearHC}, the fractional area of the region that is classified, with high confidence, as being clear of any type of cloud.

(3) $\tilde{F}_{\mathrm{CloudHC}}$ and $\tilde{F}_{\mathrm{CloudLC}}$, the fractional area of the region that is classified, with high and low confidence, respectively, as consisting of clouds excluding those detected using the BDAS test. These parameters are used as input to Level 2 aerosol retrievals.

(4) $\hat{F}^{k}_{\mathrm{CloudHC}}$ and $\hat{F}^{k}_{\mathrm{CloudLC}}$, the fractional area of the region that is classified, with high and low confidence, respectively, as consisting of clouds detected using the original terrain-projected RCCM only, for camera *k*.

This last metric ($\hat{F}$) is calculated for each of the MISR view angles, while the other metrics are calculated based on the stereo reference camera (nominally An) RCCM. Also, the F and $\tilde{F}$ fractions use the RCCM only if the region is classified as snow/ice free.

14.2.5 Overview of the Cloud Mask and Cloud Fraction Validation

Validation of the cloud masks and cloud fractions is conceptually much the same as that for the RLRA. However in addition to lidars and cloud penetrating radars, the use of broadband total and diffuse irradiance measurements will be used to detect the presence of clouds and to estimate the local cloud fraction [Long 1996].

In the pre-launch time frame, validation will involve the use of AirMISR to generate cloud masks over a variety of surface targets. The AirMISR cloud masks will then be compared with both (1) other airborne observations (such as those from MAS) and (2) ground based measurements (such as those from a 94 GHz cloud radar). If AirMISR uses all 9 MISR angles, it views only a relatively small target area, about 10 km on a side. (This is because AirMISR has only one camera whose pointing angle is adjusted during flight). However, in principal all three cloud masks can be generated using only a few camera positions, allowing larger areas to be utilized.

In the post-launch time frame, automated comparison between the MODIS cloud masks and the nadir RCCM will be routinely examined and areas or situations where these two cloud mask disagree further investigated using additional airborne measurements as necessary. Also, the RCCM mask for all MISR view angles will be compared. Of course both the MODIS and MISR cloud masks can agree i.e., both can indicate cloud or no cloud, and still be erroneous. These com-

parisons will focus primarily near regions where long term ground-based measurements can be obtained. These measurement sites offers the best option for long term monitoring, composition of statistical measures of success, and identification of problems related to atmospheric and surface conditions which may occur infrequently. Because the RCCM success may be highly dependent on the surface conditions, a wide array of surface types will be monitored.

In principle, validating the cloud masks will validate the cloud fractions. In practice, cloud fractions will be used as a primary validation check, and sample comparisons applied to help isolate the problems. In general, a sample-by-sample comparison between MODIS and MISR will require projecting the MISR cloud masks onto the same grid system used by MODIS, or vice versa, and may prove difficult due to differences with resolution and viewing angles. However this reprojection should have only a minimal effect on the cloud fractions.

14.3 ALBEDO PRODUCTS AND TEXTURE INDICES

Once the average RLRA has been determined for each 2.2 km x 2.2 km region of the surface, a number of “reflecting level parameters” are associated with it. In terms of MISR standard cloud products, this includes three texture indices, counts of the number of unobscured pixels, and two average bidirectional reflectance factors, one associated with RLRA tops and one associated with RLRA sides.

What is meaning of “unobscured pixels”, “RLRA tops” and “RLRA sides”? When viewing a scene from an angle other than nadir, the image of one surface may be blocked by the presence of another surface, e.g., by other clouds or nearby terrain. “Unobscured pixels” are those pixels which are not blocked by some other surface. However, MISR is not able to detect the thickness of clouds. Therefore, a cloud is considered to be a square prism or column stretching from the surface to its RLRA. The expression “RLRA tops” refers to those image pixels located on the tops of these prisms and the expression “RLRA sides” refers to the sides of the prisms. Therefore, radiation which is said to originate from the “RLRA sides” is not necessarily originating from the sides of clouds, but could be representative of area underneath the clouds, or other clouds at a lower altitude. Alternatively, those pixels which are described as “RLRA tops” are not necessarily the tops of clouds, if the cloud coverage is fragmentary on spatial scales less than 2.2 km x 2.2 km.

The Bidirectional Reflectance Factors (BRFs) are ratios of the scattered radiance to the incoming solar radiance, and are used to determine the scene albedo. At a basic level, the study of the Earth energy balance requires knowledge about the ratio of the irradiance reflected from a given surface to the irradiance incident on that surface. This quantity is often referred to as the albedo and can be obtained by summing, or more precisely, integrating the bidirectional reflectance factors of the surface over all scattering angles. Satellites, however, do not measure the scattered radiance from the Earth’s surface at all possible directions. That is, satellites measure radiances, not irradiances. Therefore, satellite determination of the albedo requires application of some model of

the scattered radiances in directions which are not measured. Previous instruments, such as ERBE, measured scattered radiances at only one angle. The nine MISR zenith view angles provide good coverage in zenith angle and can be expected to produce improvement in the albedo determination. However, the fore and aft views provide sampling at only two azimuthal angles and a model for the azimuthal dependence of the surface reflectance is still required. Again, data from the nine view angles can be expected to help in scene classification or modeling and hence better selection of azimuthal models.

Because the azimuthal dependence of the scattering depends strongly upon the shape, roughness and composition of the scatterer, it is desirable to classify and select azimuthal scattering models on a scale which is consistent with the variation in these characteristics. However, because of changes in height of the reflecting surface, be it from nearby clouds or terrain, some MISR view angles may be obscured as described above. This obscuration has led the MISR science team to develop three types of albedos, which are called the Local Albedo, the Restrictive Albedo, and the Expansive Albedo.

14.3.1 Texture Indices and the Average Bidirectional Reflectance Factors (BRFs)

The top of each 2.2 km x 2.2 km region has up to 64 275-m pixels in each of the nine MISR zenith view angles. A fraction of these 64 pixels may be “unobscured RLRA tops”, depending on the view angle and the height of nearby RLRA columns. Also, different portions of the sides of each RLRA rectangle may be visible depending on the view angle and height of nearby RLRA surfaces.

The standard MISR cloud data set will contain the BRFs averaged separately for pixels designated as RLRA column tops or as RLRA column sides at each wavelength. In addition to the average BRFs, three measures of the variation in the RLRA top pixels are calculated: (1) the standard deviation divided by the mean BRF for all RLRA top pixels, (2) the standard deviation of the difference in adjacent pixels in the along track direction, and (3) the standard deviation of the difference in adjacent pixels in the cross track direction. These three standard deviations are referred to as texture indices because they provide a measure of cloud homogeneity [Chen et al 1989]. All of the texture indices are calculated at 672 nm.

14.3.2 The Local Albedo and Methodology Flags

To obtain he local albedos, the azimuthal models are applied at the relatively high resolution of 2.2 km x 2.2 km. The local albedos are later summed to obtain (a portion of) the restrictive and expansive albedos over larger 35.2 km x 35.2 km areas. There may at times be considerable heterogeneity even at 2.2 km resolution. However, the presence of such heterogeneity should be identified when it occurs, through the accompanying texture indices.

The local albedo is defined in the MISR Level 2 Top-of-Atmosphere Albedo Algorithm Theoretical Basis Document to be the ratio of the *unobscured* upwelling irradiance through the RLRA to the downwelling TOA irradiance above the RLRA. That is to say, (1) the local albedo is calculated using the BRF of those pixels which are located only on the top of the RLRA columns, and (2) no correction is applied to account for absorption and scattering by the atmosphere. The second point means that there will be small differences between the local albedo as defined above and the albedo that would be conventionally measured in situ, owing due to absorption and scattering in the atmosphere above the cloud.

The local albedo is restricted to the RLRA tops because only the BRFs associated with these pixels can reasonably be associated with an Azimuthal Model (AZM). (As explained above, the source of the pixels assigned to the RLRA sides is not known). The restrictive albedo described in the following section does incorporate the RLRA sides, but no azimuthal dependence is assumed.

The unobscured fractions and average BRFs for each of the nine view angles used in the local albedo evaluation are stored together with other scene classifiers in the standard MISR cloud data set. Therefore users who, for whatever reason, would prefer to calculate the albedo without the azimuthal corrections, or using different models than currently intended can easily do so. In practice, three types of azimuthal models are used for cloudy skies: (1) a deterministic model, (2) a stochastic model and (3) a solid angle weighting model.

In the deterministic model, one of several AZMs is chosen based on the relative direction of the sun, the RLRA, the phase (ice/water) of the cloud, and the nine average BRFs at 672 nm. The AZM consists of a set of weights which given the BRF at *one* view angle can be used to determine the total albedo or a portion of the total albedo. (Recall that the albedo is given by a summation of the BRFs over a hemisphere above the scattering surface. So, the albedo can be thought of as a sum of partial albedos, one associated with each MISR zenith view angle). The appropriateness of the AZM for each of MISR view angle is examined by comparing how consistently the AZM predicts the partial albedo based on radiance measurements at neighboring view angles. More specifically, if the calculation of the partial albedo at *one* particular view angle based on the BRF at *that* view angle matches the partial albedo calculation based on the BRF from at least one *neighboring* view angle (to within some threshold value), then the partial albedo is taken as the average of the partial albedo associated with that view angle and its neighboring view angles. If the partial albedo calculations do not match, then the stochastic model is tried next. The deterministic AZM models will be used only for homogeneous clouds, to approximate plane-parallel clouds. The determination of scene homogeneity is based upon a thresholding of the texture indices. The AZM model weights have largely been determined through numerical simulations, the full details of which are given by Varnai [1996].

If the deterministic approach fails, a generic model for all clouds is used to provide a statistical best guess for the azimuthal correction. This second method is referred to as the stochastic method. The stochastic model is similar to the deterministic model in that it also consists of a set of weights which given the BRF at *one* view angle can be used to determine a portion of the total albedo associated with each MISR zenith view angle. These weights are applied in a manner analogous to the deterministic approach (described in the proceeding paragraph).

If the measurements fail to satisfy the criteria for the deterministic and the stochastic models, then no azimuthal correction is made and albedo calculations assuming no azimuthal dependence are used. This third technique is referred to as the solid angle weighting method and is always used for the nadir camera.

Note that for a given calculation of the local albedo, it is possible for each partial albedo contribution to be determined by a different method. It is possible, for example, for deterministic weighting to be applied at two angles, stochastic weight for one angle, and solid angle weighting for the remaining six angles. An AZM model indicator and methodology flags are included in the MISR cloud product data set which completely describe how the local albedo is calculated for each 2.2 km x 2.2 km subregion.

If the RLRA is the surface terrain, a modified form of an empirical model known as the Coupled Surface-Atmosphere Reflectance (CSAR) equation is fit to the measured radiances [Rahman et al. 1993]. The CSAR equation has three free parameters which are determined by a least squares fit to the measured radiances. A χ^2 test is used to evaluate the effectiveness of the CSAR model relative to the measured values. If the test is passed the CSAR model is used to determine the albedo. If the test fails the local albedo is determined using the solid angle weighting approach, that is, no azimuthal correction is applied.

14.3.3 The Restrictive Albedo

The restrictive albedo is calculated for 35.2 km x 35.2 km regions and is defined as the ratio of the irradiance reflected from *all* surfaces within the region to the downwelling TOA irradiance above that region. The relevant reflected irradiance from all RLRA surfaces (both column tops and column sides) are used in this calculation. The restrictive albedo is thus due in part to the sum of the unobscured irradiances already associated with the local albedos. These irradiances are azimuthally corrected using the best technique for each local region (that is, using the local albedo). The remainder of the restrictive albedo is due to the contributions from the RLRA sides. The albedos of RLRA sides are determined using solid angle weighting.

14.3.4 The Expansive Albedo

The expansive albedo differs from the other two albedos in being referenced to the top of the atmosphere instead of to a surface just above the cloud tops. The expansive albedo is defined as the ratio of the upwelling irradiance through a region at the top of atmosphere (defined at 30 km altitude) to the downwelling TOA irradiance. Since the TOA reference surface is never obscured, this albedo is identical to what would be obtained from airborne measurements at an altitude of 30 km. Like the restrictive albedo, the expansive albedo will be determined for 35.2 km x 35.2 km regions. However, the reflecting surface (i.e., the RLRA columns) contributing to the upwelling irradiance at TOA is much larger than the 35.2 x 35.2 km area underneath this surface. In fact, the Earth surface area contributing to the expansive albedo is many hundreds of kilometers. The expansive albedo will, consequently, generally be different than the restrictive albedo and generally involves substantially greater scene inhomogeneity.

14.3.5 Overview of the Cloud Albedo Validation

Validation of the cloud BRFs, and albedos represents a significant challenge. For the most part, the validation of these quantities will be restricted to the post-launch time frame.

To validate the local albedo, one really wants to validate the measured radiances and the azimuthal models. To completely validate these quantities, the surface BRFs would have to be measured at all azimuthal and zenith angles, or more precisely, with at least enough angles to fully characterize the fluctuations in the BRF. Because airborne vehicles are needed to make such measurements and because clouds are often highly spatially, as well as temporally variable, such complete measurements are extremely difficult. Therefore, validation efforts for local albedos will initially concentrate on relatively homogeneous stratus cloud scenes.

In general, we will validate the local and restrictive albedos using two methods: (1) making airborne hemispherical albedo measurements just above the cloud tops and comparing these results with MISR local albedos, modified to account for scattering and absorption above the cloud and (2) making AirMISR measurements as close as possible in time and space to the MISR overflights both along the satellite ground track and at azimuthal angles other than those measured by MISR. We will also study the use of ground-based downwelling measurements to infer the cloud top albedos. However, there remains at this time some uncertainty in the absorption of shortwave radiation by clouds, which may limit the applicability of this approach. The expansive albedo, on the other hand, will be approximately measured using downward looking hemispherical radiometers flown on board the ER-2 at altitudes of roughly 20 km.

Other approaches which we hope to investigate involve sorting MISR measured BRFs (as a function of azimuthal and solar zenith angles) and MISR calculated albedos with reference to cloud scene classifiers, such as cloud top altitude, cloud bottom temperature, texture indices, and cloud

fractions. Ideally, these cloud scene classifiers can serve as a basis from which to essentially construct a set of azimuthal models from the measured BRFs.

Also, for many applications, the surface albedo is defined as a broadband quantity; however, MISR makes measurements at only four wavelengths. Therefore, another model which converts the narrowband albedos to a broadband quantity is generally needed. Airborne measurements using the Airborne Visible/Infrared Imaging Spectrometer (AVIRIS) or the Solar Spectral Flux Radiometer (SSFR), as well as both narrowband and broadband hemispherical radiometers will be used to study conversion of the narrowband cloud albedos to broadband albedos.

15. REFERENCES

Chen, D.W., S.K. Sengupta, and R.M. Welch (1989) Cloud field classification based upon high spatial resolution textural features. 2. Simplified vector approach. *J. Geophys. Res.* **97**, 14749.

Di Girolamo, L. (1992) On the detection of cirrus clouds from satellite measurements. Master of Science thesis, Dept. of Meteorology, McGill Univ., Montreal, PQ.

Di Girolamo, L. and R. Davies (1994) A Band-Differenced Angular Signature technique for cirrus cloud detection. *IEEE Trans. Geosci. Rem. Sens.* **32**, 890-896.

Long, Charles N. (1996) Surface Radiative Energy Budget and Cloud Forcing: Results for TOGA COARE and Techniques for Identifying and Calculating Clear Sky Irradiance, Ph.D Thesis, Penn State University.

Marchand, R. T., E. E. Clothiaux, and T. P. Ackerman (1998) A One-Year Cloud Climatology for the Southern Great Plans Site, American Meteorological Society Conference on Cloud Physics, 17-21 August .

Rahman, H., B. Pinty, and M.M. Verstraete (1993). Coupled surface-atmosphere reflectance (CSAR) model 2. Semiempirical surface model usable with NOAA Advanced Very High Resolution Radiometer data. *J. Geophys. Res.* **98**, 20,791-20,801.

Varnai, T. (1996). Reflection of solar radiation by inhomogeneous clouds. Ph.D Thesis, McGill University, Montreal.

Science Data Validation Plan

Appendix

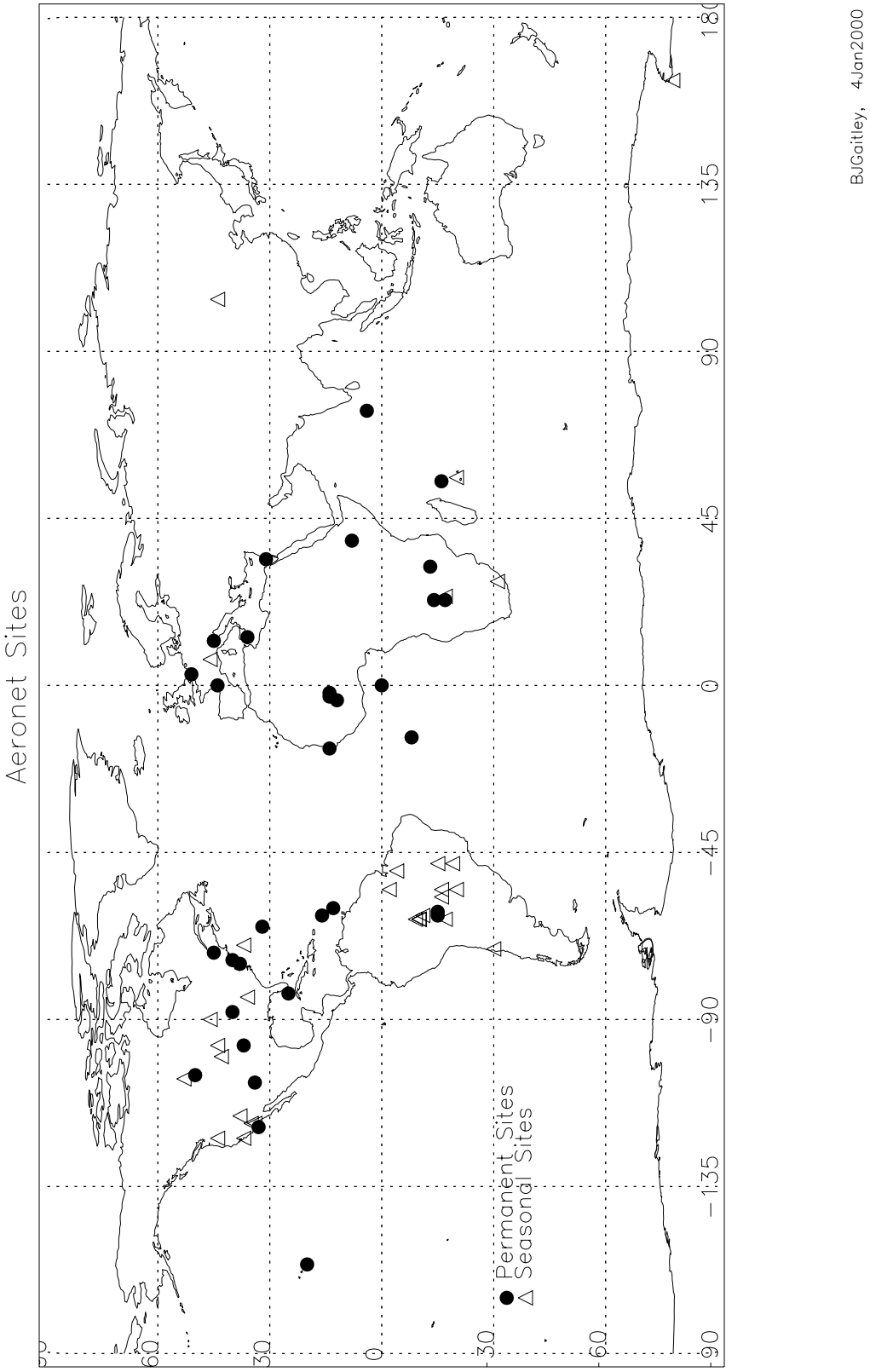

Figure A-1: Distribution of permanent (solid circle) and seasonal (open triangle) AERONET stations corresponding to MISR Local Mode sites, for use in validation of retrieved MISR aerosol optical depth and aerosol microphysical models.

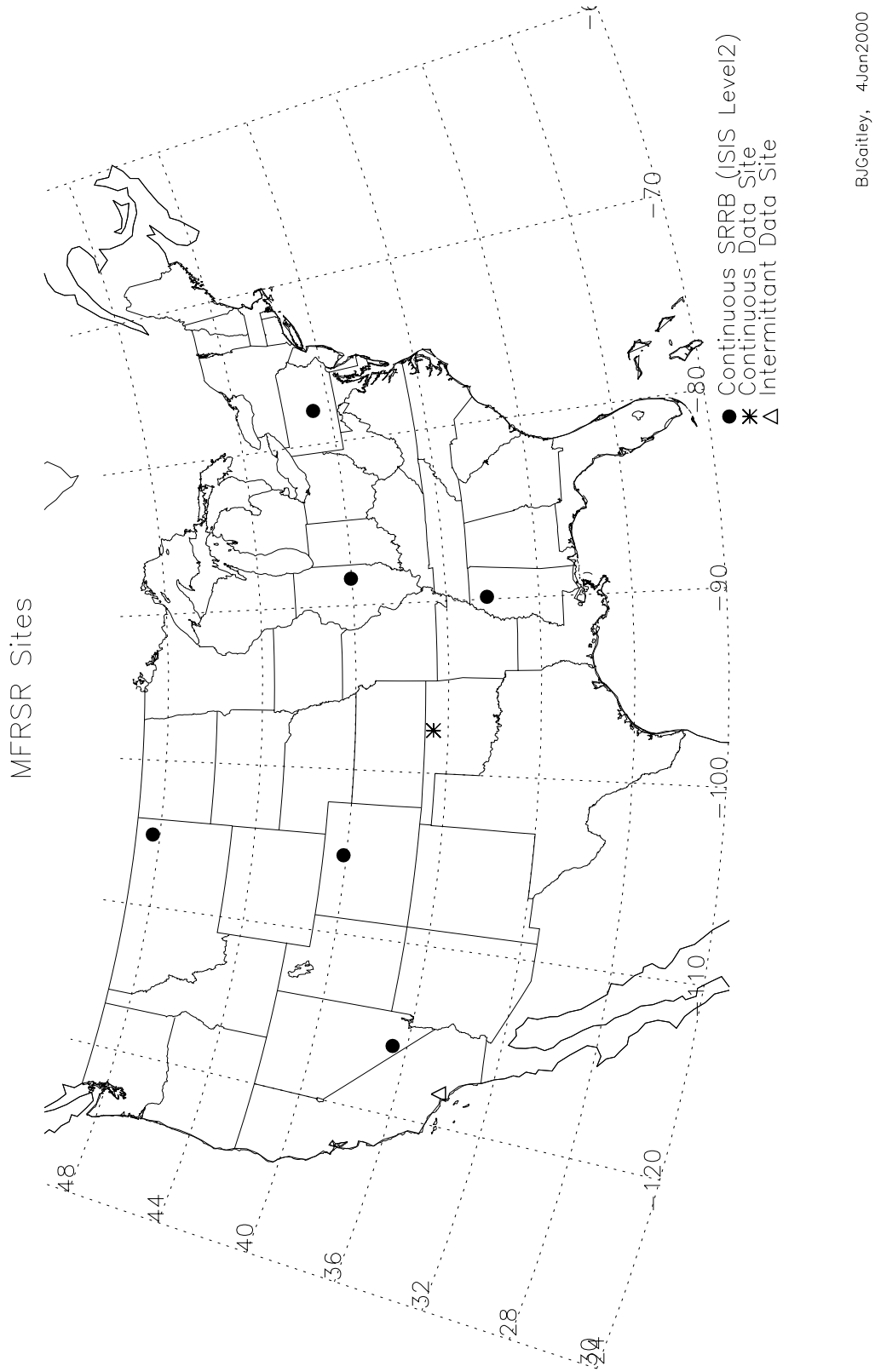

Figure A-2: Distribution of Surface Radiation Budget Network (SURFRAD) and other sites to be used in vaidation of MISR calculated irradiance at the surface.